

NIL ✓  
(NASA-CR-159564) CF6 JET ENGINE PERFORMANCE  
IMPROVEMENT PROGRAM. SHORT CORE EXHAUST  
NOZZLE PERFORMANCE IMPROVEMENT CONCEPT  
(General Electric Co.) 113 p HC A06/MF A01

N79-33206

CSSL 21E G3/07

Unclas

38429



National Aeronautics and  
Space Administration

# CF6 JET ENGINE PERFORMANCE IMPROVEMENT PROGRAM

## SHORT CORE EXHAUST NOZZLE PERFORMANCE IMPROVEMENT CONCEPT

by

W. A. FASCHING

GENERAL ELECTRIC COMPANY

SEPTEMBER 1979

Prepared For

**National Aeronautics and Space Administration**



## FOREWORD

The work was performed by the CF6 Engineering Department of General Electric's Aircraft Engine Group, Aircraft Engine Engineering Division, Cincinnati, Ohio. The program was conducted for the National Aeronautics and Space Administration, Lewis Research Center, Cleveland, Ohio, under Subtask 2.2 of the CF6 Jet Engine Performance Improvement Program, Contract Number NAS3-20629. This report was prepared by W.A. Fasching, General Electric Program Manager, with the assistance of H. Word, B. Bonini, F. Keenan and B. Safriet. The NASA Project Engineer for this program was F.J. Hrach. The program was initiated in February 1978 and was completed in February 1979.

**PRECEDING PAGE BLANK NOT FILMED**

TABLE OF CONTENTS

<u>Section</u>		<u>Page</u>
1.0	SUMMARY	1
2.0	INTRODUCTION	2
3.0	DESCRIPTION OF SHORT CORE NOZZLE CONCEPT	5
4.0	DESIGN AND FABRICATION	12
	4.1 Overall Design Approach	12
	4.2 Design Description	12
	4.3 Core Cowl and Pylon Design	14
	4.4 Maintainability	14
	4.5 Reliability	15
	4.6 Safety	16
5.0	PERFORMANCE TEST	17
	5.1 Test Configurations	17
	5.2 Test Facility	17
	5.3 Instrumentation	21
	5.4 Test Procedure	25
	5.5 Test Results	26
6.0	ACOUSTIC TEST	35
	6.1 Test Configurations	35
	6.2 Test Facility	35
	6.3 Instrumentation	39
	6.4 Test Procedure	41
	6.5 Test Results	43
7.0	ENDURANCE TEST	92
	7.1 Test Configuration	92
	7.2 Test Facility	92
	7.3 Test Procedure	92
	7.4 Test Results	92

CONFIDENTIAL

TABLE OF CONTENTS

<u>Section</u>		<u>Page</u>
8.0	ECONOMIC ASSESSMENT	99
9.0	SUMMARY OF RESULTS	101
APPENDIX A -	QUALITY ASSURANCE	103
APPENDIX B -	LIST OF SYMBOLS	106
REFERENCES		108

## 1.0 SUMMARY

The purpose of the Short Core Exhaust Nozzle Program was to develop the technology and to demonstrate the technical feasibility of this performance improvement concept on a CF6-50 turbofan engine

Back-to-back performance and acoustic tests were conducted in order that direct comparisons could be made between the short core and the long core exhaust nozzles. In addition, development endurance testing was performed for mechanical design assurance.

The sea level performance testing substantiated within test accuracies the expected uninstalled performance improvement (~0.3% improved nozzle thrust coefficient) which is predicted to be 0.9% internal sfc improvement at cruise. Flight tests conducted outside this program indicate a cruise sfc reduction of at least 0.9% can be obtained with the Short Core Exhaust Nozzle on the Airbus Industrie A300B and the Douglas DC-10-30 aircraft. The acoustic tests demonstrated that this performance gain was achieved without an increase in engine noise. The nozzle hardware successfully completed 1000 simulated flight cycles of endurance testing without any signs of distress.

An economic assessment of the improvement applied to engines on the Boeing 747 and the Douglas DC-10 is included in the report

## 2.0 INTRODUCTION

National energy demand has outpaced domestic supply creating an increased U.S. dependence on foreign oil. This increased dependence was dramatized by the OPEC oil embargo in the winter of 1973 to 1974. In addition, the embargo triggered a rapid rise in the cost of fuel which, along with the potential of further increases, brought about a changing economic circumstance with regard to the use of energy. These events, of course, were felt in the air transport industry as well as other forms of transportation. As a result of these experiences, the Government, with the support of the aviation industry, has initiated programs aimed at both the supply and demand aspects of the problem. The supply problem is being investigated by looking at increasing fuel availability from such sources as coal and oil shale. Efforts are currently underway to develop engine combustor and fuel systems that will accept fuels with broader specifications.

Reduced fuel consumption is the other approach to deal with the overall problem. A long-range effort to reduce consumption is to evolve new technology which will permit development of a more energy efficient turbofan or the use of a different propulsive cycle such as a turboprop. Although studies have indicated large reductions in fuel usage are possible (e.g., 15 to 40%), the impact of this approach, in any significant way would be 15 or more years away. In the near term, the only practical propulsion approach is to improve the fuel efficiency of current engines. Examination of this approach has indicated that a 5% fuel reduction goal starting in the 1980 to 1982 time period is feasible for the CF6 engine. This engine is, and will continue to be, a significant fuel user for the next 15 to 20 years.

Accordingly, NASA is sponsoring the Aircraft Energy Efficiency (ACEE) program (based on a congressional request) which is directed at reducing fuel consumption of commercial transports. The Engine Component Improvement (ECI) program is the element of the ACEE program directed at the fuel efficiency of current engines. The ECI program consists of two parts: engine diagnostics and performance improvement. The engine diagnostics effort is to provide information to identify the sources and causes of engine deterioration. The performance improvement effort is directed at developing engine performance improvements and retention components for new production and retrofit engines. The initial effort consisted of a feasibility analysis which was conducted in cooperation with the Boeing and Douglas aircraft companies and American and United Airlines. The study consisted of:

- The identification of engine and component modifications which exhibited a fuel savings potential over current practice in CF6 engines.
- The technical and economic assessment of the modifications, including the impact on airline acceptability and the probability of production introduction of the concepts by the 1980 to 1982 time period as well as their retrofit potential.
- The assessment of fuel savings for the DC-10-10, DC-10-30, and the B-747-200 aircraft.

- The selection of the most promising concepts and the preparation of Technology Development Plans for their development and evaluation in ground test facilities

The results of the feasibility analysis are reported in Reference 1.

One of the concepts selected for development was the Short Core Exhaust Nozzle, hereafter referred to as the Short Core Nozzle. This report presents the results of the development work on the concept.

In 1974/1975, General Electric and the Douglas Aircraft Company conducted a series of model tests directed at performance improvement of the CF6-50 core engine exhaust system. The CF6-50 engine was initially designed to provide core engine thrust reversing, however, many airline operators subsequently deactivated the core reverser or adopted a fixed nozzle system that had the same aerodynamic flowpath but did not provide the reversing function. The elimination of core engine thrust reversing capability on many aircraft provided the necessary flexibility for design changes and potential performance improvements through reduced internal pressure losses and external drag reduction.

The model tests cited above confirmed the potential for improvement, and preliminary design studies were initiated by General Electric and Douglas. Subsequent work effort included additional model tests and full-scale flight tests. The additional model tests included wind tunnel tests with wing-on in which Douglas determined an interference drag reduction potential; full-scale tuft and pressure surveys conducted on a DC-10 by Douglas substantiated that the interference drag observed on the model actually exists on the airplane. In August 1977, a static model test was conducted by General Electric to improve the internal flowpath to achieve the desired nozzle flow area for engine thermodynamic cycle matching. Further wind tunnel scale model tests were conducted by General Electric in October 1977 on the selected configuration. These tests confirmed the results of the initial tests.

In late 1977, the Short Core Nozzle performance improvement concept was selected for development and evaluation in ground test facilities by the NASA Engine Component Improvement Program because of its high fuel saving potential and high payback for the DC-10-30 aircraft.

The objective of the program was to develop the technology of the Short Core Nozzle system and to verify the predicted fuel savings by full-scale engine ground tests. Mechanical, cycle, performance, acoustic, and installation design studies were conducted in support of the engine tests.

In the program, a back-to-back sea level static performance test was conducted in a test cell on a CF6-50 engine equipped with a Long Fixed Core Nozzle and appropriate cowl doors and the same engine equipped with the Short Core Nozzle and a new core cowl. The acoustic test consisted of a back-to-back test of a CF6-50 engine equipped with the Core Reverser Nozzle and the same engine equipped with the Short Core Nozzle in an outdoor noise test facility. Endurance testing of a CF6-50 engine with the Short Core Nozzle was performed in order to establish the life capability of the new exhaust system.

The performance test objective was to demonstrate with a back-to-back engine test the overall thrust coefficient improvement of the Short Core Nozzle versus the Long Fixed Core Nozzle configuration to substantiate scale model test results. The objectives of the acoustic test and subsequent data analysis were

- To establish the acoustical effect of the Short Core Nozzle on CF6-50 engine noise.
- To assess the impact of the engine modification on community noise levels for typical aircraft approach and takeoff flight conditions

The objective of the endurance test was to demonstrate the structural integrity of the Short Core Nozzle by subjecting it to 1000 simulated flight cycles



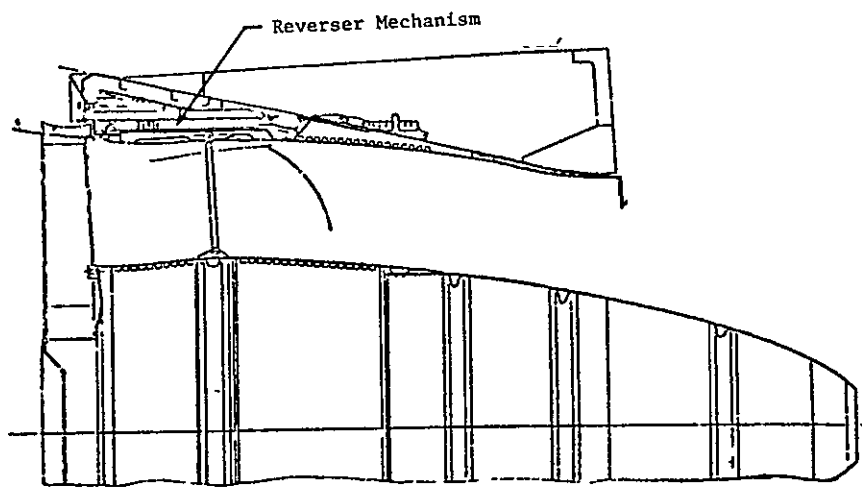
### 3.0 DESCRIPTION OF SHORT CORE NOZZLE CONCEPT

The Short Core Nozzle is a replacement for a deactivated Core Reverser Nozzle or the Long Fixed Core Nozzle, both of which are in use on the CF6-50 high bypass turbofan engine (Figure 1). A comparison of the Short Core Nozzle with the Long Fixed Core Nozzle is shown in Figure 2. A comparison of the nacelle and pylon for the short exhaust system with the production DC-10-30 installation is shown in Figure 3.

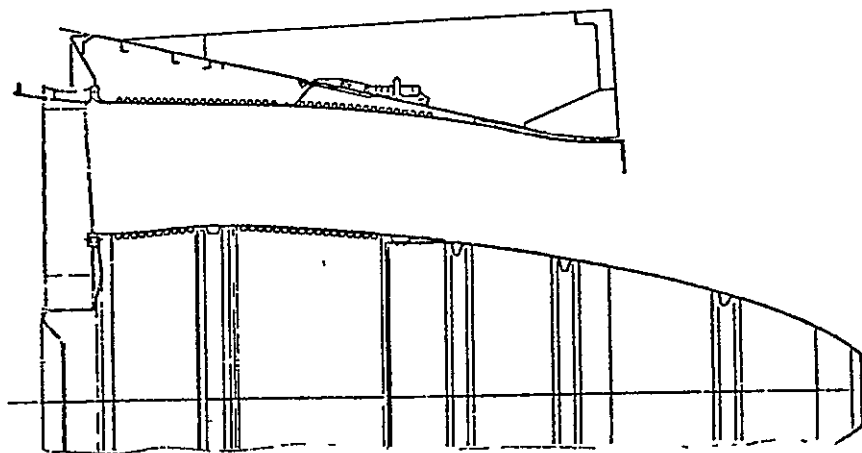
The Long Fixed Core Nozzle was introduced for DC-10 and 747 aircraft for those airlines which do not require core stream reversing to meet their landing requirements. The lighter weight A300B aircraft do not require a core exhaust reverser, and Long Fixed Core Nozzles are used. These nozzles have essentially the same flow lines as the Core Reverser Nozzle. Both the Long Fixed Core Nozzle and Short Core Nozzle systems provide significant weight reductions by removal of the deflector structure, blocker doors, and actuation and position sensing hardware.

As can be seen in Figure 3, the Short Core Nozzle system requires reduced diameter fan flow lines aft of the fan reverser, therefore, recontouring the engine core cowl as well as the core nozzle is needed. The reduced diameters are due to the elimination of the exhaust reverser function. The reverser hardware, in particular the stationary deflectors and reverser actuators, requires a larger cowl diameter at the engine turbine rear frame. This requires the boattail angle in the core nozzle region to be approximately 12 degrees with the reverser rather than the 15 degrees, which is possible with the deflector structure removed. The reduced diameter cowl and shorter nozzle, therefore, reduce weight, core pressure loss and scrubbing drag. This drag and pressure loss reduction along with a recontoured lower pylon fairing was estimated to result in a significant sfc reduction during cruise. A weight reduction of 45 kg (100 lbs) over the Long Fixed Core Nozzle, and 147 kg (325 lb) over the Core Reverser Nozzle would be achieved with the Short Core Nozzle.

An assessment of Short Core Nozzle performance improvement was obtained from isolated nacelle model tests at FluidDyne in March 1978. The model test included evaluation of both the Long Fixed Core Nozzle and the Short Core Nozzle to obtain a direct measure of the improvement with the Short Core Nozzle. The gross thrust coefficients for these nozzles are presented in Figure 4 for the static testing and in Figure 5 for the external flow wind tunnel testing. It can be seen from Figure 4 that the static test demonstrated improvements in gross thrust coefficient with the Short Core Nozzle of 0.0036 and 0.0037 at maximum cruise power and normal cruise power pressure ratios, respectively. At lower nozzle pressure ratios, there is more scatter in the test data and the improvement is approximately 0.0035 in gross thrust coefficient. From Figure 5, it can be seen that the improvement with the short nozzle is 0.0039 in gross thrust coefficient at M 0.82 cruise. The insert in Figure 5 shows that this improvement is approximately 1% net thrust (~1% sfc) at 40,000 N (9,000 lb) of net thrust and 10,668 m (35,000 ft) altitude. This improvement in cruise thrust coefficient is exactly the



Core Reverser Nozzle



Long Fixed Core Nozzle

Figure 1. Current CF6-50 Core Nozzles.

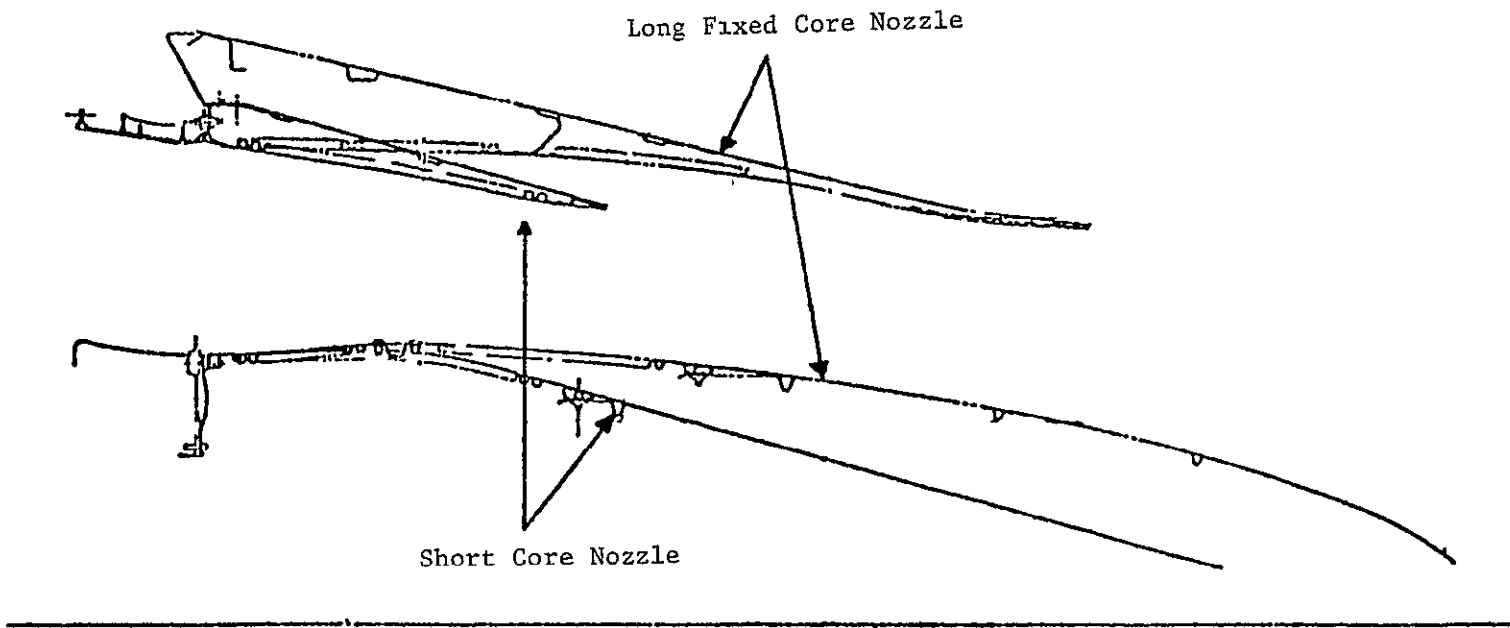
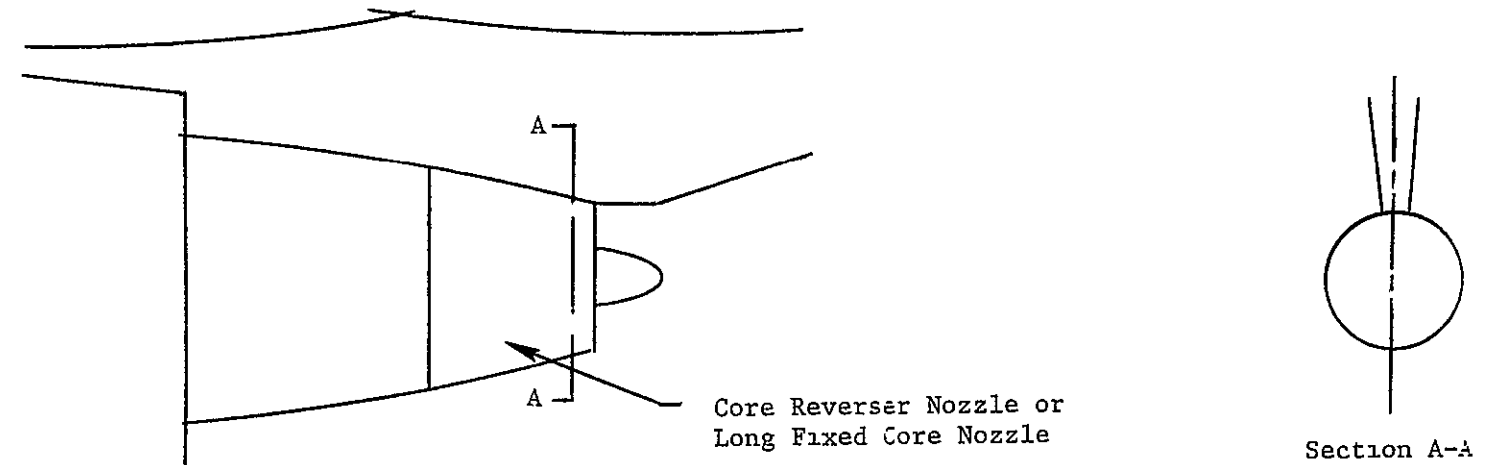
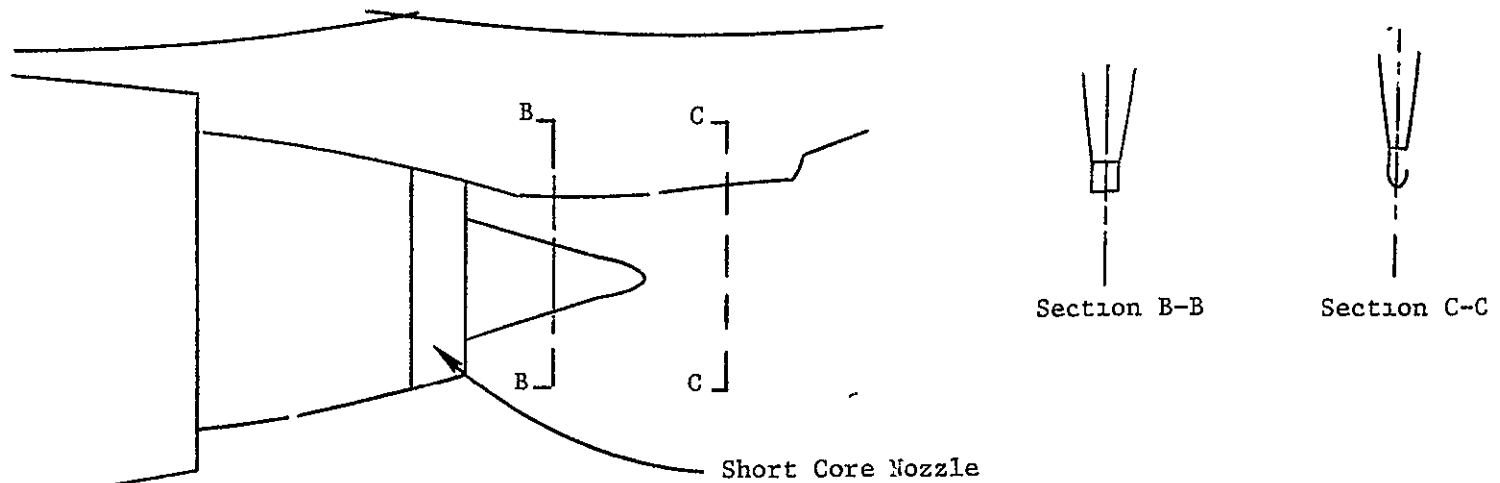


Figure 2 Comparison of Short Core Nozzle to Long Fixed Core Nozzle



a) Production DC-10-30 Nacelle and Pylon - CF6-50 Engine with Core Reverser Nozzle or Long Fixed Core Nozzle.



b) Modified Nacelle and Pylon Fairing - CF6-50 Engine with Short Core Nozzle.

Figure 3. CF6-50 Nacelle-Pylon-Core Nozzle Comparison.

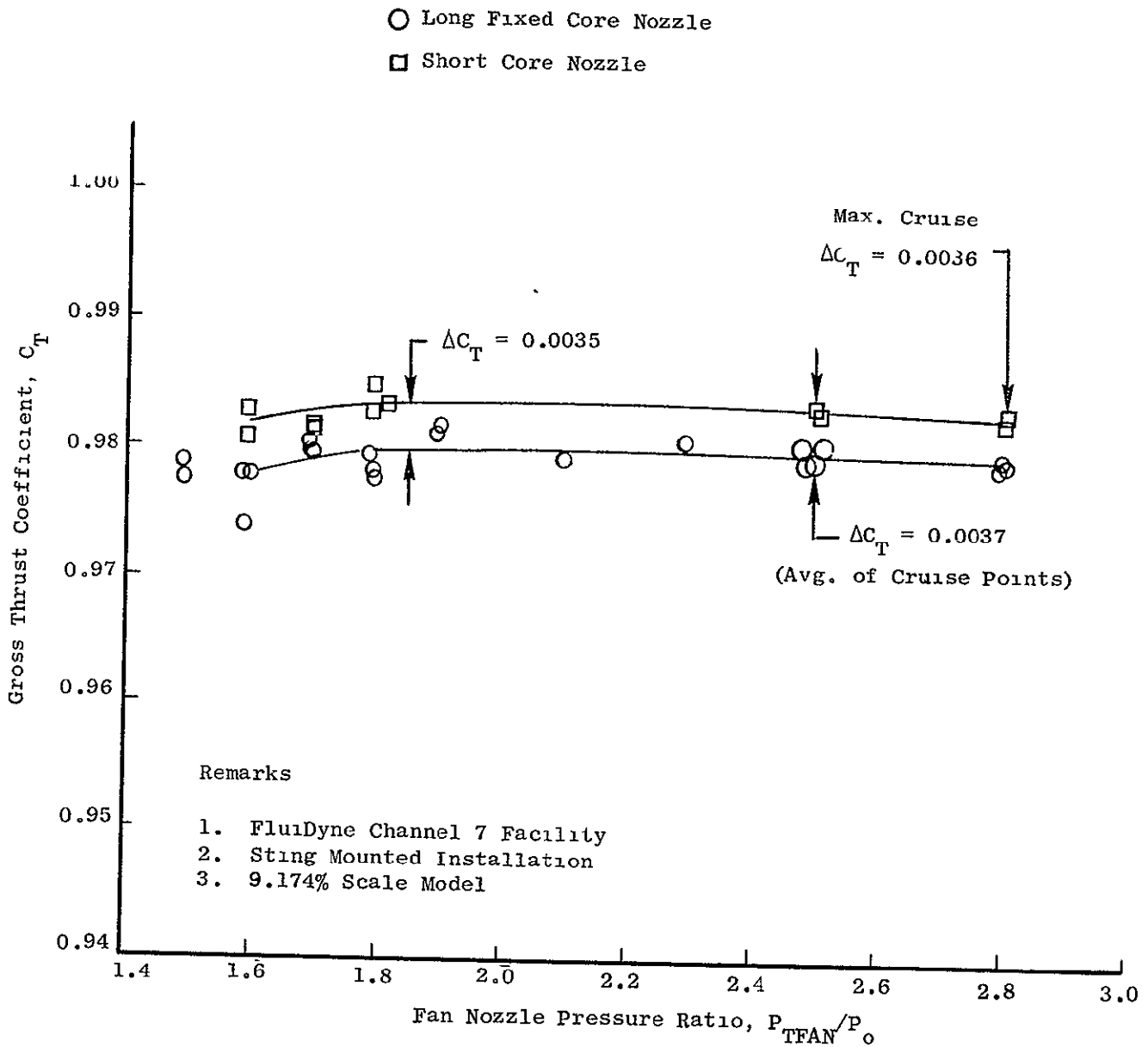


Figure 4. CF6-50 DC-10 FluiDyne Test Results, Static Test Data, Isolated Nacelle.

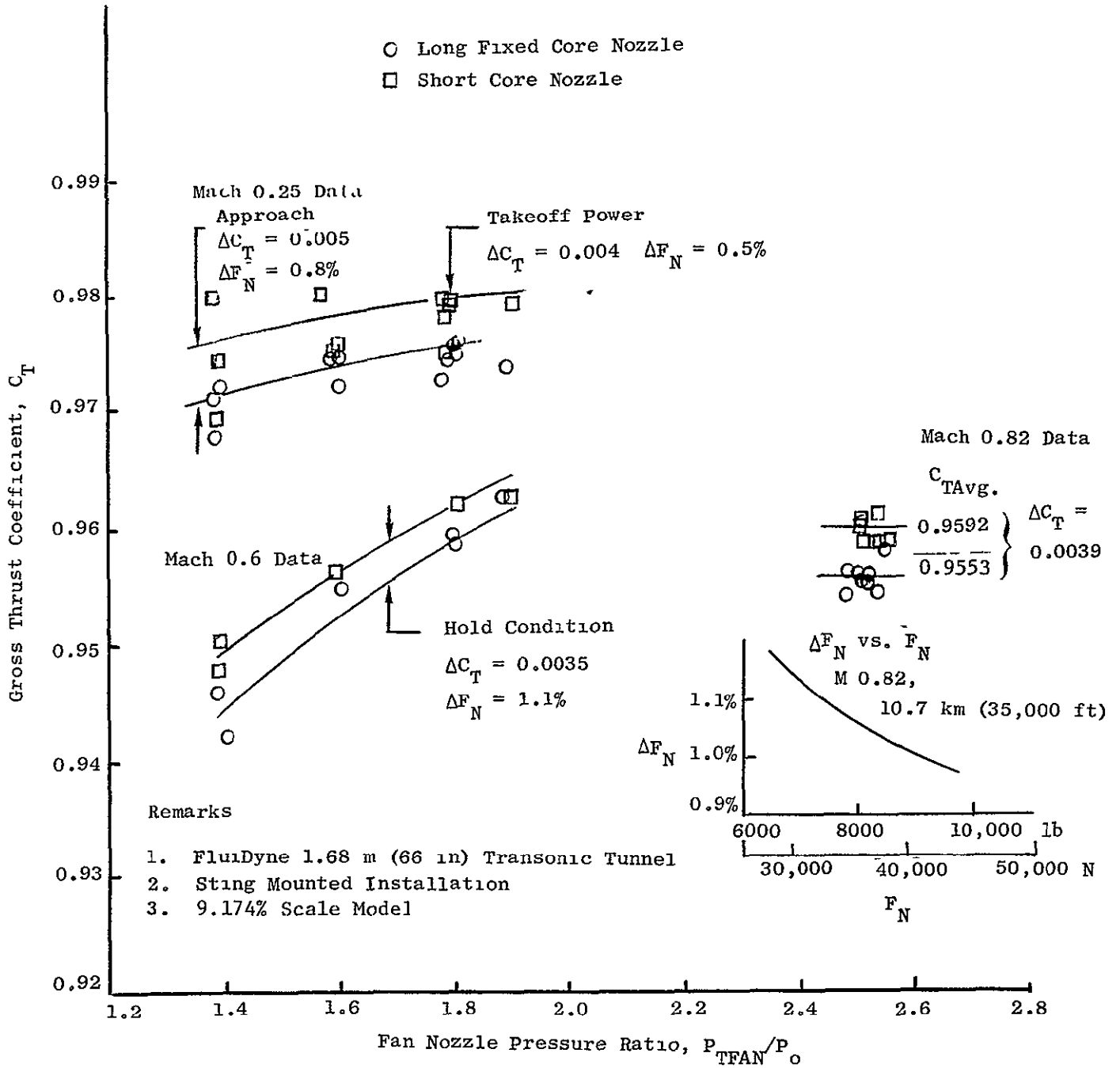


Figure 5. CF6-50 DC-10 FluiDyne Test Results, Wind Tunnel Test Data, Isolated Nacelle.

improvement that was obtained in the 1975 model test of an earlier version of the Short Core Nozzle. At lower Mach numbers (Mach 0.6 and 0.25 on Figure 5), there is more data scatter but the Short Core Nozzle shows an improvement at all conditions

Installation of the Short Core Nozzle is readily adaptable to all CF6-50 series engines on the A300, DC-10-30, and 747 airplanes. Utilization of the Short Core Nozzle requires a different core cowl and lower pylon fairing.

## 4 0 DESIGN AND FABRICATION

### 4.1 OVERALL DESIGN APPROACH

The Short Core Nozzle is functionally similar to the CF6-50 Long Fixed Core Nozzle. In designing the Short Core Nozzle, core cowl and core nozzle contours were established which result in reduced scrubbing area and, therefore, drag. The cowl diameter aft of the fan reverser and core nozzle length and diameter were reduced. The effect is that the boattail (divergence) angle aft of the fan was increased from 12 to 15 degrees providing the drag improvement. The nozzle is converging-diverging with an area ratio of 1.035.

The Short Core Nozzle requires a minimum of modification to the engine. No changes in the fan reverser are made. Bolting flanges for the Short Core Nozzle, the Core Reverser Nozzle, and the Long Fixed Core Nozzle are common. However, since the core cowl diameter over the turbine rear frame is reduced, the envelope available for the supply and scavenge tubing in the vicinity of the turbine rear frame is also reduced. These tubes were formed to more closely follow the turbine rear frame contour than was previously the case. Also, the core cowl hinge line on the pylon and pylon apron required modification to accommodate the new flow lines. Since the Short Core Nozzle does not translate as does the Core Reverser Nozzle, it no longer is necessary to provide a horizontal split line at the fairing juncture with the pylon. Therefore, it is advantageous to support the total fairing directly from the pylon rather than splitting the fairing and carrying half on the nozzle and half on the pylon.

### 4 2 DESIGN DESCRIPTION

The Short Core Nozzle is depicted in Figure 6. The design includes an outer cowl with an integral core cowl support ring, exhaust nozzle liner, forward centerbody, aft centerbody, replaceable core cowl wear pads, baffle, and associated mounting hardware. There are no provisions for pylon fairings or pylon fairing attachment structure, these fairings are part of the air-frame pylon structure.

The material used in this lightweight, high temperature structure is Inco 625 for the sheet metal and stiffeners and the rolled and welded flanges. Wear surfaces are provided by plasma spraying of a wear-resistant coating, tungsten carbide. Bolting hardware is Inco 718 due to the high temperature locations and the frequent removal/reassembly operations.

Both the inner and outer nozzle sections and the centerbodies are full 360 degree bodies of revolution. The sheet metal components are butt-welded together, and reinforcing "hats" and doublers are attached by brazing.



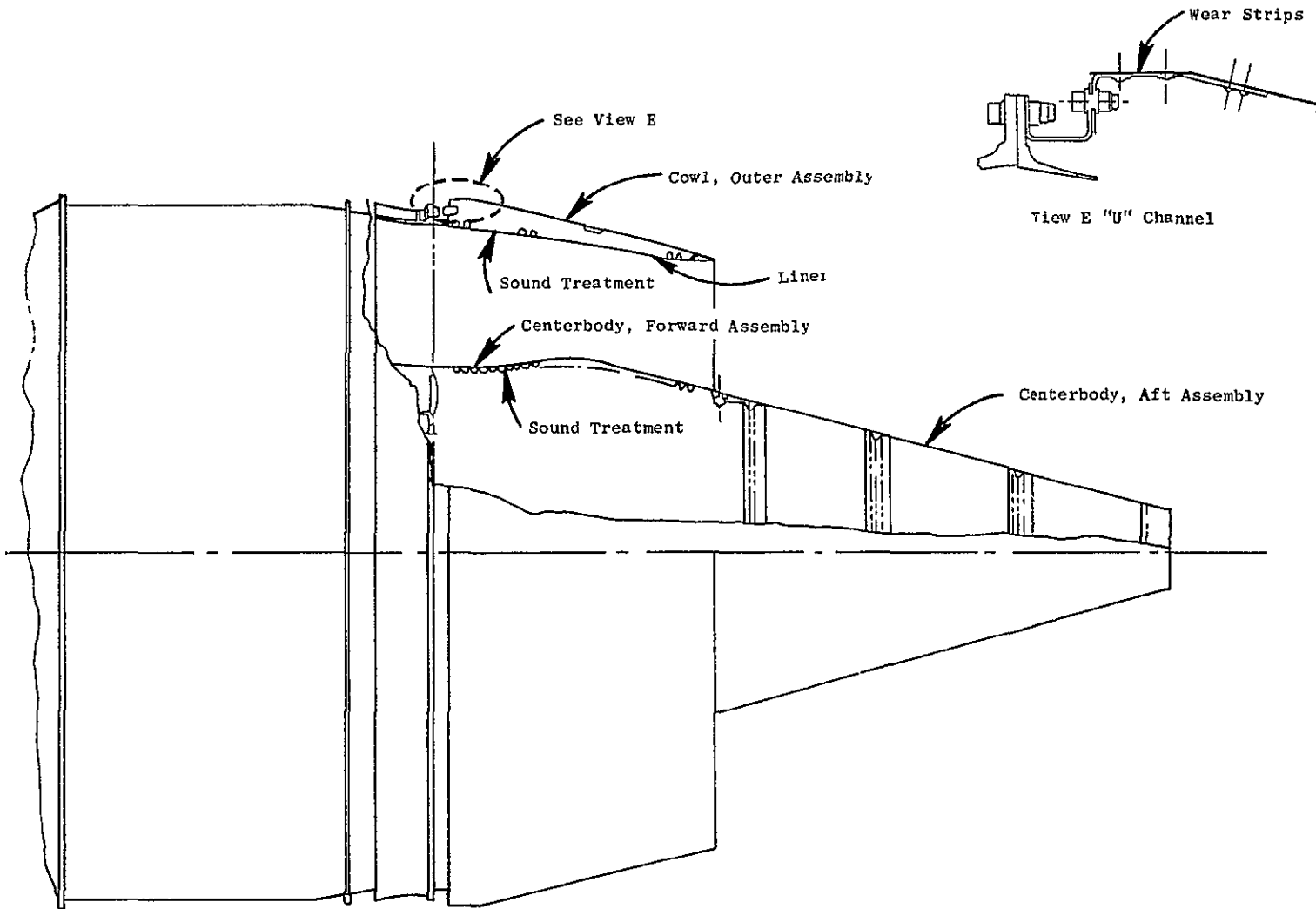


Figure 6. CF6-50 Short Core Nozzle.

The sound treatment design is the same type as that used on the Core Reverser Nozzle, i.e., the corrugated "top hat" type treatment. In this design, the face sheets are perforated with 1.6 mm (0.063 in.) diameter holes on a 60 degree staggered pattern to obtain the required  $9\% \pm 2\%$  open area. To provide acoustic chambers, 0.19 mm (0.0075 in.) Inco 625 sheet metal is formed into circumferential corrugates to a height of approximately 9.5 mm (0.375 in.) dependent upon the tuning required and brazed to the nonflowpath side of the face sheet. Full height 9.5 mm (0.375 in.) sheet metal partitions placed at every 76 mm (3 in.) of circumference in the corrugate serve to reduce any rotational wave propagation. Drain holes are provided in each corrugate at bottom vertical to prevent accumulation of unburned fuel during "hot" starts. In the concept utilized, there are approximately  $1.44 \text{ m}^2$  (15.5  $\text{ft}^2$ ) of sound treatment area in the outer liner and  $0.88 \text{ m}^2$  (9.5  $\text{ft}^2$ ) in the centerbody for a total of  $2.32 \text{ m}^2$  (25.0  $\text{ft}^2$ ) which is comparable to that for the current exhaust system.

#### 4.3 CORE COWL AND PYLON DESIGN

Douglas Aircraft Company designed the core cowl and pylon modifications. The nacelle modification, exclusive of the pylon, involves the area aft of the fan reverser. New, steeper external loft lines for the core cowl and core nozzle necessitated a change to the core cowl attachment to the pylon. The present center and aft core cowl hinges were redesigned to a lower location so as not to protrude into the airstream. The pylon apron which seals the interface between the core cowl and the pylon was redesigned to relocate it to follow the new loft line. The aft pylon fairing was redesigned to match the new short nozzle contour and the aerodynamic lines developed for this shorter exhaust system.

Stress analyses were conducted to establish material gages for strength requirements. Material selections utilizing aluminum, steel, and titanium were made to minimize cost and weight consistent with the temperature environment. Detailed design drawings were made for fabrication of the hardware.

Three sets of prototype core cowl doors were furnished by General Electric for engine test and the flight test program on the Airbus A300B. The Douglas flight test program was conducted with Douglas production cowling. These flight test programs are described in Section 4.6.

Installation/rework drawings were made for all the new components so that the production airplanes used for flight testing could be readily configured for test and reworked back to the original production quality for later delivery to the airplane customer.

#### 4.4 MAINTAINABILITY

Compared to the Core Reverser Nozzle, maintainability is improved, because with the Short Core Nozzle, there are no actuating components, and, therefore, rigging after assembly is not required. No parts have to be free to translate, thus eliminating fretting and wear.

With regard to the Long Fixed Core Nozzle, however, there is no major change in maintainability with the Short Core Nozzle. Reducing the weight of the outer cowl of the nozzle is expected to simplify handling of that component. The cowl door support land on the Short Core Nozzle has replaceable wear strips whereas the Long Fixed Nozzle core cowl support has wear coating plasma sprayed directly on the support cone land and is more difficult to refurbish.

Access to the core cowl compartment is achieved in the same manner as before, through opening the core cowl doors. The nozzle is a true body of revolution, and there are no pylon fairings mounted to it. The pylon fairings attached to the pylon are not provided with "skirt" extensions, and there is no contact between the cowl surface and the pylon-mounted fairing.

The bolting hardware attaching the outer cowl and the forward and aft centerbodies is made of Inco 718 with silver-plated Waspalloy nuts to accommodate the high temperatures. The outer cowl has lifting brackets attached to facilitate handling.

The sheet metal and flange material used in the nozzle is Inco 625 which is readily repair welded and requires no subsequent heat treatment to re-establish its properties. The thickness of the aft centerbody and the sound treatment face sheet has been increased from 0.36 mm (0.014 in.) and 0.46 mm (0.018 in.), respectively, to 0.63 mm (0.025 in.) in order to lessen handling damage.

#### 4.5 RELIABILITY

Compared to the Core Reverser Nozzle, the reliability of the exhaust system is greatly improved because of the elimination of the translation mode. All actuation and position sensors utilized in the turbine reverser were removed.

The Short Core Nozzle was designed to achieve a total useful life, with repair, of at least 35,000 projected flight cycles or 50,000 aircraft operating hours, whichever occurs first. It was designed to operate for the power settings and within the flight envelope defined in the Engine Model Specification.

Maneuver limit load factors for flight and landing, including landing impact, have been established. Loads were established consistent with methods used on the Long Fixed Core Nozzle for combining translation accelerations, angular velocities, and thrust or drag. The additional constraint of engine operation with higher inertia loadings due to a fan blade-out was also met.

The temperatures and pressures to be encountered in the nozzle were taken from the GF6-50 cycle deck. The applicable General Electric Design Practices were utilized in the design process.

#### 4.6 SAFETY

A detailed stress analysis of the individual components utilizing the maneuver, pressure and thermal inputs has been completed and documented. All flight envelope cases analyzed gave a positive margin of safety. FAA Air-Worthiness Standards Aircraft Engines Part 33 Revised 10/31/74 and FAA Advisory Circular AC33-1B guided the design.

The construction features and materials utilized are quite similar to the well-proved Long Fixed Core and Core Reverser Nozzles.

In order to substantiate both reliability and safety, a series of engine tests was run. The endurance test described in Section 7.0 is one such test. Other tests included the following

<u>Type of Test</u>	<u>Exposure</u>
Ground Test	88 simulated flight cycles
Airbus Industrie A300B Flight Test	19 flights accumulating 47 hours and 30 minutes on each nozzle plus a total of 10 hours and 18 minutes of ground running
Douglas Aircraft Co DC-10 Flight Test	382 hours and 15 minutes of flight testing including 415 total engine cycles cumulative on all nozzles flown

For the ground test, the Short Core Nozzle was instrumented with accelerometers on both the nozzle and centerbody to establish response frequencies from ground idle to takeoff power. Good agreement with calculated data was obtained and accelerations were well within capability.

This nozzle was then used in the Airbus Industrie A300B flight test program. A total of 21 pressure taps installed on the outer cowl was monitored during flight testing to establish pressure distributions on the cowl.

## 5.0 PERFORMANCE TEST

### 5.1 TEST CONFIGURATIONS

The test vehicle was the CF6-50 engine. Figure 7 shows the Long Fixed Core Nozzle configuration including the pylon fairing simulating the wing position on the airplane. Figure 8 shows the Short Core Nozzle configuration with the Short Core Nozzle Core cowl doors. The Long Fixed Core Nozzle test hardware consisted of:

- Fan Reverser
- Core Cowl Doors
- Long Fixed Core Nozzle
  - Outer Cowl
  - Forward Centerbody
  - Aft Centerbody
- Nozzle Fairing

Changes made to install the Short Core Nozzle were:

- Core Cowl Doors
- Short Core Nozzle
  - Outer Cowl
  - Forward Centerbody
  - Aft Centerbody

A flight-type engine cowling, a test inlet bellmouth for measurement of inlet airflow and an inlet screen for foreign object damage protection were used for the test.

### 5.2 TEST FACILITY

Figure 9 is a schematic of engine test cell 7 in Building 500 of General Electric's Evendale Plant. It is a large turbofan or turbojet test facility with inlet air heaters capable of up to 66° C (150° F) at 907 kg/sec (2000 lb/sec) airflow. The cell exhausts are water-cooled with sound-controlled vertical intakes and discharges. Overhead thrust frames can handle thrust loads up to 445,000 N (100,000 lbs). All cells are equipped for automatic data handling, including transient recording up to 400 analog channels at speeds ranging from 200 to 10,000 channels per second. Printed data are available within 2 minutes after initiation of a reading.



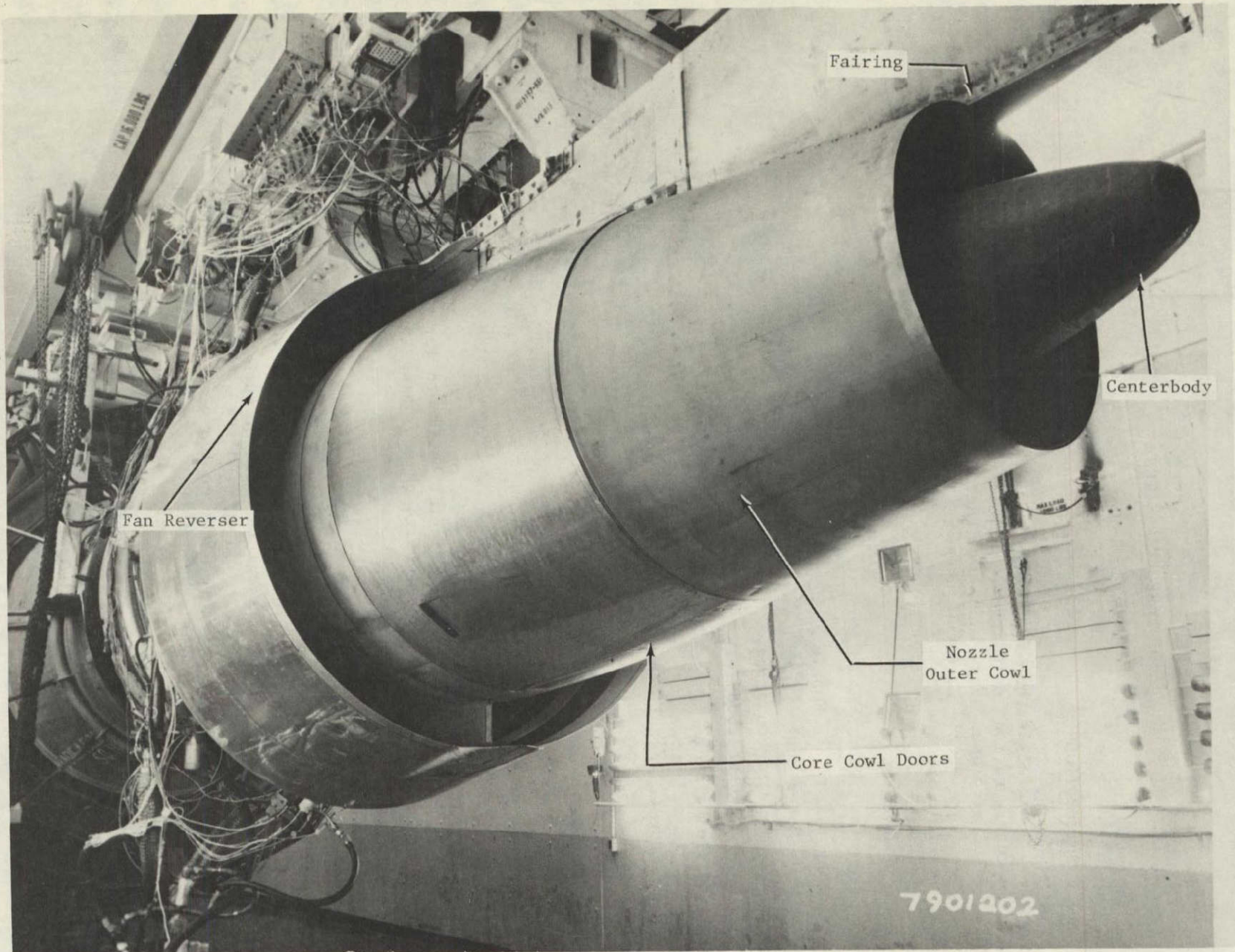


Figure 7. Long Fixed Core Nozzle.



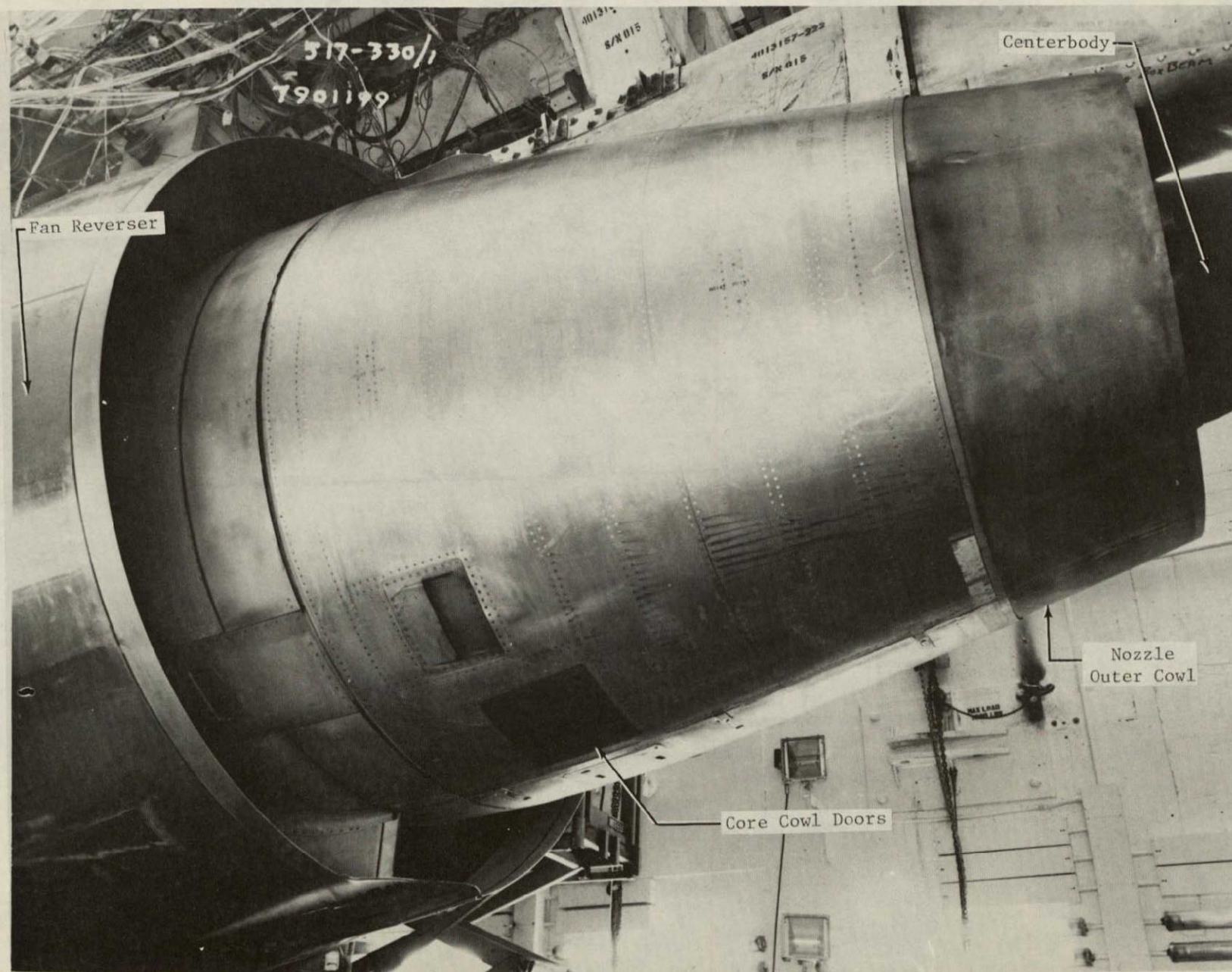


Figure 8. Short Core Nozzle.



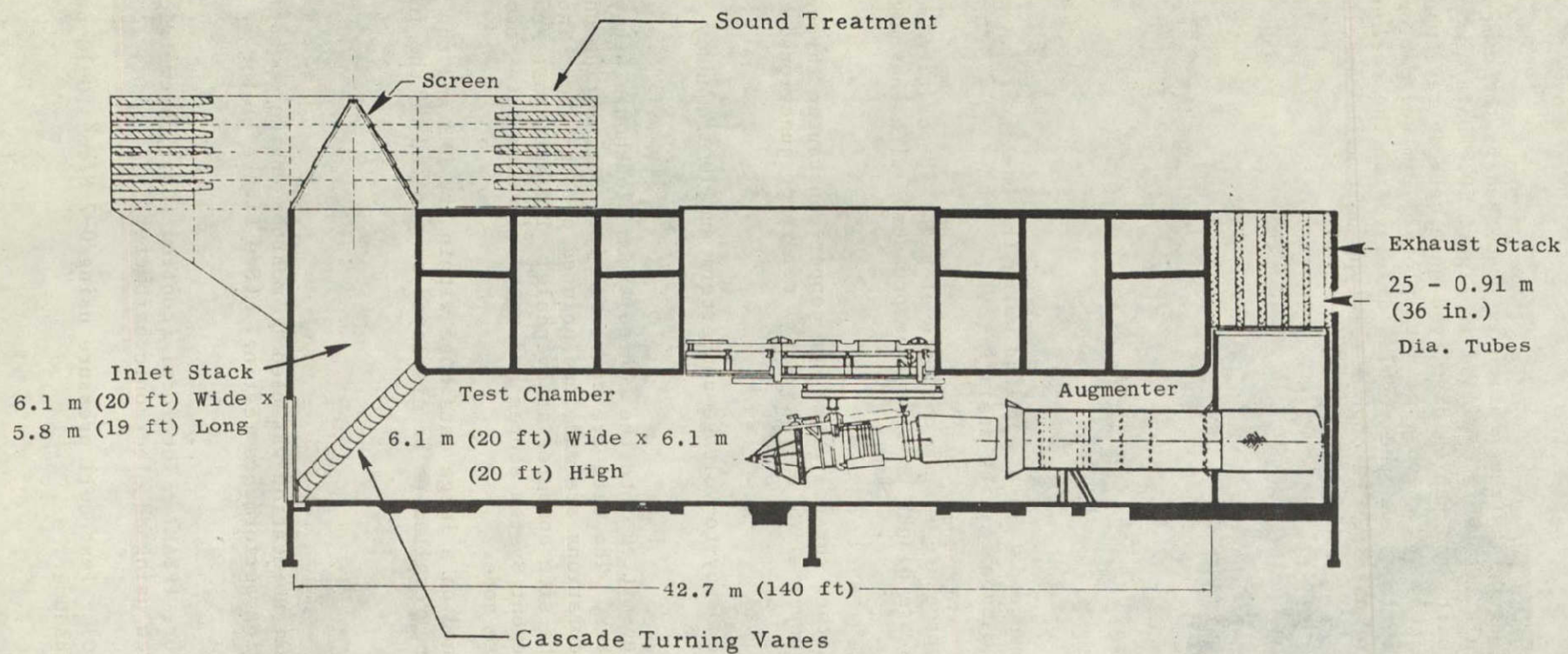


Figure 9. Cell 7, Building 500.



Engine control and safety instrumentation is processed by the computerized control console. This system is depicted in Figure 10. Data are converted into engineering units and can be displayed on a cathode ray tube (CRT) by addressable call-up pages, bar graphs, or data plots. Limited performance calculations can be accomplished and the results displayed on the call-up pages. Hard copy data are obtained through a teletype unit with capacities as follows:

- Pressure - 39 channels
- Potentiometer Position - 6
- Frequency - 9
- Thrust - 1 channel
- Thermocouple - 43
- Vibration - 8

Steady state performance data are acquired using the on-site Data Management System (DMS). System capabilities are:

345 Pressures - The pressure system consists of eight 48-position scanner valves. Thirty positions are blanks or reference pressures with the number varying by scanner valve.

400 Temperatures - Either chromel-alumel or copper-constantan through the use of CATS blocks (copper alloy thermal sink) reference junctions at the engine facility interface.

There are also 10 frequency-to-voltage converters and 10 frequency counters.

Once the data are transmitted into the control room blockhouse, they are input into the cell computer. The data are converted into engineering units and basic performance calculations are made and printed out on-line. The data are transferred to the site computer at Evendale. The data base manager within the new Data Management System stores and retrieves each data item via its six character data base code.

All data are maintained on a large data base within the DMS and the central computer and can be recalled to be displayed or plotted on the interactive graphic terminals.

### 5.3 INSTRUMENTATION

The following test instrumentation was used to monitor engine operation and engine performance during performance testing. (See Figure 11 for station designation.)

- Barometric Pressure (PBAR) - The local (control room) barometric pressure was taken using an electronic barometer.
- Cell Pressure (PO) - Test cell pressure using 0-7 N/cm<sup>2</sup> (0-10 psi) differential transducer.



ORIGINAL PAGE IS  
OF POOR QUALITY

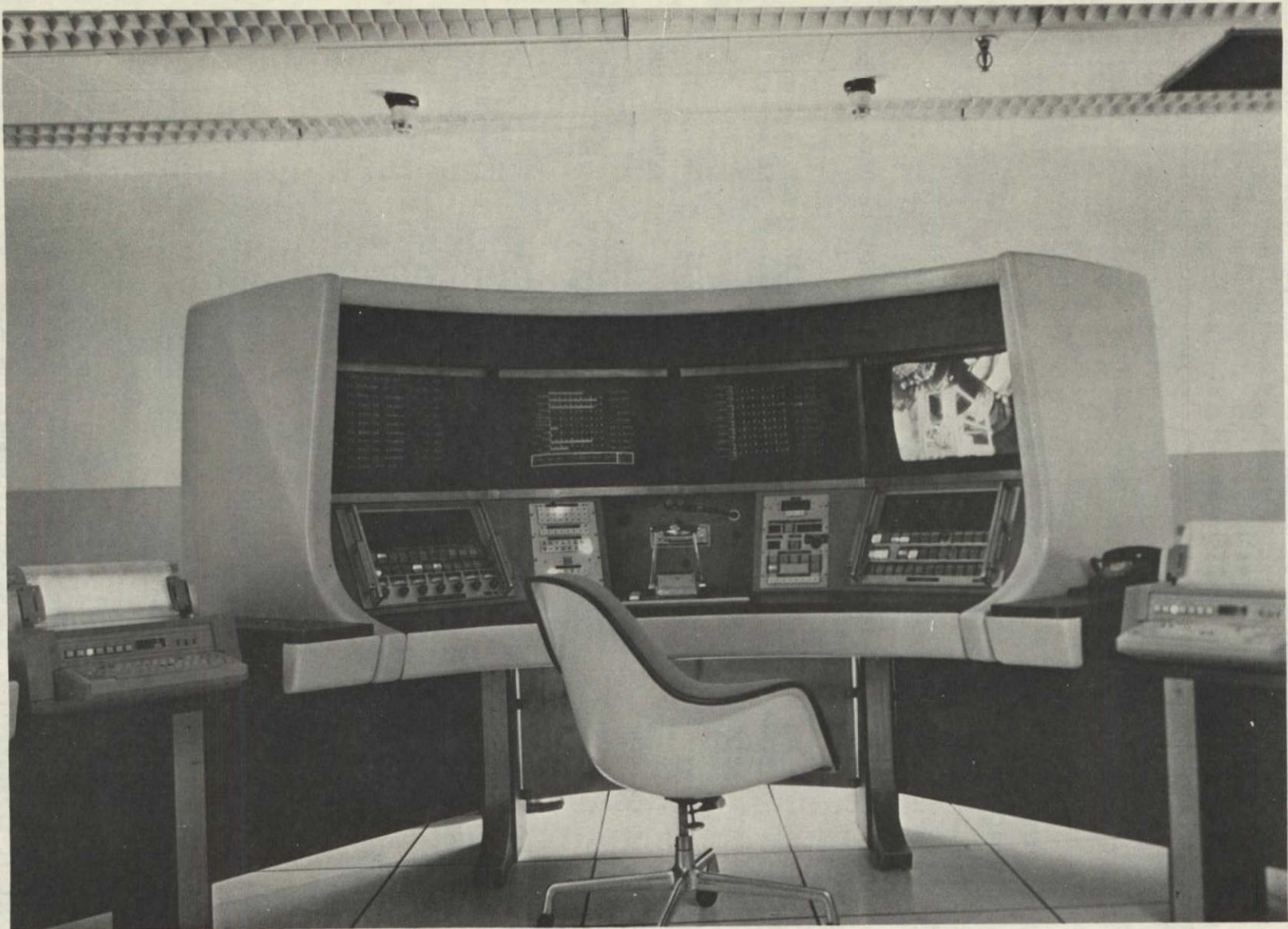


Figure 10. A Computerized Control Console.

- Humidity (HUM) - The absolute humidity in grains of moisture per pound of dry air was recorded using a wet/dry bulb sling psychrometer
- Inlet Total Pressure (PT2) - Four 6-element total pressure rakes located in the engine inlet at the fan face and measured with 0-7 N/cm<sup>2</sup> (0-10 psi) differential transducers and pressure scanning valves were used. The circumferential locations of these rakes measured from the engine top vertical centerline were 45, 135, 225, and 315 degrees
- Inlet Static Pressure (PS2) - Four 6-element rakes identical to the total pressure rakes were used
- Compressor Inlet Static Pressure (PS25) - One static pressure tap located on the outer wall of the fan frame core flowpath was recorded. Measurements were made using a 0-10 N/cm<sup>2</sup> (0-15 psi) differential transducer and pressure scanning valve.
- Compressor Inlet Temperature (TM25) - One ungrounded copper constantan thermocouple, replacing one of the mounting bolts for the CIT sensor, was utilized.
- Compressor Discharge Temperature (TT3) - One ungrounded chromel-alumel probe mounted in the condition monitoring port of the compressor rear frame was utilized.
- Compressor Discharge Static Pressure (PS3) - A wall static pressure tap was located in a combustor borescope port and measured on a 0-345 N/cm<sup>2</sup> (0 to 500 psi) absolute transducer.
- Low Pressure Turbine Inlet Total Pressure (PT49) - Five 4-element probes were manifolded by probe and measured on a 0-103 N/cm<sup>2</sup> (0 to 150 psi) absolute transducer.
- Exhaust Gas Temperature (T49) - The low pressure turbine inlet temperature indicating system consisted of 11 dual-immersion chromel-alumel thermocouples electrically averaged. The system was composed of four harnesses which were joined together by means of an aft lead which, in turn, connected to a forward lead. The forward lead had another electrical connector for transmission of the signal to the EGT indicator
- Low Pressure Turbine Discharge Pressure (PT5) - Four 5-element rakes were manifolded together and located in the turbine rear frame. PT5 was measured with a 0-10 N/cm<sup>2</sup> (0-15 psi) differential transducer and pressure scanning valves.
- Low Pressure Turbine Discharge Temperature (TT5) - Two 5-element rakes were located in the turbine rear frame. The signals were electrically averaged thermocouples.

- Fan Discharge Pressure (PT13) - Four strap-on rakes Two each with four elements and two each with three elements for a total of 70 pressures were read by each immersion and located on the strut in the fan frame. The measurement was made with a 0-10 N/cm<sup>2</sup> (0-15 psi) differential transducer and pressure scanning valve.
- Fan Speed (N1) - Low pressure rotor speed was measured using two fan speed sensors.
- Core Speed (N2) - High pressure rotor speed was measured using an engine core speed sensor driven off the end of the lube and scavenge pump.
- Main Fuel Flow (WFM) - Facility engine fuel flow was measured on a volumetric turbine flowmeter.
- Verification Fuel Flow (WFV) - Facility engine fuel flow was measured in series with WFM.
- Fuel Temperature (TF) - Facility engine fuel temperature was measured at the flowmeters using a copper-constantan thermocouple.
- Thrust (FGM) - 222,400 N (50,000 lb) three bridge load.

#### 5.4 TEST PROCEDURE

The Long Fixed Core Nozzle configuration was tested first. Normal pre-fire checks, idle leak check, and mechanical checkout were completed. The power calibrations conducted for the test consisted of 15 steady state speed settings from 2093 to 3980 rpm or 61 to 116% corrected speed. At each speed point, two readings were taken after a stabilization time of 3 minutes

The first power calibration was completed and the first six points were repeated before instrumentation problems with PT49 (low pressure turbine inlet pressure) and PS3 (borescope compressor discharge static pressure) occurred. Further attempts to complete the second power calibration resulted in failure due to icing on the inlet airflow rakes. Bad weather forecasted for the next three or four days was the deciding factor in the decision to use the inclement weather period to install the Short Core Nozzle configuration. The six top points of the second power calibration demonstrated good repeatability of the data and the total points completed were, therefore, considered adequate for representing the Long Fixed Core Nozzle characteristics

The Short Core Nozzle configuration was installed and the power calibration was completed twice with no further problems.

## 5.5 TEST RESULTS

At sea level test cell operating conditions, the performance indicator for the Short Core Nozzle improvement is primarily the difference in overall gross thrust coefficient. The thrust coefficient is defined as follows:

$$C_T = \frac{F_{GM}}{(F_{1Fan} + F_{1Core})}, \text{ where}$$

$F_{1Core}$  = Ideal core nozzle thrust based on core measured pressures and calculated core gas flow.

$F_{1Fan}$  = Ideal fan nozzle thrust based on fan duct measured pressures, inlet total airflow, and calculated core flow.

Two methods were used in calculating the overall gross thrust coefficient difference. The first method utilized the scale model data nozzle flow coefficient difference. The first method utilized the scale model data nozzle flow coefficients to determine core airflow and the second method utilized the low pressure turbine effective area to determine core airflow. The fan flow was obtained by subtracting the calculated core flow from the total flow determined from the inlet total pressure rakes.

Both methods indicated overall gross thrust coefficient improvements in the order of 0.0025 as shown in Figures 12 and 13. The first method is dependent on accurate physical area measurements of both Long Fixed and Short Core Nozzles and accurate flow coefficient characteristics both in shape and in absolute level from the model test data. Any slight characteristic change between model and full scale hardware is to be reflected as a Root Sum Square (RSS) error in the overall gross thrust coefficient ( $C_T$ ) calculation. Calculating the overall gross thrust coefficient with the second method eliminates the above-mentioned potential errors but transfers the potential RSS error to the repeatability of the test instrumentation since none of the hardware changes made influence the low pressure turbine effective area. Because of this, the second method can result in a more consistent gross thrust coefficient curve shape but contain the same amount of data scatter as in the first method. In this test, the second method did result in more consistent curve shape characteristics as indicated in Figure 13.

It can be noted from Figure 13 that the data show an unexplained shift in calculated fan nozzle flow coefficient. This indicates data inaccuracies and, to some extent, appears to validate the 0.3% improvement in overall gross thrust coefficient. However, thrust at fan speed, thrust at engine pressure ratio, and sfc at thrust show conclusive evidence of having demonstrated approximately 0.3% improvement in gross thrust with the Short Core Nozzle.

Figure 14 shows the low pressure turbine pressure ratio comparison between the Long Fixed and Short Core Nozzles. This figure indicates the relative effective core nozzle throat area for the two nozzles. Note the crossover point of the curve occurs at a low pressure turbine discharge to engine

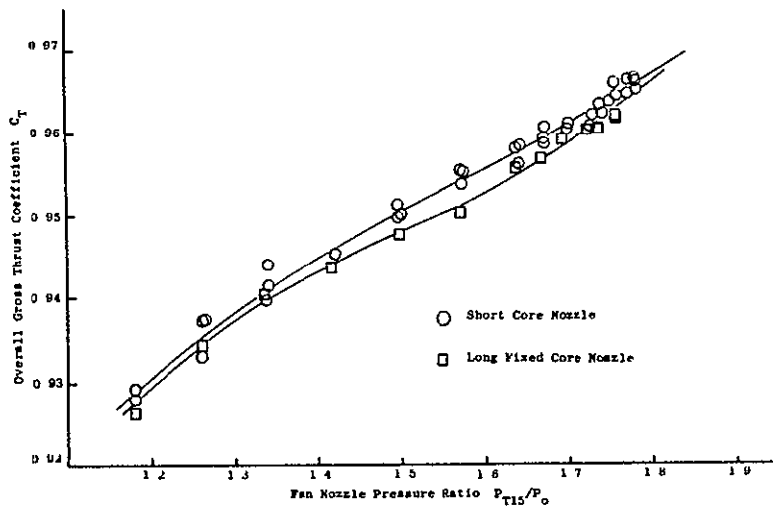


Figure 12. Test Cell Data, Overall Gross Thrust Coefficient, Core Flow Obtained Using Measured Areas and Flow Coefficients.

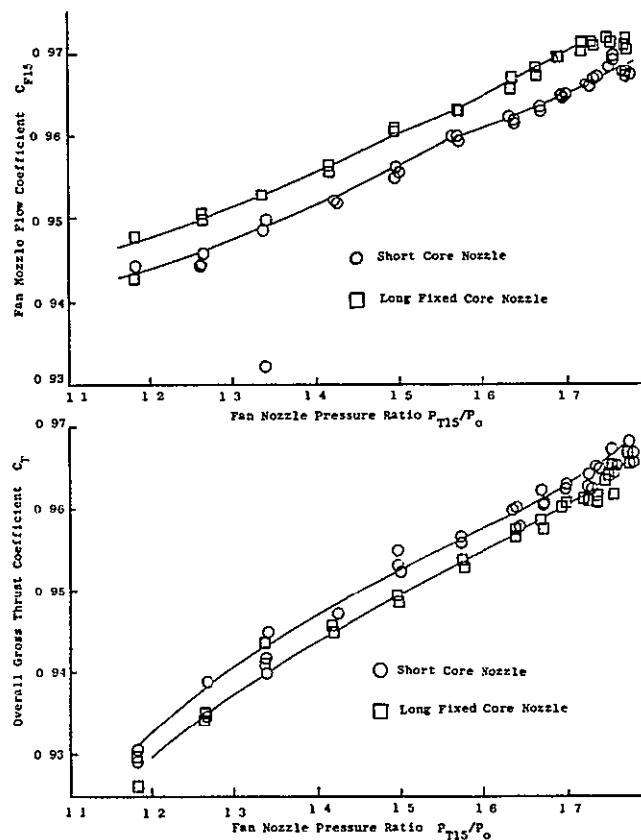


Figure 13. Test Cell Data, Fan Nozzle Flow Coefficient and Overall Gross Thrust Coefficient, Core Flow Obtained from Low Pressure Turbine Flow Function.

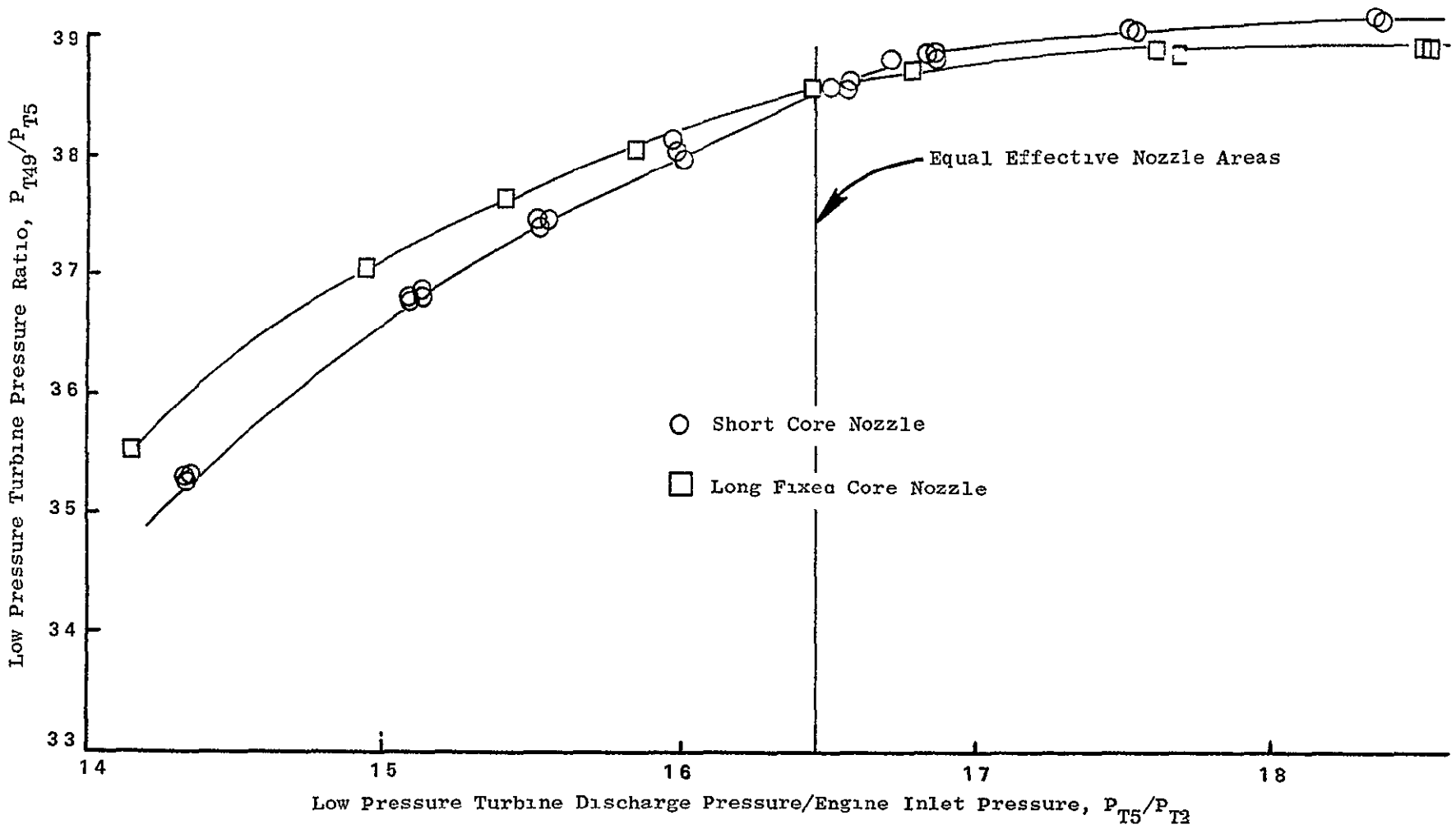


Figure 14. Test Cell Data - Low Pressure Turbine Pressure Ratio.

inlet pressure ratio of approximately 1.65. This corresponds to a thrust of approximately 226,860 N (51,000 lb). This region of equal effective throat areas (a condition of equal ideal thrust) should reflect the improvement due to the Short Core Nozzle in a measured thrust difference and also in an sfc improvement of equal magnitude. This improvement is shown in Figures 15a and b established from the test data which indicates that at a corrected fan speed corresponding to  $PT5/PT2 = 1.65$ , the Short Core Nozzle improvement is approximately 0.33% in thrust of 0.37% in sfc. The thermodynamics of the engine above and below this crossover point of equal effective nozzle areas is influenced by the fact that the core nozzle effective areas are different, thereby making it difficult to see the short core nozzle improvement in parameters other than overall gross thrust coefficient.

The test results from the standpoint of pretest predictions for sea level conditions are consistent with  $\Delta$  thrust versus fan speed,  $\Delta$  thrust versus engine pressure ratio, and  $\Delta$  sfc versus thrust curves shown in Figures 16, 17, and 18. The figures show differences based on the Long Fixed Core Nozzle test data since the cycle deck used reflects an average engine and not specific characteristics of the particular engine tested. Figure 19 indicates a small amount of adjustment is needed to the cycle to exactly match the effective area characteristic of the two nozzles. The cycle was modified to model the measured nozzle effective area characteristics and resulted in approximately the same overall performance improvement in corrected gross thrust at corrected fan speed, and sfc at corrected gross thrust as the model used for pretest predictions.

Power management changes for converting to the Short Core Nozzle are not necessary since the thrust at fan speed increases as shown in Figure 16. A small amount of exhaust gas temperature ( $\sim 3^\circ$  C) margin can be realized, however, if the improvement in thrust at corrected fan speed for the Short Core Nozzle is used to lower the power management.

The following summarizes the results of the performance test

1. The full scale engine back-to-back Long Fixed Core versus Short Core Nozzle testing indicates an improvement in overall thrust coefficient of approximately 0.3%. Test data, in the region of equal effective exhaust nozzle areas, show improvements in gross thrust at engine pressure ratio and at fan speed, and improvements in sfc at thrust for the Short Core Nozzle configuration. The close agreement between full scale and model test data at sea level verifies the 0.35% overall gross thrust improvement with the Short Core Nozzle as determined from scale model tests.
2. Based on the agreement of full scale with model test results at sea level, the model test results simulating altitude operation can be used for estimating "on-wing" Short Core Nozzle improvements.
3. The Short Core Nozzle does not require a power management change to meet minimum engine thrust at fan speed.



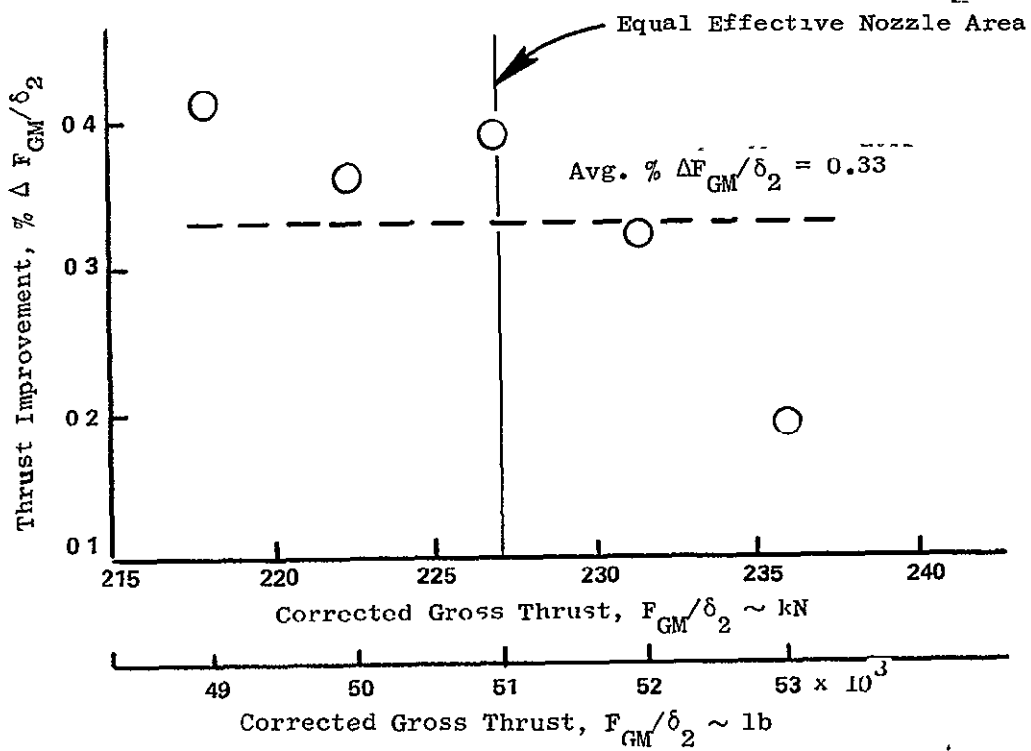


Figure 15a. Test Cell Data, Thrust Improvement with Short Core Nozzle.

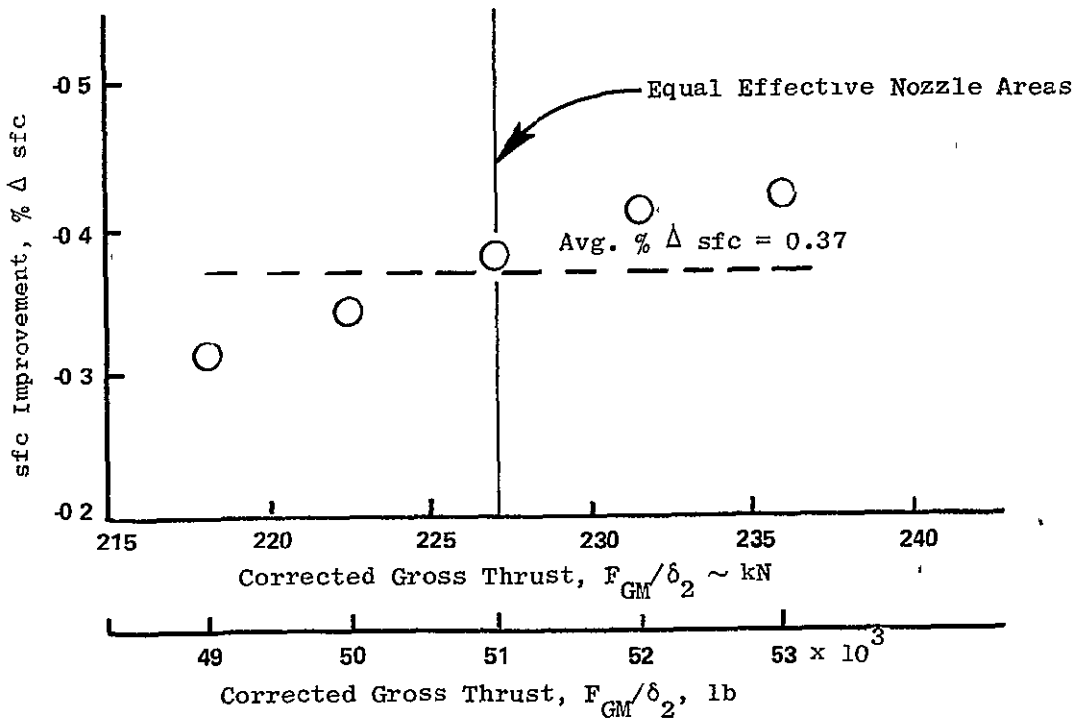


Figure 15b. Test Cell Data, SFC Improvement with Short Core Nozzle.

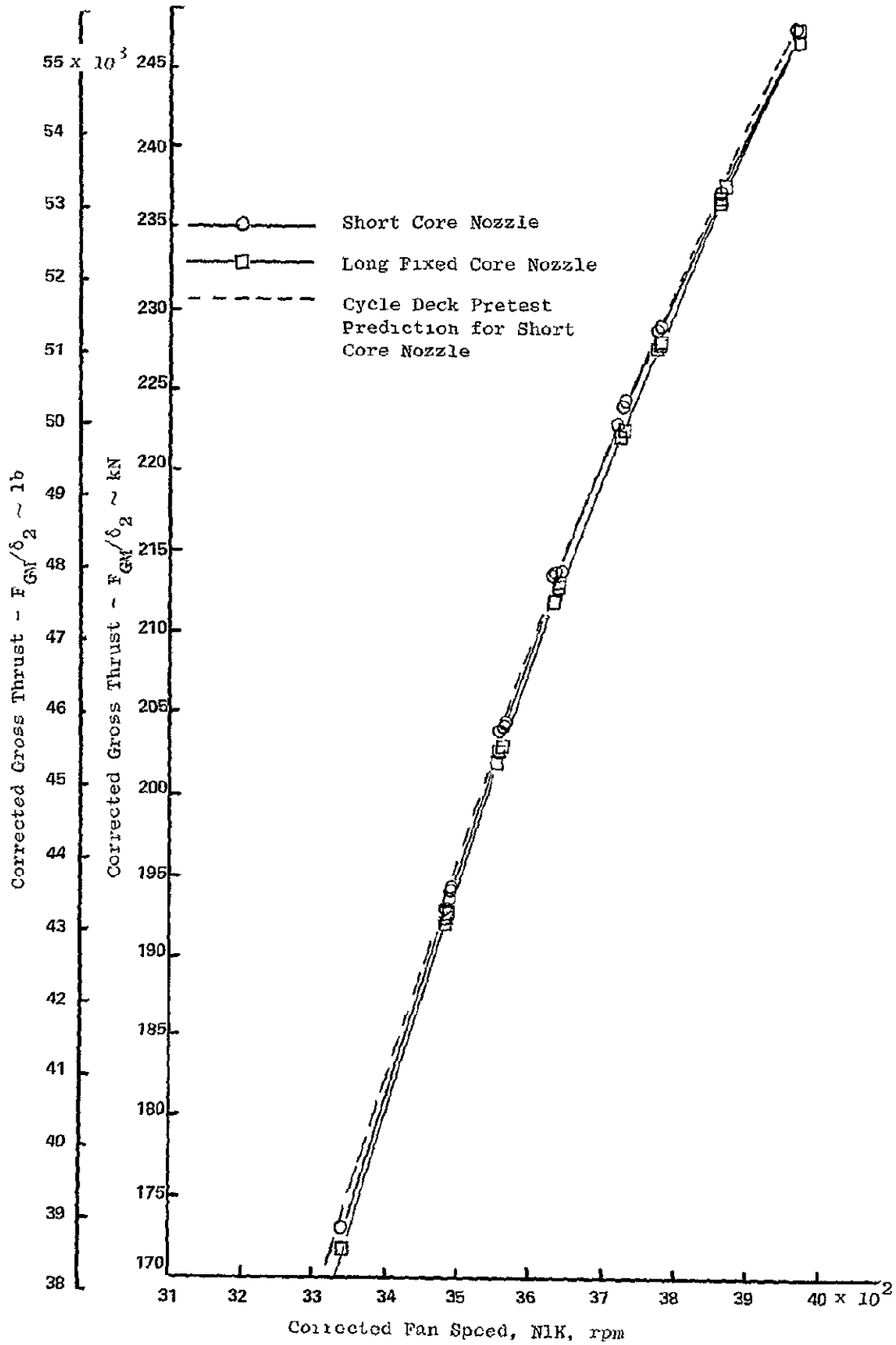


Figure 16. Test Cell Data, Corrected Gross Thrust vs. Corrected Fan Speed.

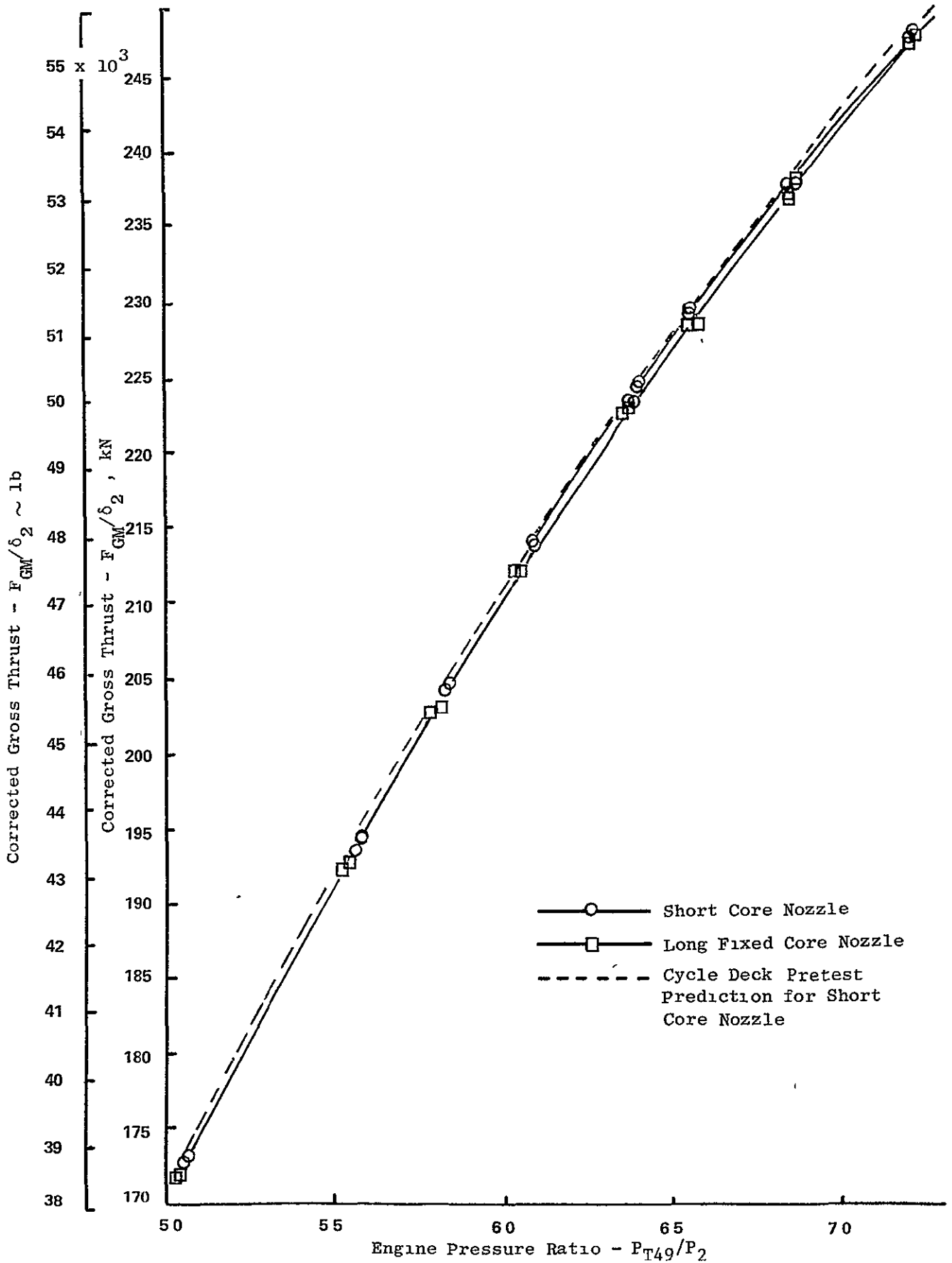


Figure 17. Test Cell Data, Corrected Gross Thrust vs. Engine Pressure Ratio.

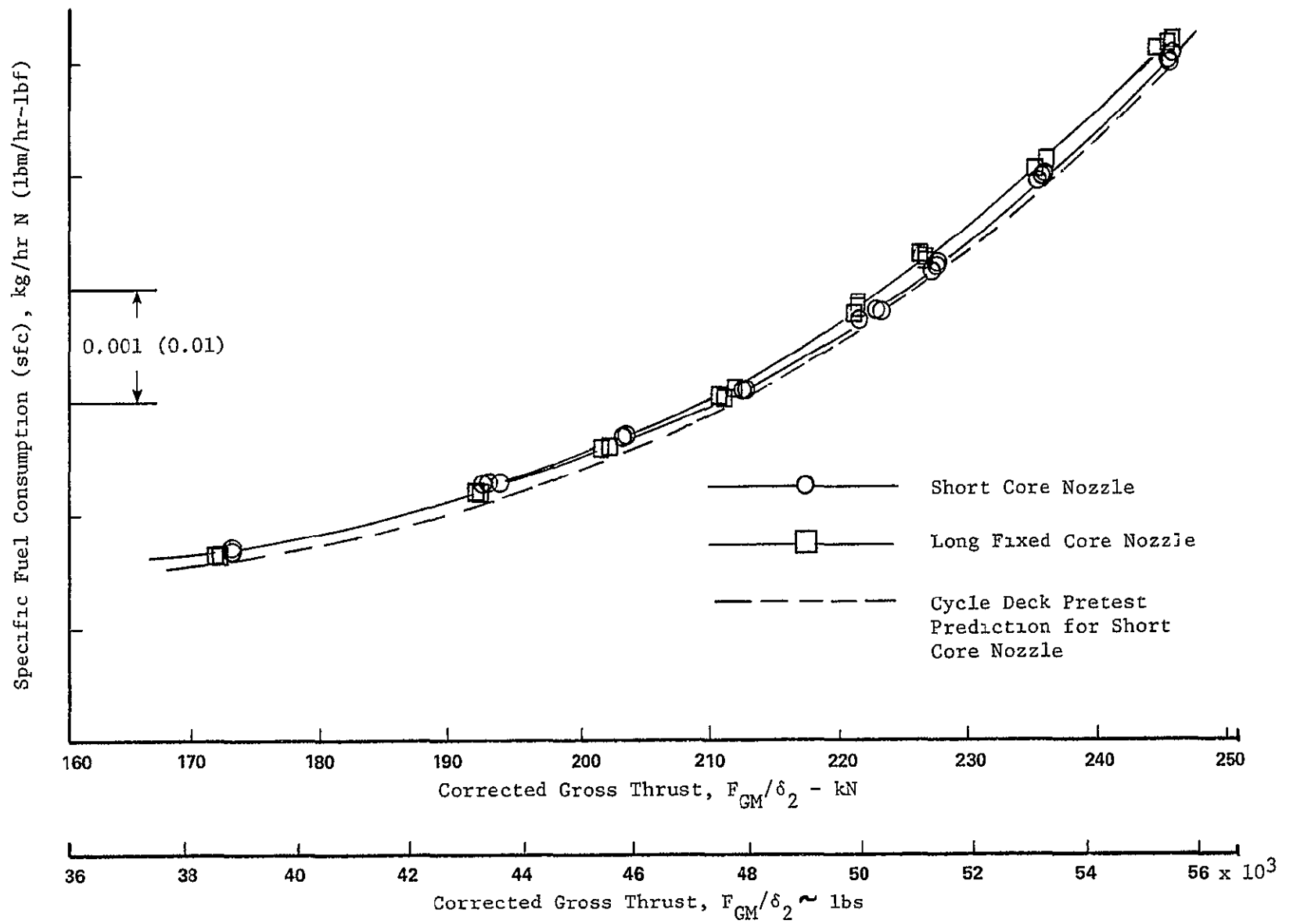


Figure 18. Test Cell Data, Specific Fuel Consumption vs. Corrected Gross Thrust.

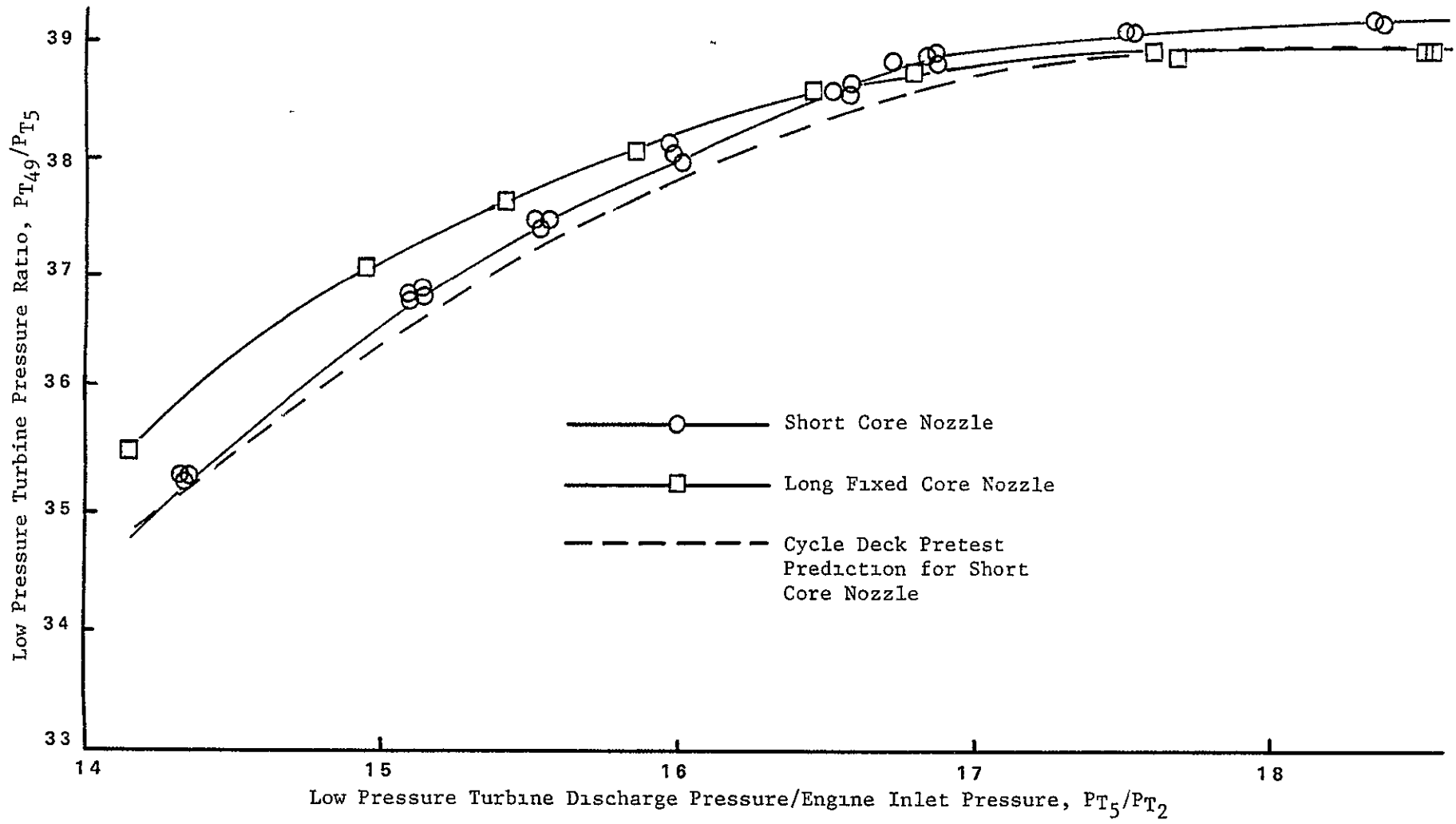


Figure 19. Test Cell Data, Low Pressure Turbine Pressure Ratios.

## 6.0 ACOUSTIC TEST

### 6.1 TEST CONFIGURATIONS

A series of static back-to-back noise tests was conducted on a CF6-50 engine with the Short Core Nozzle and the Core Reverser Nozzle.

The production CF6-50 engine was fitted with a reference acoustic inlet and bellmouth lip and production fan and core exhaust duct acoustic treatment. A description of the acoustic treatment is shown in Table I below:

Table I. Acoustic Treatment.

Location	Treatment Type	Treatment Area
Fan Inlet	Single Degree of Freedom (SDOF)	5.57 m <sup>2</sup> (60 ft <sup>2</sup> )
Fan Casing	Multiple Degree of Freedom (MDOF)	5.85 m <sup>2</sup> (63 ft <sup>2</sup> )
Fan Exhaust Duct	Single Degree of Freedom (SDOF)	4.65 m <sup>2</sup> (50 ft <sup>2</sup> )
	Multiple Degree of Freedom (MDOF)	4.37 m <sup>2</sup> (47 ft <sup>2</sup> )
Short Core Nozzle	"Tophat" (SDOF)	2.32 m <sup>2</sup> (25 ft <sup>2</sup> )
Core Reverser Nozzle	"Tophat" (SDOF)	1.95 m <sup>2</sup> (21 ft <sup>2</sup> )


The engine was configured with the advanced fan blades and a smooth micro-balloon shroud with a fan tip clearance of 1.9 mm (0.075 in.).


All performance rakes were excluded from the fan inlet, fan exhaust, and core exhaust ducts for these tests. A comparison of the flow lines and the acoustic treatment between the Core Reverser and Short Core Nozzle is made in Figure 20.

### 6.2 TEST FACILITY

The static back-to-back noise tests were performed at the General Electric Peebles Test Operation Site 4D at Peebles, Ohio. The site is paved with concrete extending a minimum of 6.1 m (20 ft) beyond the microphone positions. The acoustic field is free of obstructions for 45.7 m (150 ft) minimum distance beyond the far field microphone locations. The engine was mounted to a thrust frame supported by an open-trussed cantilever structure as shown in Figure 21. The engine centerline was located 4 m (13 ft) above the concrete.

Acoustic Treatment Area - m<sup>2</sup> (ft<sup>2</sup>)

 Core Reverser Nozzle - 1.95 (21)

 Short Core Nozzle - 2.32 (25)

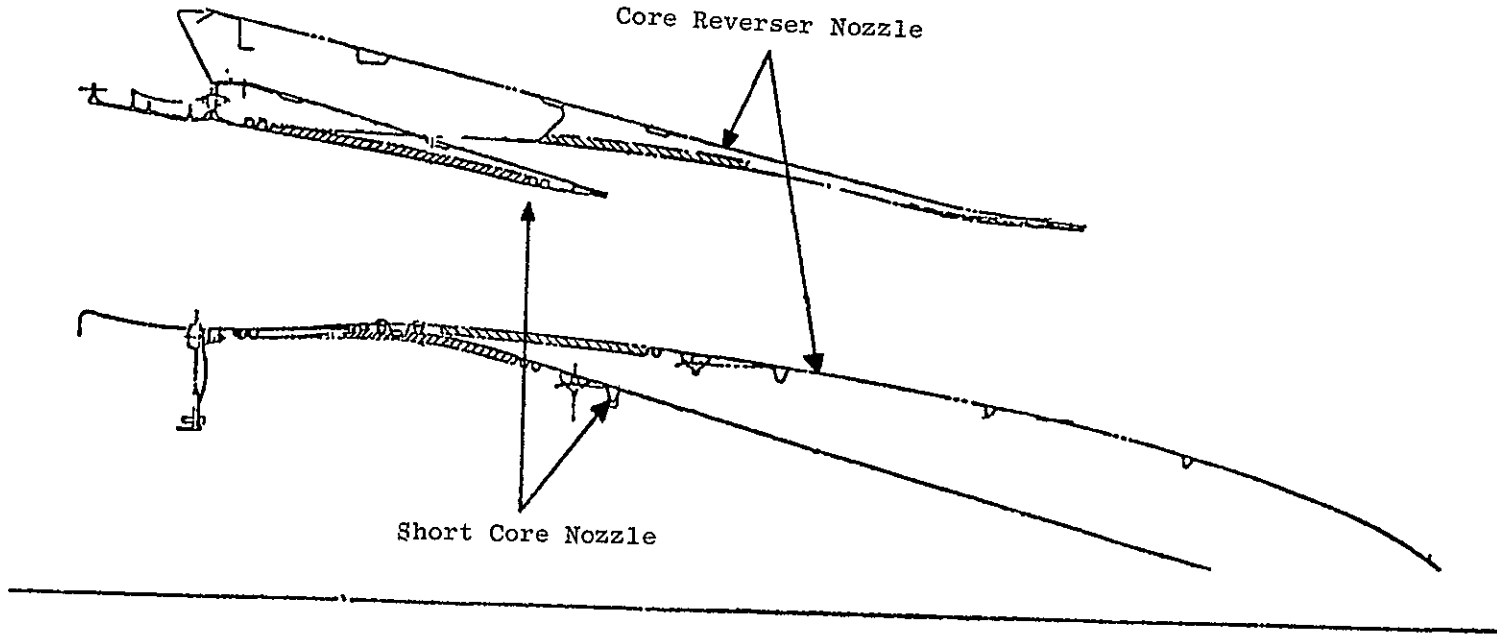


Figure 20. Comparison of Short Core Nozzle to Core Reverser Nozzle.

ORIGINAL PAGE IS  
OF POOR QUALITY

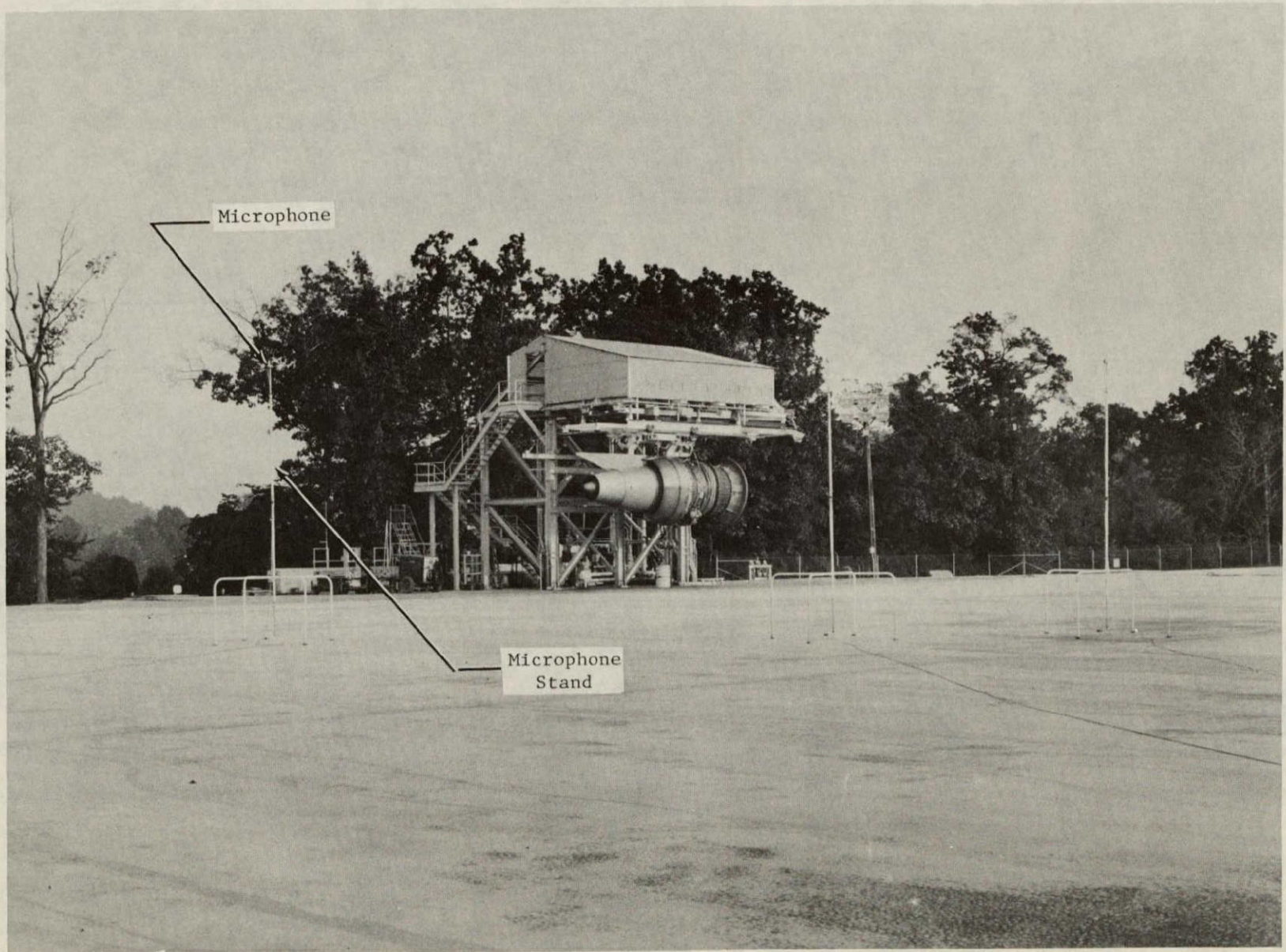


Figure 21. CF6-50 Acoustic Sound Field.



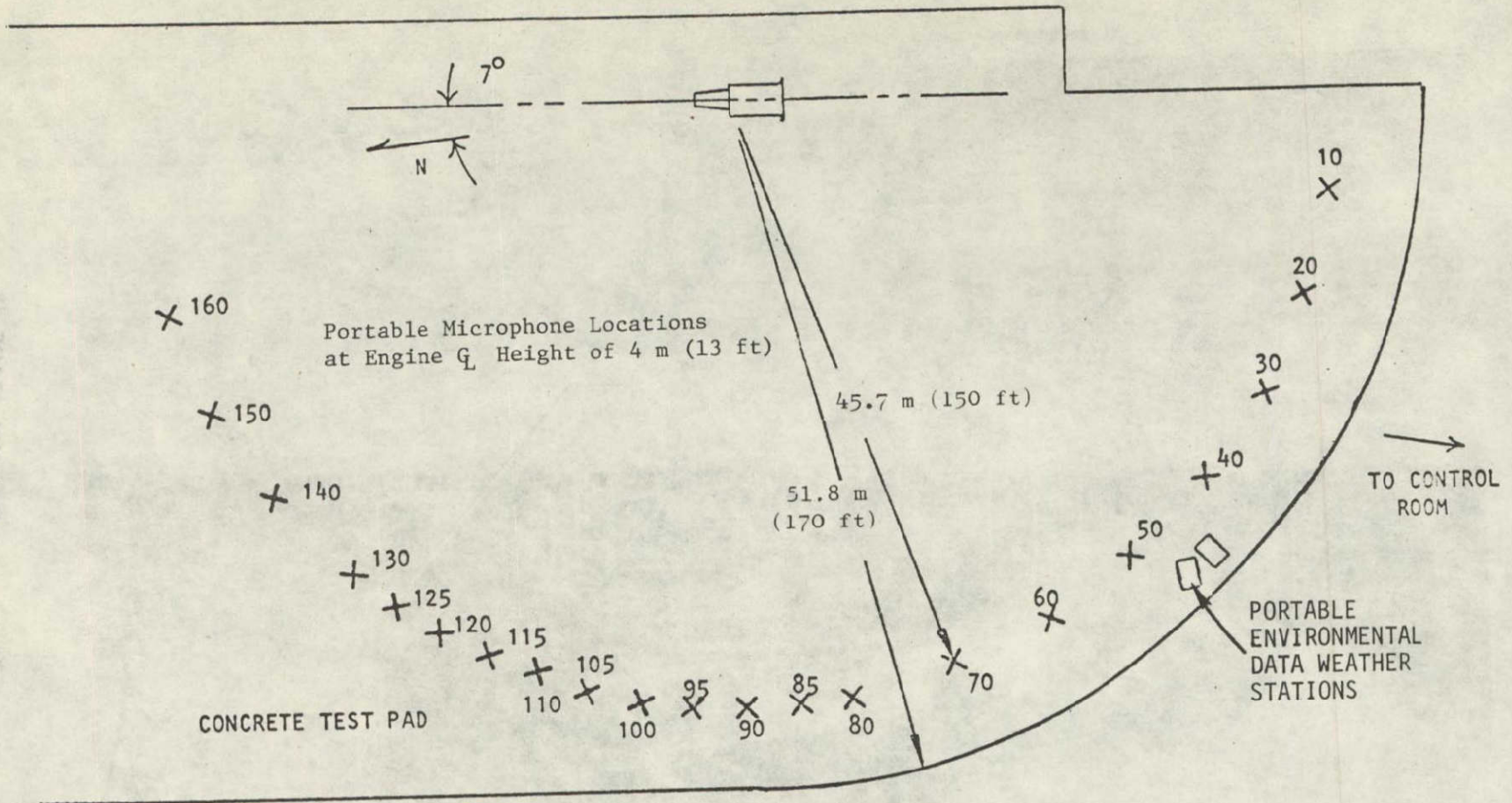


Figure 22. CF6-50 Sound Field Layout.

The microphone cartridge was replaced and, prior to each test, a 124 dB pistonphone, traceable to the National Bureau of Standards, was applied to each microphone. The microphone sensitivity was compared to the most recent laboratory calibration data to assure compliance within  $\pm 1.5$  dB; any system falling outside this band was replaced. The microphone outputs were then normalized using variable attenuators in order to record the same voltage level with the pistonphone source input. At the conclusion of each test, the pistonphone was reapplied and the voltage level was recorded as a verification of microphone system integrity.

On several occasions throughout the test series, 2-minute recordings of ambient noise were made with "facility on" and "facility off". These recordings were made at gain settings used during the sound measurements to assure acceptable signal-to-noise ratios for the acoustic data.

#### Turbine Sound Separation Probe

A water-cooled sound separation probe was used to record dynamic pressure fluctuations at the core exhaust nozzle. Two Kulite pressure transducers spaced 12.7 cm (5.0 in.) apart in a line parallel to the engine axis were flush-mounted on a 0.95 cm (0.375 in.) diameter tube. Water flowed through the tube, cooling the transducers, thereby greatly extending the temperature operating range. A laboratory calibration of the transducers to determine pressure response was performed prior to probe assembly.

The probe tip containing two transducers was positioned 90 degrees to the probe stem which was installed in an actuator to permit a radial traverse. The downstream transducer was positioned inside the core nozzle 1.27 cm (0.5 in.) from the exit plane. A box beam support attached to the concrete pad held the probe stem horizontal to the ground at the 9 o'clock engine position, aft looking forward. A shield was positioned around the actuator in order to reduce buffeting due to the fan exhaust flow.

The probe aft transducer was immersed to four positions when testing the Short Core Nozzle (2.0, 6.4, 10.8 and 16.0 cm relative to the outer wall). Data were recorded at 76.2 cm/sec (30 ips) for 1 minute at each immersion. A 2-minute stabilization time was allowed between engine speed changes. The data were recorded at average corrected fan speeds of 2207, 2400, 2598 and 2841 rpm. Prior to and following the test, a  $3.45 \text{ N/cm}^2$  (5 psi) static pressure was applied to the rear face of each Kulite diaphragm to verify probe calibration.

#### Atmospheric Test Condition Instrumentation

Barometric pressure was recorded for each test point. Wind speed, direction, air temperature and dew point were all measured using a Portable Environmental Data Station (PEDS). Two of these stations were located approximately 45 degrees from the inlet on a 51.2 m (168 ft) arc (Figure 22). The sensors were positioned at a 4 m (13 ft) height. Wind speed and direction measured on one of the PEDS were recorded continuously on strip charts. The second PEDS incorporated wind speed and  $V \cos\theta$  wind direction instrumentation.

These signals were also recorded continuously on strip charts. Ambient temperature and dew point temperature were measured by aspirator resistance temperature devices. The dew point measurement was made with a hygrometer which sampled air from the 4 m (13 ft) location. These measurements were all recorded on the DMS computer system.

#### 6.4 TEST PROCEDURE

##### Atmospheric Test Condition Limits

Atmospheric condition limits were set prior to the test. Any data recorded outside these limits (listed below) were discarded:

Relative humidity	20%	$\leq$ RH $\leq$ 95%
Temperature	264° K (-9° C)	$\leq$ T $\leq$ 305° K (32° C)
Headwind	$\leq$ 4.1	m/sec (including gusts)
Crosswind	$\leq$ 2.6	m/sec (including gusts)
Tailwind	0	m/sec (including gusts)
Gusts	$\leq$ 1.5	m/sec

##### Engine Test Conditions

The two engine configurations were run to obtain data for comparisons at the same corrected thrust over a range of conditions that encompass the approach, cutback, and takeoff power ranges for aircraft powered by the CF6-50 engine. The nominal test conditions consisted of 19 fan speeds covering the range of 2090 to 3905 rpm equivalent to the thrust range of 53,632 to 234,421 N (12,057 to 52,700 lb).

For each configuration, the 19 test conditions were repeated twice in the same order for a total of three readings at each power setting. A shutdown of at least 30 minutes occurred between each test series. At each power setting, the engine was stabilized for at least 2 minutes prior to recording acoustic data.

The engine performance data were corrected to standard sea level pressure, zero humidity, zero wind day using the measured atmospheric data for ambient temperature and pressure, absolute humidity, wind velocity, and wind direction.

##### Acoustic Data Recording

Acoustic data were recorded on magnetic tape using a 28-channel FM tape recorder system operated in the interrange instrumentation group (IRIG) wide

band Group 1 mode at a tape speed of 76.2 cm/sec (30 ips). The recorder was set up for 40% carrier deviation ( $\pm 40\%$ ) at full scale record level. Signal amplification was provided by a a.c/d.c preamp module. During testing, the tape recorder input and output were monitored to assure that adequate amplification was used and to assure proper operation of the recorder. Data were recorded for at least 2 minutes at each speed point.

#### Acoustic Data Reduction

Off-line data reduction was performed using an automated 1/3 octave reduction system. The recorded data were played back on a 28-track system operating in the IRIG wide band Group 1 mode.

In the automatic operating mode, control of the system was provided by means of a minicomputer and operator-provided information. The data to be sampled were located by means of a time code reader, indexing from the time code signal recorded on the data tape. This tape-shuttling was continued for each data channel with sampling performed over the same time increment until all channels of a particular reading were processed. The system then advanced to the next data point, based on the operator-supplied time reference, and repeated the shuttling process. After the processing information (including reading identification, reading time, gain changes, etc.) was set up by the operator, the system ran without further operator assistance until a magnetic tape change was required.

All 1/3 octave analyses were performed using a 1/3 octave analyzer. The frequency range of the data reduction process was 50 Hz through 10 kHz. A normal integration time of 32 seconds was used to provide adequate sampling of the low frequency portion of the data signal. The data sampling for the spectrum analysis was done within the 52-second time interval for which the average performance and ambient weather conditions were determined.

Each data channel output was passed through an interface to the minicomputer where data were corrected for both the frequency response of the acquisition and reduction system (as determined from the pink noise calibration) and for the microphone head response. The minicomputer was interfaced to a main frame computer to generate a file containing the 1/3 octave band data for further processing. The 1/3 octave band data were also punched on paper tape as a backup for the communication interface system.

The noise data at each test point were processed using a digital computer program to normalize the data to a 298 K (77° F)/70% relative humidity standard day using the atmospheric data (ambient pressure and temperature and relative humidity) and perform data extrapolations to various sideline distances. Overall sound pressure level (SPL), perceived noise level (PNL) and tone corrected perceived noise level (PNLT) were computed for each angle at the sideline distances. The sound power level for each 1/3 octave band and overall sound power level was computed for each test point. These results were used for subsequent analysis and data comparisons.

## 6.5 TEST RESULTS

### Measurement Accuracy

The transducers utilized in the acoustic test are of two types: 1.27 cm (1/2 in.) microphones and Kulite miniature pressure transducers. The accuracy of any sound measurement is dependent on the accuracy of the acoustic data recording and reduction system which is dependent on the tolerance of each independent component in the system. A list of each component and the accuracy ( $3\sigma$  tolerances) obtained from the respective manufacturers is presented below:

	<u>Component</u>	<u><math>3\sigma</math> Tolerance (<math>\pm</math> dB)</u>
Far Field Microphone System	Microphone Cartridge Calibration	0.2 f < 10 kHz
	Cathode Follower Amplifier	0.2
	Pistonphone	0.2
	Noise Generator	0.5
	Power Supply	0.09
	Variable Gain Amplifier	0.2
Common to Both Systems	Tape Recorder	0.5
	Tape Deck	0.5
	1/3 OB Analyzer	0.25
	Computer	0.0
Kulite System	Minicomputer	0.0
	Kulite Pressure Transducer Calibration	1.5
	Voltage Source, d.c.	0.2

Since these variances are independent of each other, the estimated variance of the sound level can be computed as the RMS of the variances due to each component separately. The accuracy of the far field microphone system is then  $\pm 1.0$  dB and that of the Kulite system is  $\pm 1.7$  dB.

The accuracy of the system does not define data reproducibility which is dependent on many other factors. The intrinsic variation of acoustic data due to meteorological conditions, source variations, random instrument error, etc., defines data sample variance about the "true" absolute level of the noise source under evaluation. Hence, the instrumentation accuracy defines the tolerance (systematic error) on a "true" noise level determined from test sample statistics (random error).

Noise level differences obtained from static back-to-back tests remove any data bias introduced as a result of instrumentation systematic error. The remaining random error can be collapsed using sample statistics to determine the statistical significance of noise level differences determined from the test data. The conclusions drawn from such an analysis are independent of instrumentation system absolute accuracy.

Prior to the test, it was postulated that the change from the Core Reverser Nozzle to the Short Core Nozzle could modify engine noise through the following principal mechanisms: change in the thermodynamic cycle, change in suppression of low pressure turbine (LPT) noise, and change in jet noise. Results from the subject back-to-back static testing and data analysis to evaluate small differences between the engine configurations are discussed herein.

### Cycle Effect on Noise

Corrected thrust versus corrected fan speed data, as determined during this test series, are compared in Figure 23. Good agreement was maintained between repeat test runs and between engine configurations. Thermodynamic cycle differences between the configurations apparently do not (for acoustic purposes) significantly affect the fan speed/thrust relationship. Therefore, no acoustic effect can be attributed to cycle differences.

### Far Field Perceived Noise

The 45.7 m (150 ft) arc data were extrapolated to reference sidelines of 122 m (400 ft) and 305 m (1000 ft). Spherical divergence was used to correct for distance, and Aerospace Recommended Practice ARP866A (Reference 2) was used to correct for atmospheric absorption. These reference distances were chosen because they are typical of FAA certification altitudes for approach and takeoff, respectively. Perceived noise levels were computed at these distances to allow a general assessment of the effect of the Short Core Nozzle relative to the Core Reverser Nozzle on the far field acoustic data.

To facilitate data comparisons between the engine configurations, all data were averaged and comparative plots were made. PNL directivities at the typical takeoff and approach power settings listed in Table II are exhibited in Figures 24 through 27. The aft quadrant data comparisons should reflect any noise level changes that are related to differences between the engine configurations, since the only configuration change was the core nozzle. Differences in front quadrant noise levels, which are dominated by fan inlet

Table II. Nominal Engine Power Settings Selected For Data Presentation.

Nominal Thrust		Nominal Fan Speed rpm	Condition	Sideline Distance	
kN	(lb)			(m)	(ft)
228	51,200	3850	Takeoff	305	1000
158	35,600	3275	Cutback	305	1000
88	19,800	2610	High Approach	122	400
59	13,300	2190	Low Approach	122	400

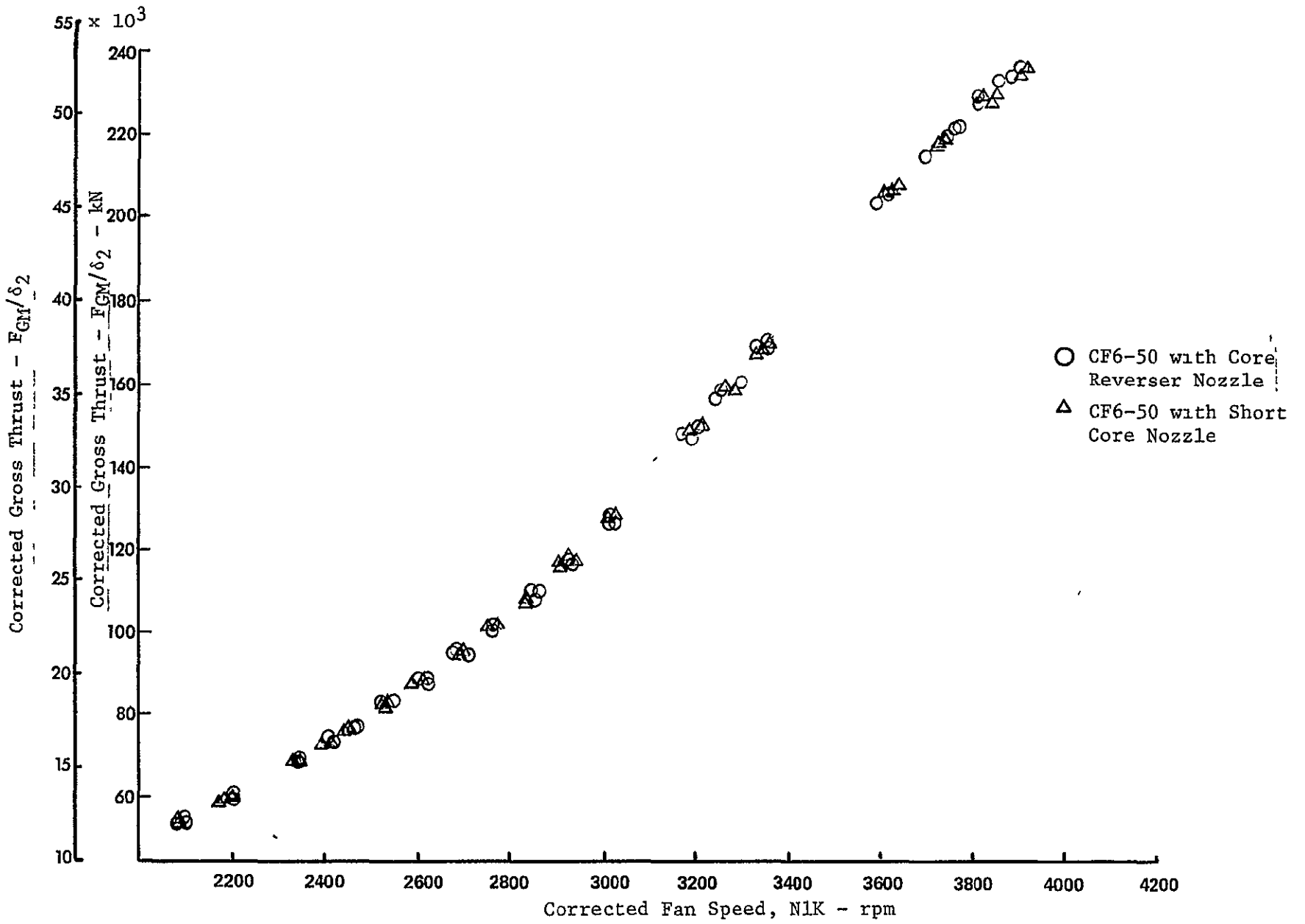


Figure 23. Corrected Thrust/Corrected Fan Speed Relationship.

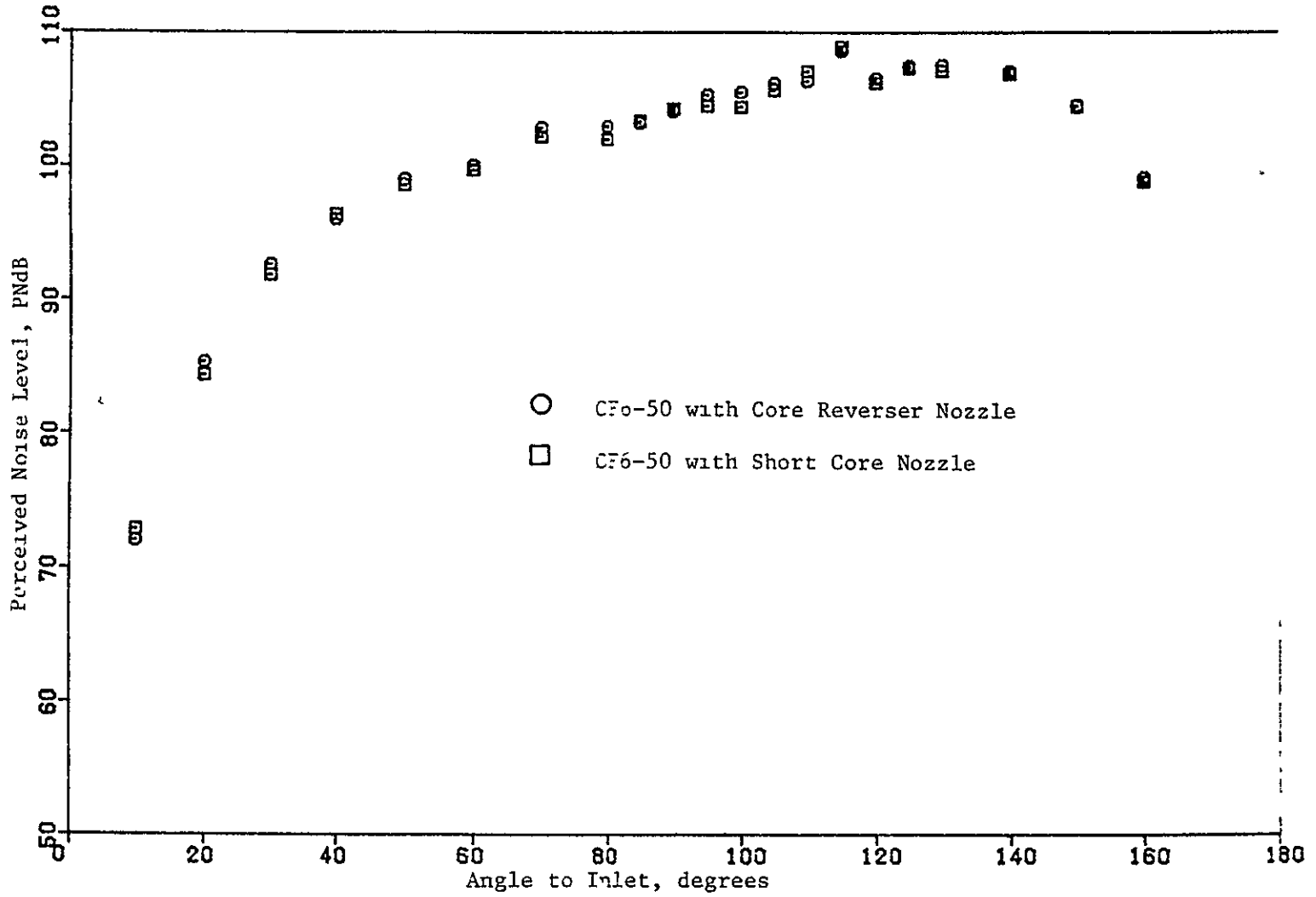


Figure 24. Perceived Noise Level Directivity Comparison of Short Core Nozzle and Core Reverser Nozzle at 305 m (1,000 ft) Sideline and 228 kN (51,200 lb) Corrected Thrust (Takeoff).



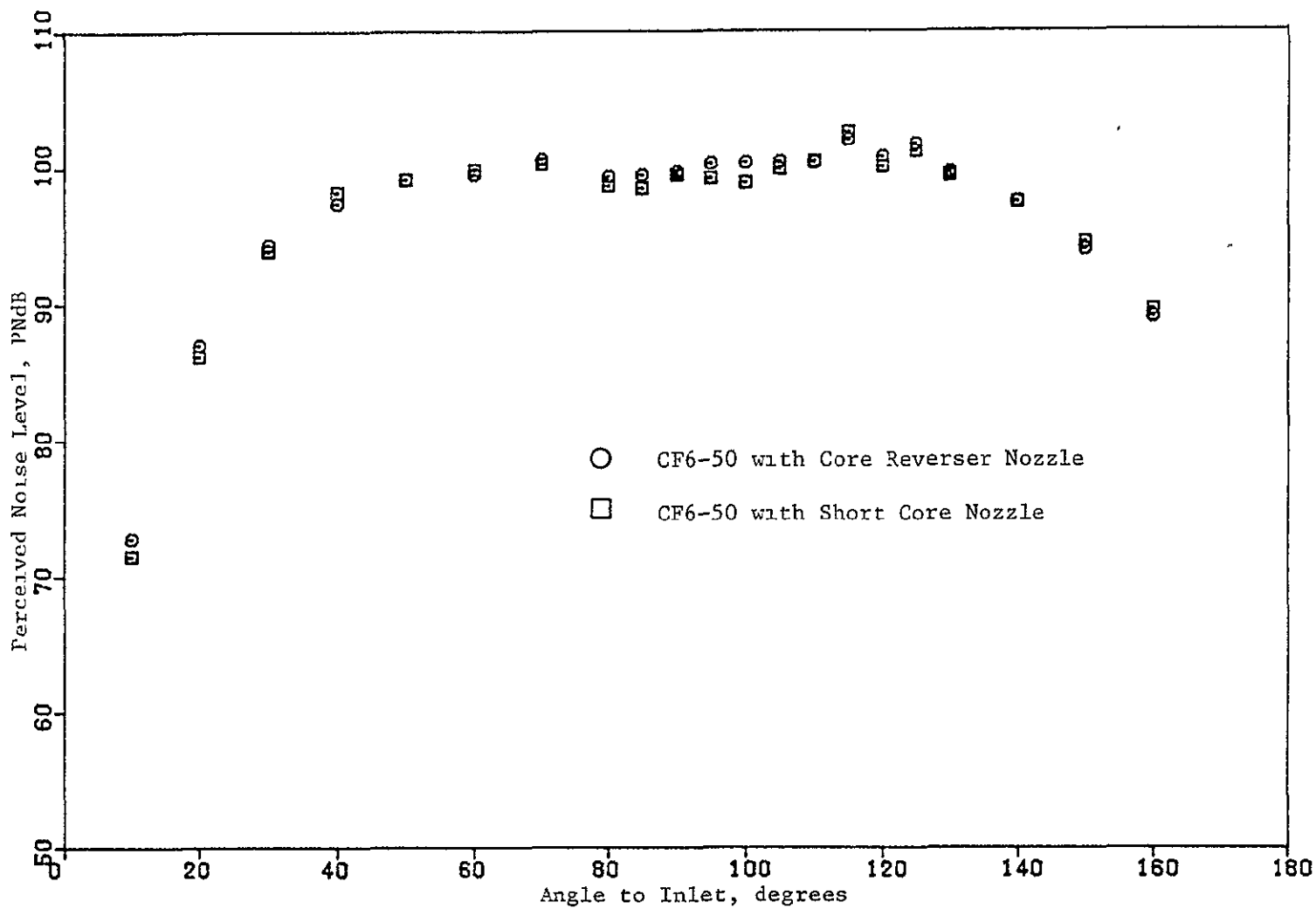


Figure 25. Perceived Noise Level Directivity Comparison of Short Core Nozzle and Core Reverser Nozzle at 305 m (1,000 ft) Sideline and 158 kN (35,600 lb) Corrected Thrust (Cutback).

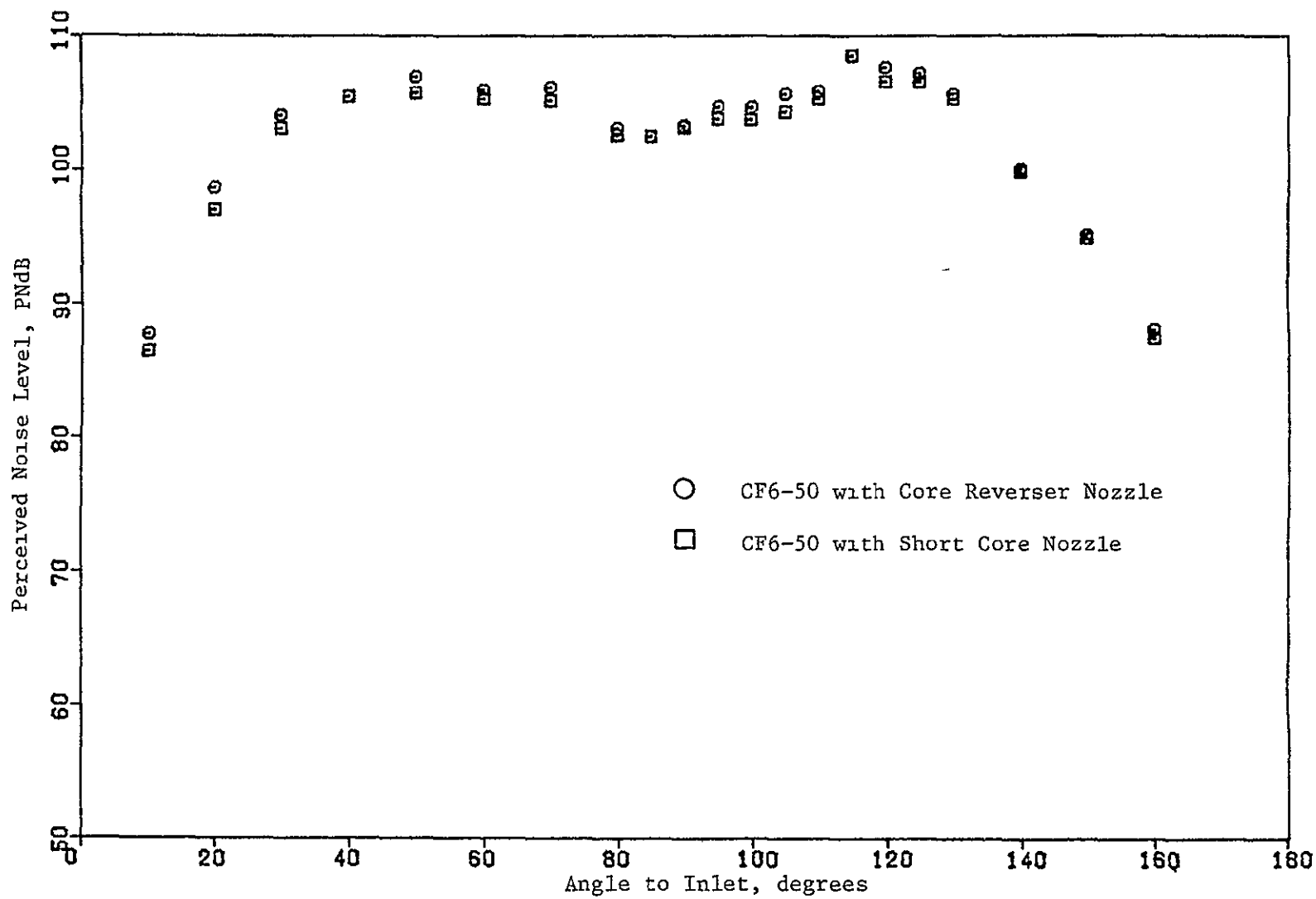


Figure 26. Perceived Noise Level Directivity Comparison of Short Core Nozzle and Core Reverser Nozzle at 122 m (400 ft) Sideline and 88 kN (19,800 lb) Corrected Thrust (High Approach).

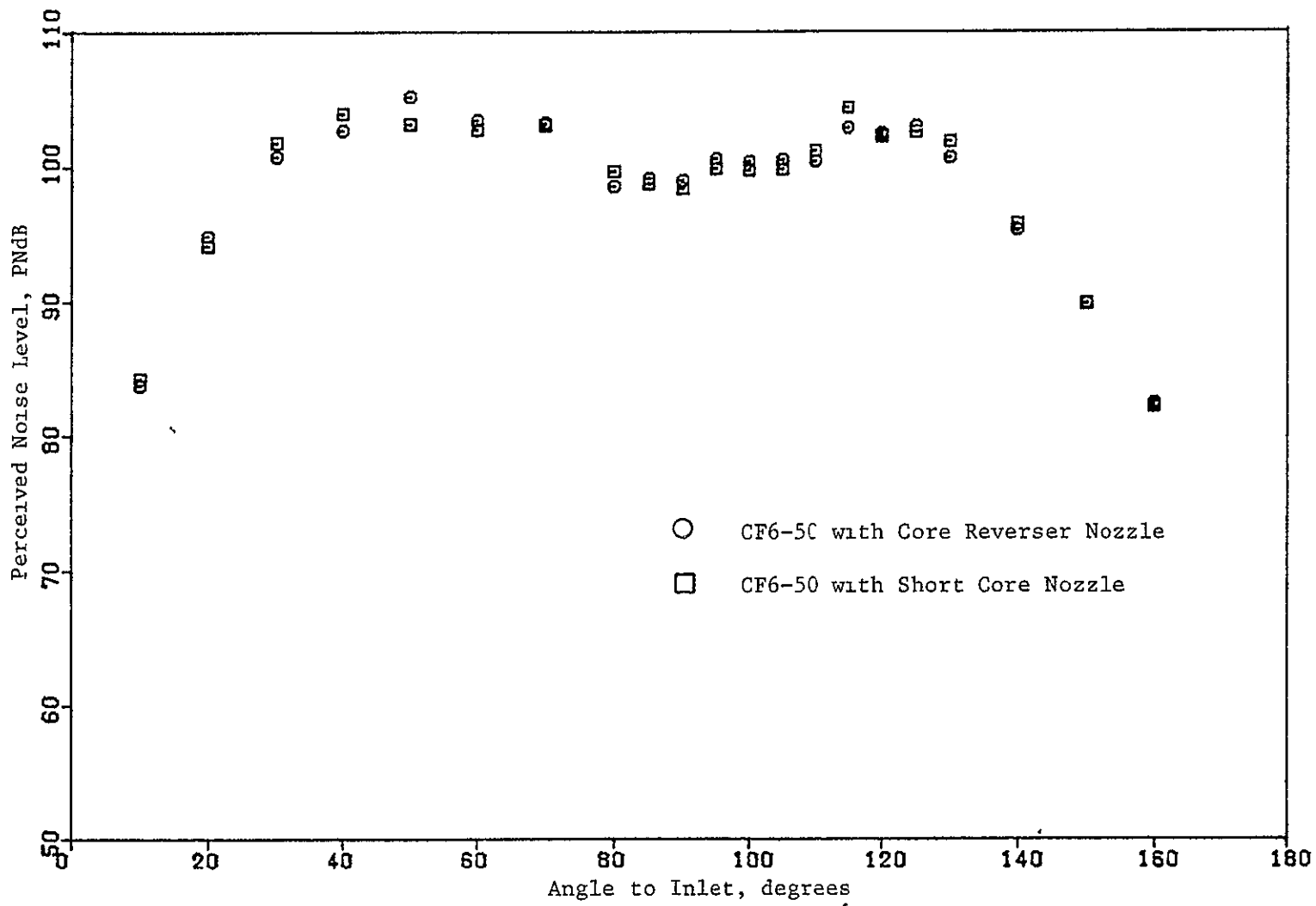


Figure 27 Perceived Noise Level Directivity Comparison of Short Core Nozzle and Core Reverser Nozzle at 122 m (400 ft) Sideline and 59 kN (13,300 lb) Corrected Thrust (Low Approach).

noise, are assumed to have been influenced by changes in meteorological conditions, possibly atmospheric turbulence, even though all tests were run within stringent wind limits. The PNL directivity behavior at the 305 m sideline distance for takeoff power settings is similar between the two configurations. This result implies that the Short Core Nozzle does not significantly affect jet noise sound levels nor directivity patterns.

PNL directivity behavior at the 122 m sideline distance at approach power settings represents a superposition of the three primary noise components of the engine: jet noise, fan and low pressure turbine (LPT) noise. Of these sources, the Short Core Nozzle should influence only the noise signatures of the LPT and the core jet. Differences in the fan noise characteristics between the two configurations should be independent of the core nozzle since the engine thermodynamic cycles are essentially identical. The small differences in the aft quadrant that occur between the configurations for approach power settings at the 122 m sideline distance (Figures 26 and 27) may be due to a difference in LPT noise levels. The apparent differences observed here are discussed further under component noise analysis.

PNL data at typical peak forward and peak aft angles determined from the directivity plots are shown versus thrust in Figures 28 through 31 for 50 and 115 degrees at both the 305 and 122 m sideline distances. No significant trends are discernible for the front quadrant angle. The PNL versus thrust data for the Short Core Nozzle at 115 degrees diverges from the Core Reverser Nozzle data at low power settings but is similar to the Core Reverser Nozzle data at high power settings. This behavior is the only difference that can be attributed to the Short Core Nozzle when the engine configuration data are compared on a PNL basis. It is possible that the LPT directivity pattern has been influenced by the Short Core Nozzle producing the observed behavior. However, this result could only affect aircraft flyover noise at the very low power approach conditions.

#### Far Field Noise Spectra

Averaged 1/3 octave spectra at angles of peak PNL (50 and 150 degrees) for the power settings listed in Table II are presented at the 305 and 122 m sideline distances in Figures 32 through 39. Noise signature component differences are discussed in a later section while salient features common to each are discussed below.

The most distinct feature common to all the noise spectra is the "null" that falls between the 160 to 315 Hz 1/3 octave bands. This is an interference phenomenon produced by the sound field. The minimum level associated with the "null" occurs in the frequency band where the path length difference between the direct path from the source to the microphone and the reflected path from the concrete surface of the pad is one-half wave length. For the 45.7 m arc microphones at 4 m centerline height, the minimum level occurs at approximately 250 Hz. Reinforcement of the engine noise occurs when the path length difference is one wave length with the maximum level occurring at approximately 500 Hz. Higher order minima and maxima effects are washed

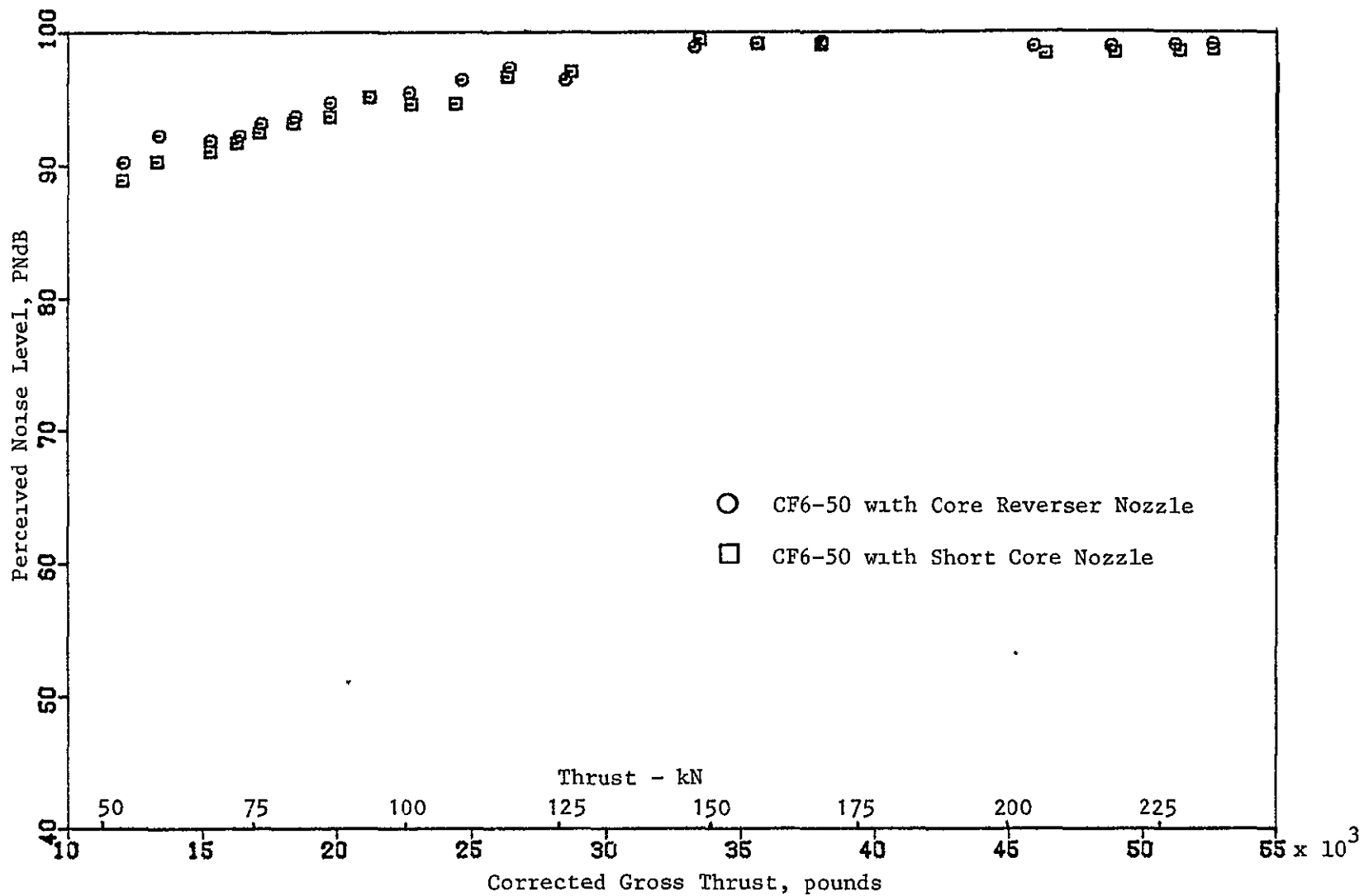


Figure 28. Perceived Noise Level Comparison of Short Core Nozzle and Core Reverser Nozzle as a Function of Thrust for 50 Degrees at 305 m (1000 ft) Sideline.

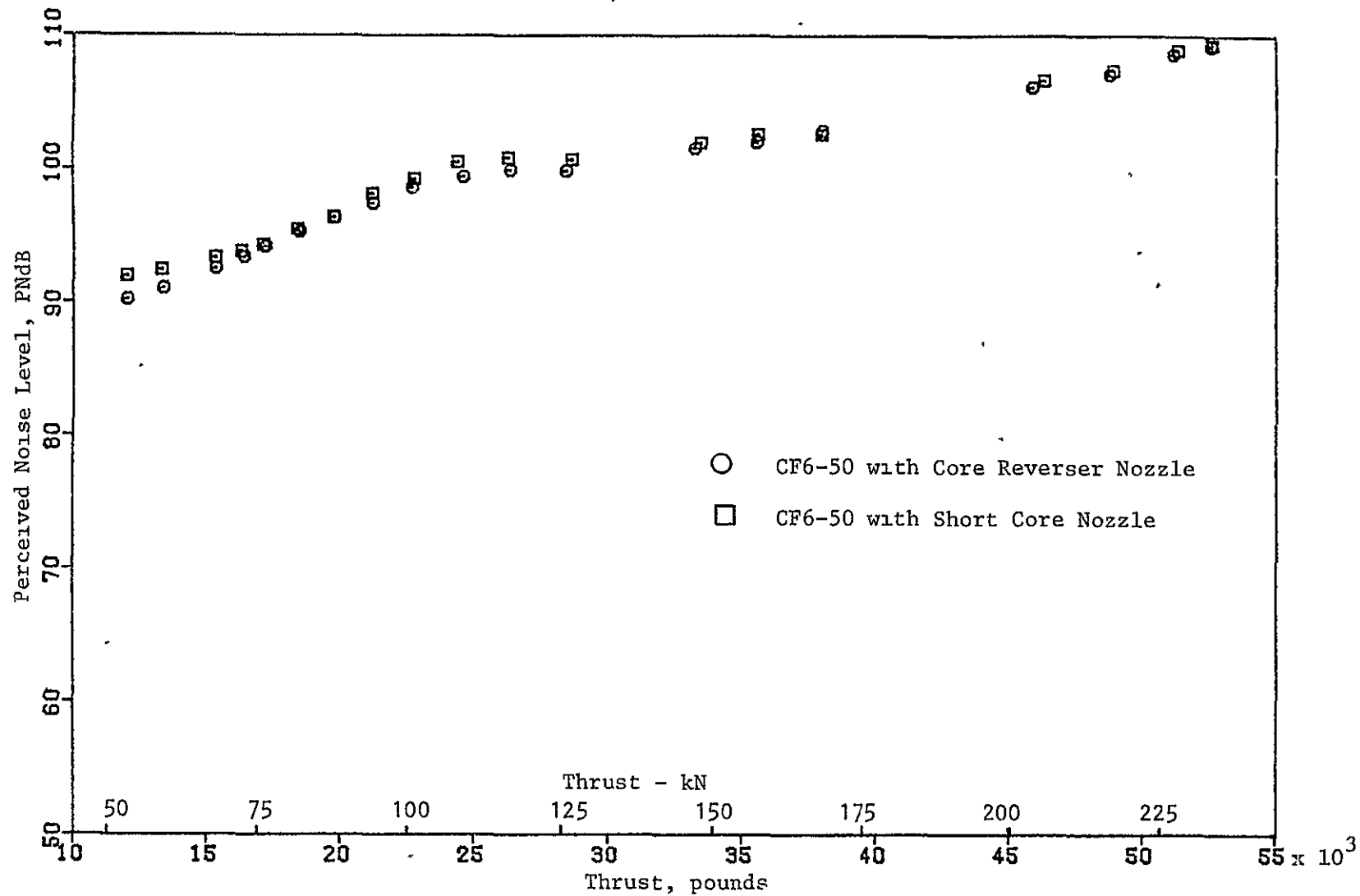


Figure 29. Perceived Noise Level Comparison of Short Core Nozzle and Core Reverser Nozzle as a Function of Thrust for 115 Degrees at 305 m (1000 ft) Sideline.

**NASA  
FORMAL  
REPORT**

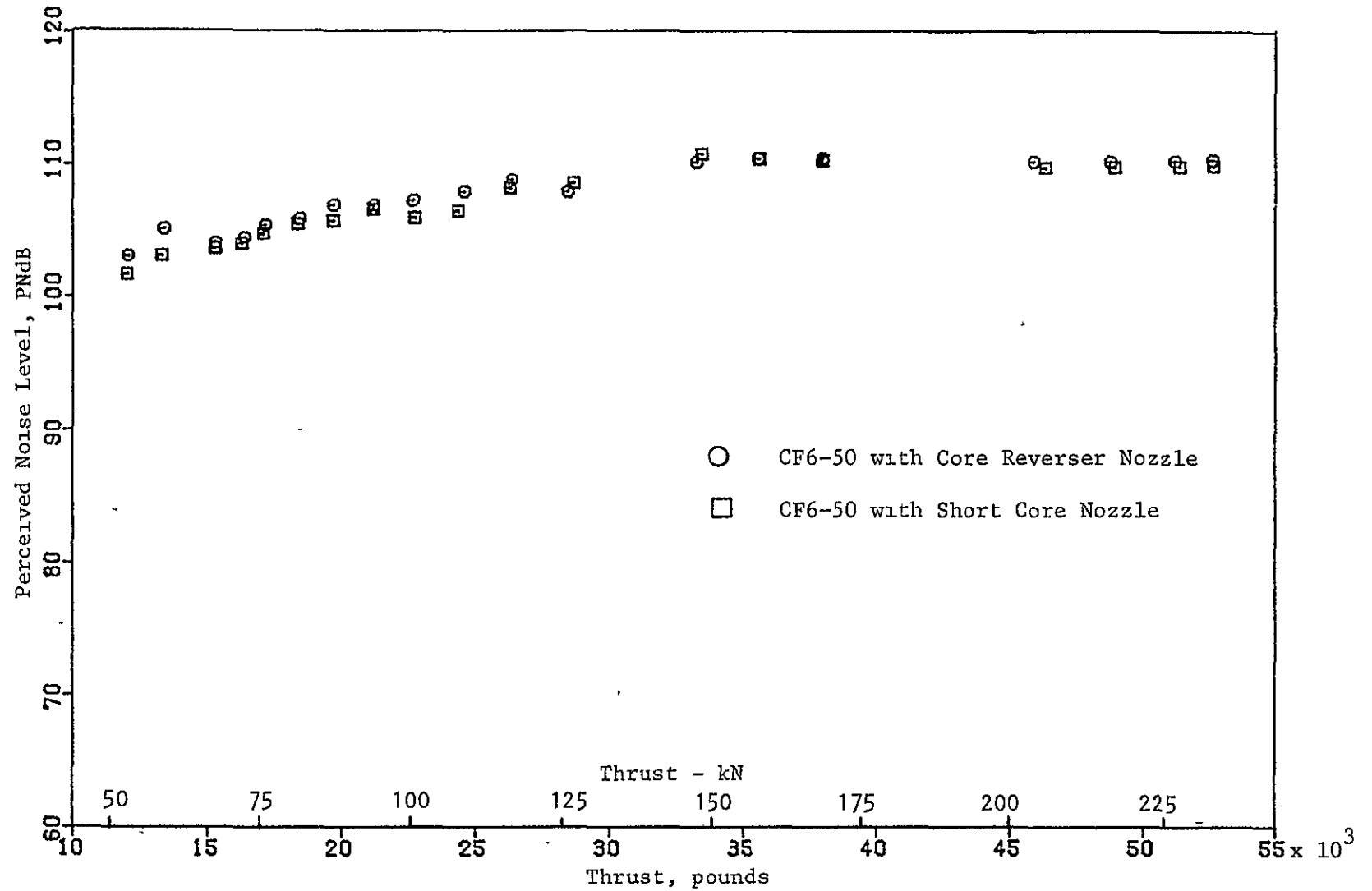


Figure 30. Perceived Noise Level Comparison of Short Core Nozzle and Core Reverser Nozzle as a Function of Thrust for 50 Degrees at 122 m (400 ft) Sideline.



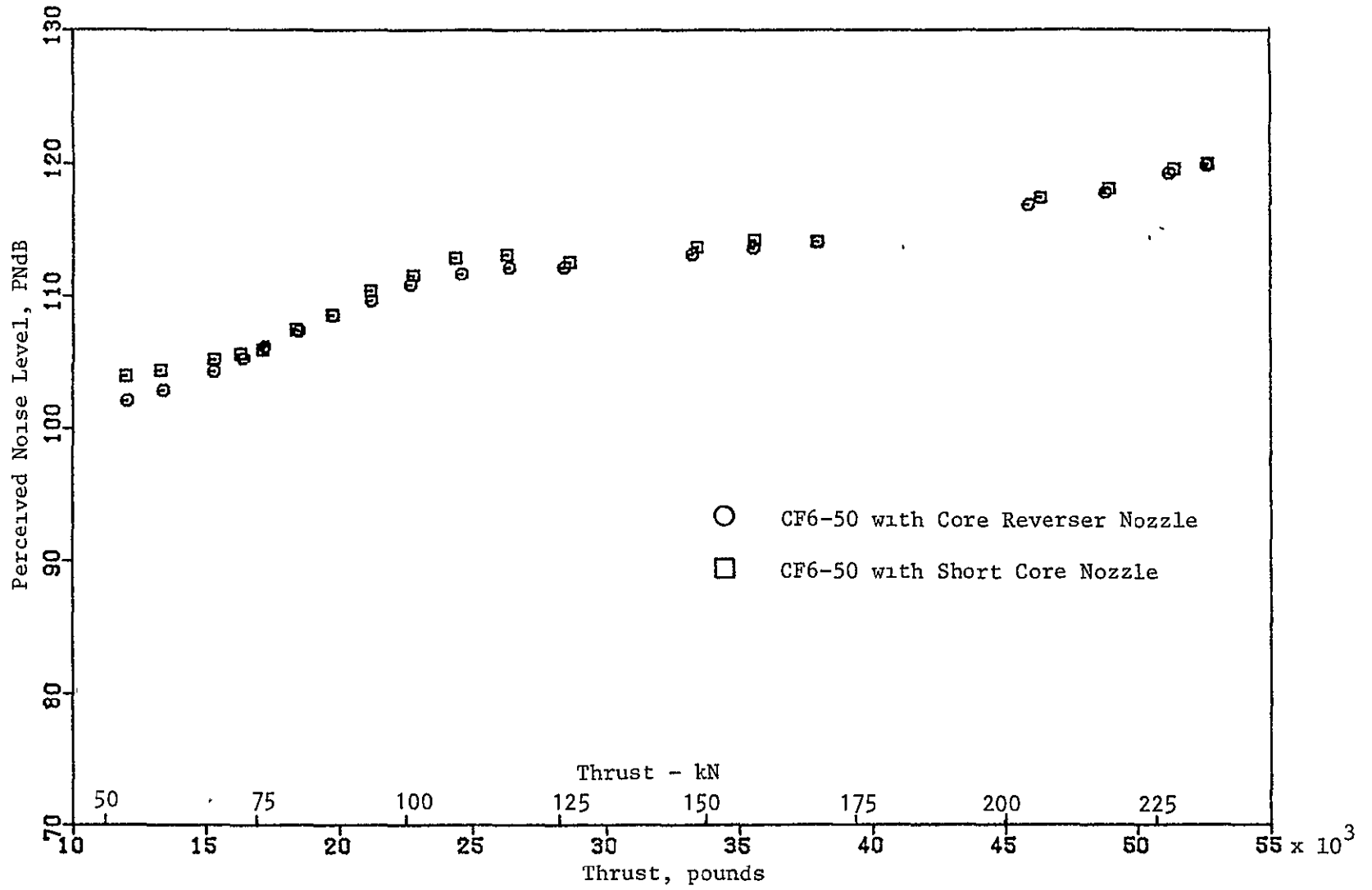


Figure 31. Perceived Noise Level Comparison of Short Core Nozzle and Core Reverser Nozzle as a Function of Thrust for 115 Degrees at 122 m (400 ft) Sideline.

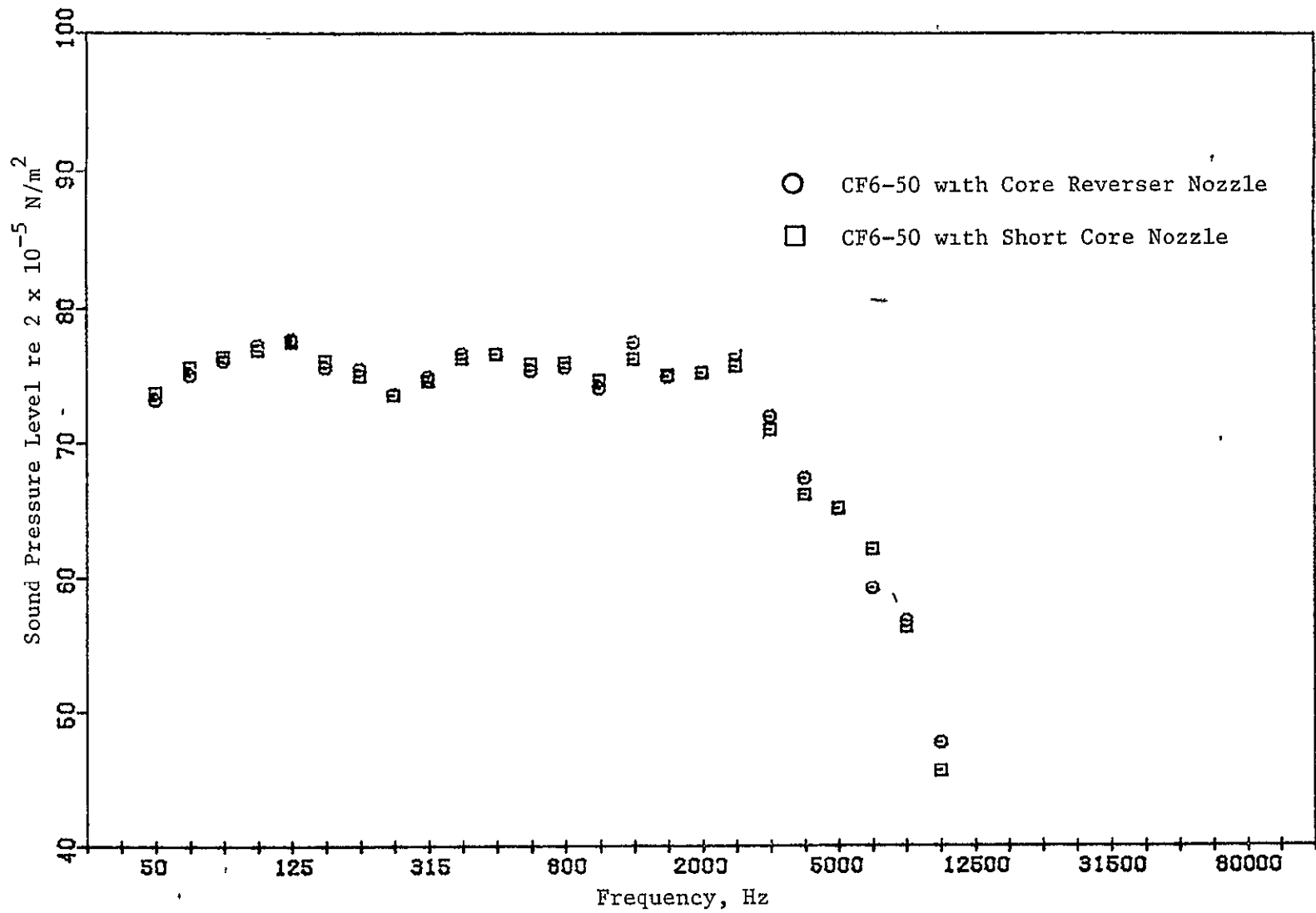


Figure 32. 1/3 Octave Spectrum Comparison of Short Core Nozzle and Core Reverser Nozzle at 50 Degrees 305 m (1000 ft) Sideline and 228 kN (51,200 lb) Corrected Thrust (Takeoff).

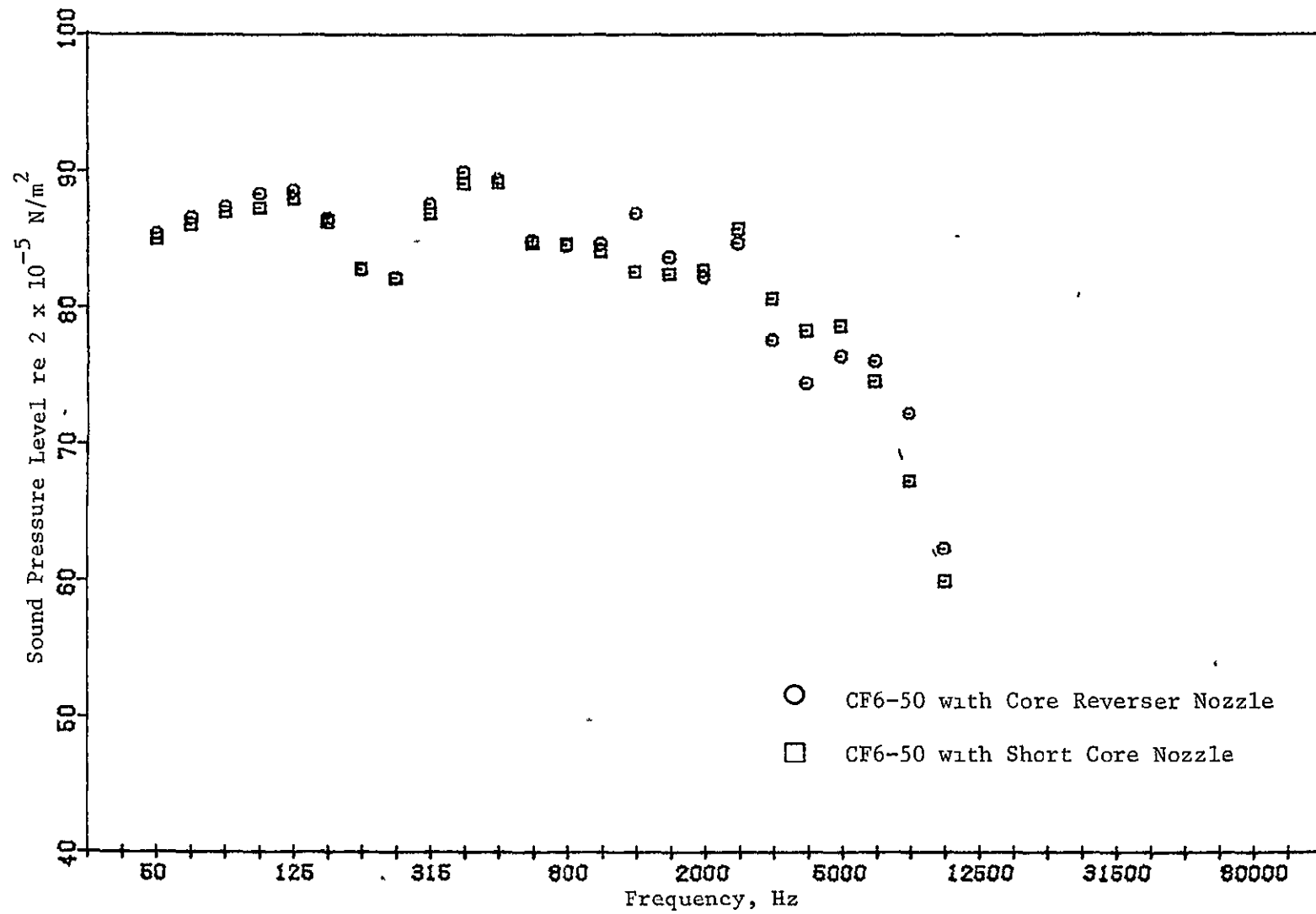


Figure 33. 1/3 Octave Spectrum Comparison of Short Core Nozzle and Core Reverser Nozzle at 115 Degrees 305 m (1000 ft) Sideline and 228 kN (51,200 lb) Corrected Thrust (Takeoff).

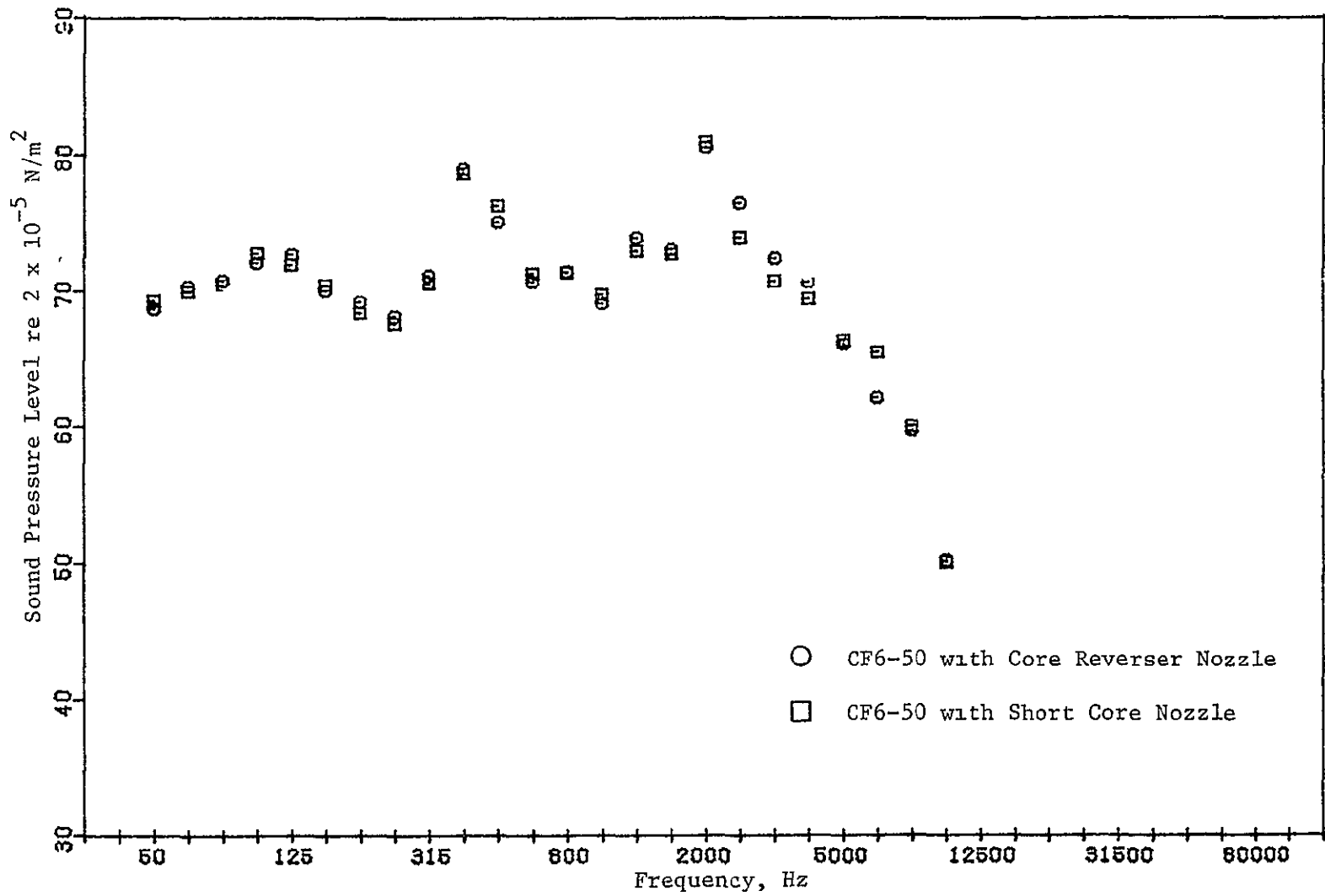


Figure 34. 1/3 Octave Spectrum Comparison of Short Core Nozzle and Core Reverser Nozzle at 50 Degrees 305 m (1000 ft) Sideline and 158 kN (35,600 lb) Corrected Thrust (Cutback).

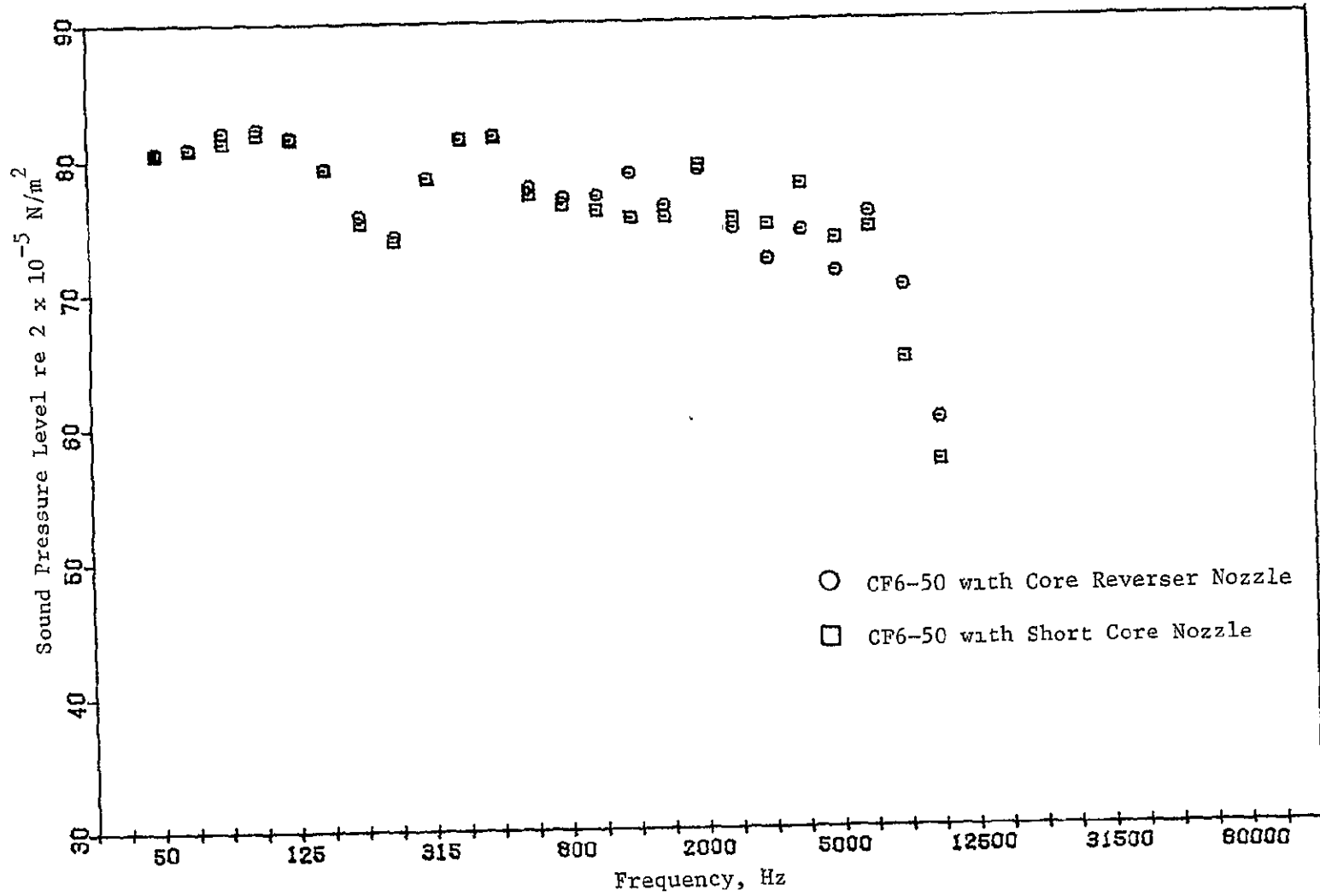


Figure 35. 1/3 Octave Spectrum Comparison of Short Core Nozzle and Core Reverser Nozzle at 115 Degrees 305 m (1000 ft) Sideline and 158 kN (35,600 lb) Corrected Thrust (Cutback).

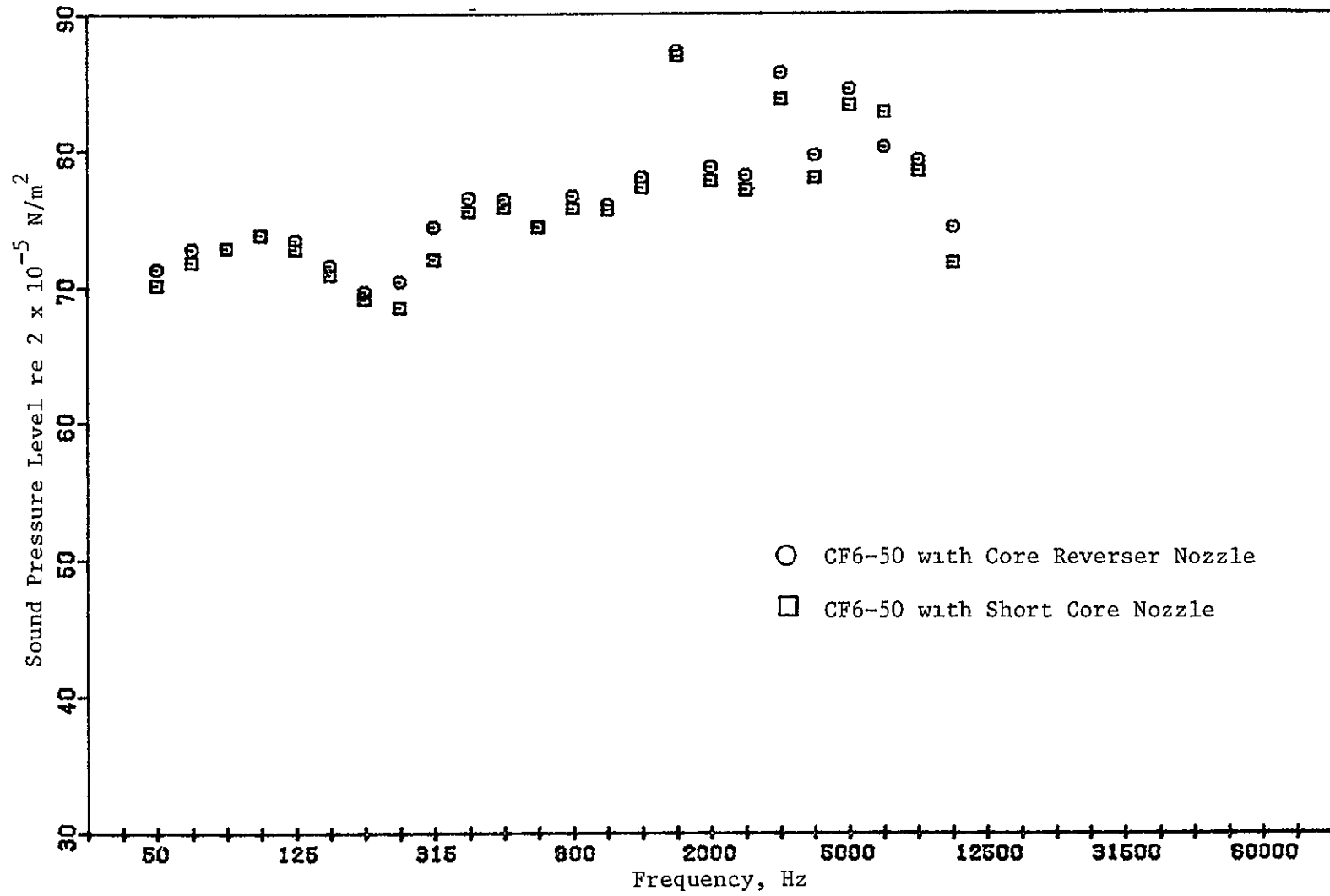


Figure 36. 1/3 Octave Spectrum Comparison of Short Core Nozzle and Core Reverser Nozzle at 50 Degrees 122 m (400 ft) Sideline and 88 kN (19,800 lb) Corrected Thrust (High Approach).

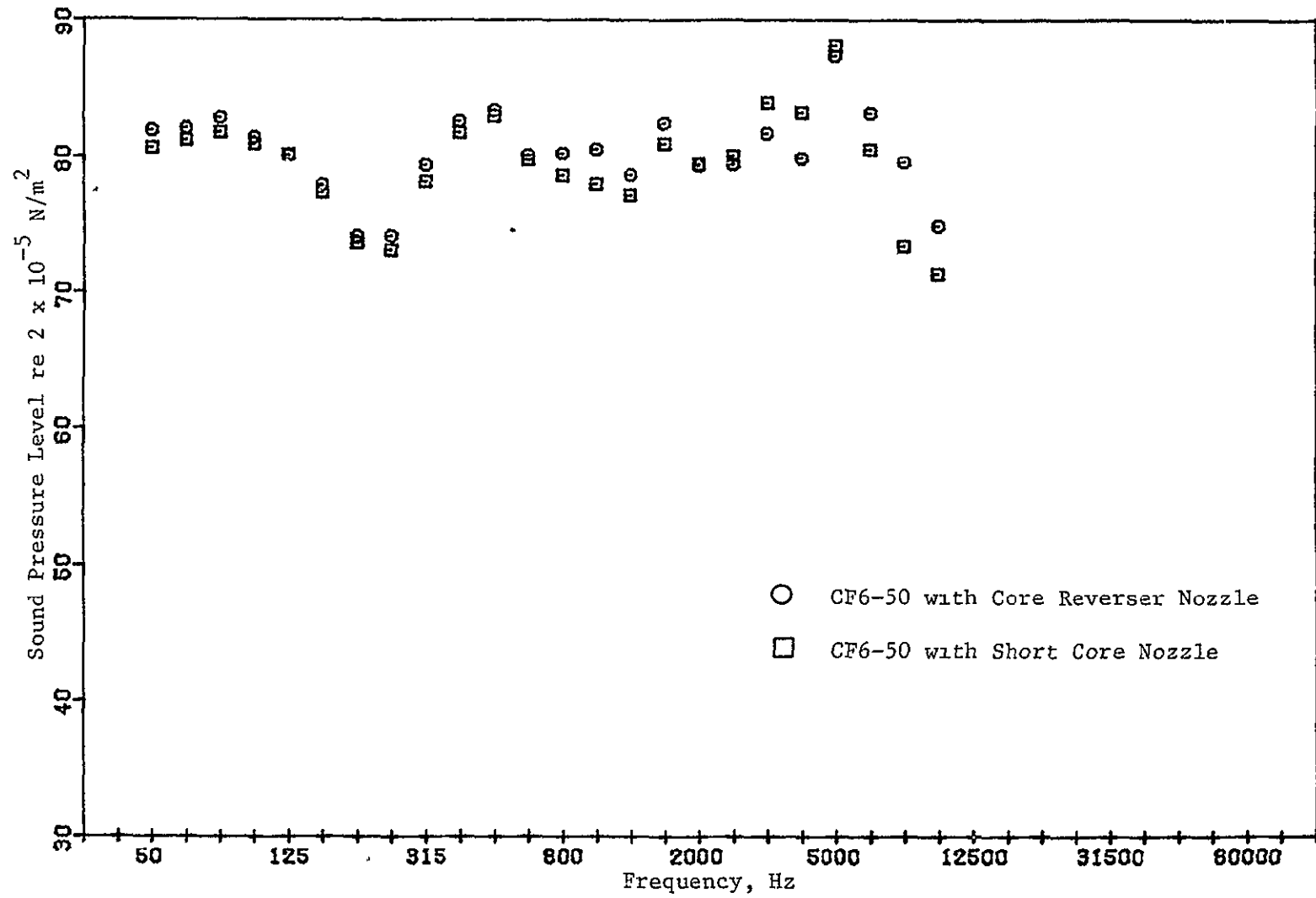


Figure 37. 1/3 Octave Spectrum Comparison of Short Core Nozzle and Core Reverser Nozzle at 115 Degrees 122 m (400 ft) Sideline and 88 kN (19,800 lb) Corrected Thrust (High Approach).

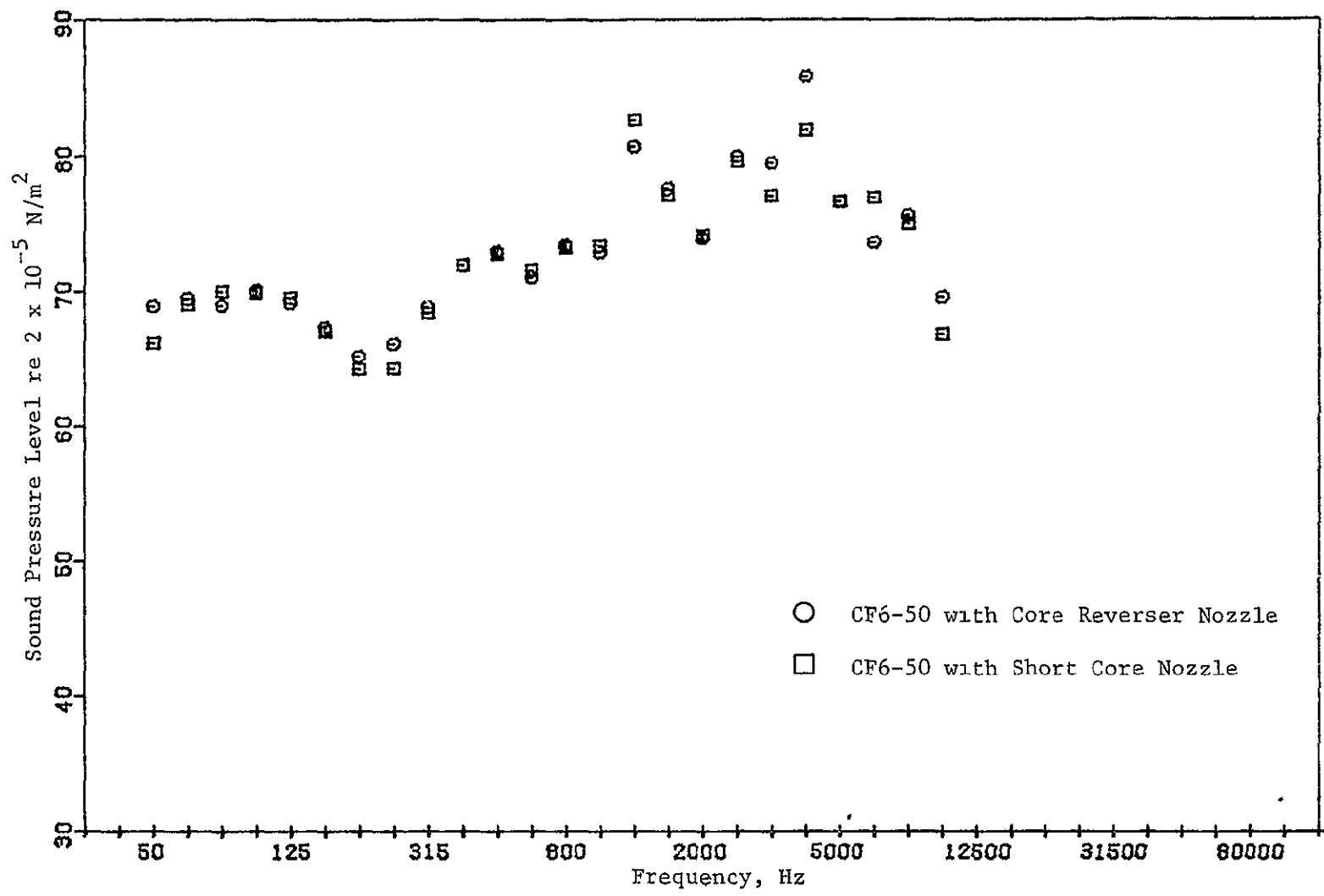


Figure 38. 1/3 Octave Spectrum Comparison of Short Core Nozzle and Core Reverser Nozzle at 50 Degrees 122 m (400 ft) Sideline and 59 kN (13,300 lb) Corrected Thrust (Low Approach).



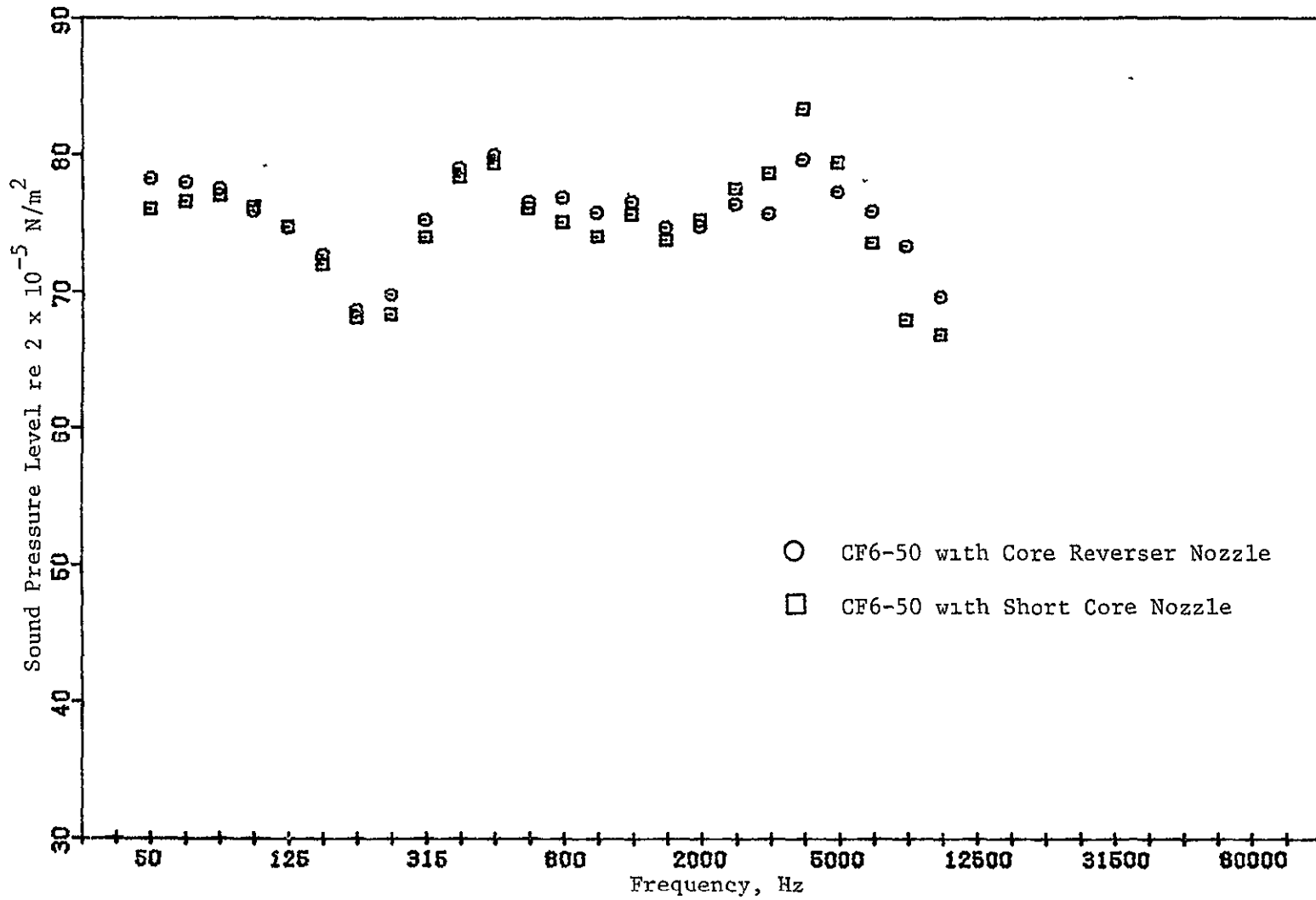


Figure 39. 1/3 Octave Spectrum Comparison of Short Core Nozzle and Core Reverser Nozzle at 115 Degrees 122 m (400 ft) Sideline and 59 kN (13,300 lb) Corrected Thrust (Low Approach).

out due to atmospheric turbulence, the extended nature of the source, broad band noise characteristics of the source, the intrinsic time variation of the source noise levels, and the band width used for data analysis. Interference effects above 1000 Hz are negligible when compared to the data scatter. No attempt was made to correct the data for interference effects. This is justified by the reproducibility of the interference effect and the direct comparisons made between the back-to-back static test results. Data corrections for this effect would have been required if the tests were performed under radically different environmental conditions.

The fan blade passing frequency (BPF) fundamental and harmonics are predominant features of the far field noise spectra at both sideline distances for all engine power settings. These tones are easily identified in the spectra. The bands that are affected are summarized in Table III for the takeoff and approach power settings listed in Table II.

Table III. Source Identification of the Far Field Tones.

Condition	Nominal Fan Speed, N1 (rpm)	Source Identification, kHz				
		Fan				LPT
		(1) F1	2F1	3F1	4F1	LPT3
Takeoff	3850	(2) 2.5	5.0	8.0	10.0	8.0
Cutback	3275	2.0	4.0	6.3	8.0	6.3
High Approach	2610	1.5	3.15	5.0	6.3	5.0
Low Approach	2190	1.25	2.5	4.0	5.0	4.0

Notes.

(1) F1 = Fan BPF fundamental  
 2F1 = Fan BPF second harmonic  
 3F1 = Fan BPF third harmonic  
 4F1 = Fan BPF fourth harmonic  
 LPT3 = LPT third stage BPF fundamental

(2) 1/3 octave band containing the specified tone, kHz

The LPT third stage fundamental BPF also contributes to the far field noise levels. The bands affected by the LPT are also listed in Table III. The LPT third stage BPF tone is in close proximity to the third harmonic BPF of the fan, always falling in the same band. Hence, the two tones cannot be differentiated in the 1/3 octave spectra.

The far field noise spectral comparisons tend to reinforce the observation made from the PNL data comparisons that the Short Core Nozzle has affected the directivity of the LPT third stage tone. The far field data at 115 degrees for low power settings show the largest differences for both the PNL and spectral comparisons. The directivity of the 4.0 kHz band data for the low approach power setting at the 122 m sideline is shown in Figure 40 for both engine configurations. The relative effects of the core nozzles are shown by the data at the aft angles. The forward angle data appear to be controlled by the third harmonic of the fan BPF.

The spectrum level differences for the forward angle data between the configurations are not significant. The 4.0 kHz band is dominated by the fan BPF third harmonic for angles less than 80 degrees. The tone level of the fan BPF third harmonic in the forward quadrant is dependent on a rotor-turbulence interaction for static testing without a turbulence control screen. Consequently, large differences between the 1/3 octave bands containing the tone may occur if atmospheric conditions (turbulence) differ between test series. However, the spectrum level of the 4.0 kHz band for the aft angles is not controlled by the fan tone. This band is controlled by the LPT third stage and fan broad band noise which is discussed in the Low Pressure Turbine Noise paragraph which follows. The 5 kHz band width spectra shown in Figures 41 through 50 show that the LPT third stage "haystack" and fan broad band noise are controlling the band level.

### Jet Noise

Before the test series was performed, it was postulated that jet noise could be affected by the change in core nozzle geometry even with no change in the magnitude of the fan and core jet velocities. Shortening of the core nozzle tends to reduce turbulence and could reduce jet noise slightly. The increase in boattail angle was expected to have no significant effect on jet noise level or directivity. Data analyses to evaluate the above effects are discussed here.

One-third octave band sound power level (PWL) data for the engine configurations are compared in Figure 51 at two typical takeoff power settings. The noise signature of the engine is seen to be dominated by jet noise (frequencies below ~1000 Hz). As shown in Figure 51, there was no significant change in the sound power level between the engine configurations.

Noise spectra at a 305 m sideline distance for takeoff power are compared in Figures 52 through 59 for 130 through 160 degrees angular locations. Again, there were no significant differences observed between the two engine configurations.

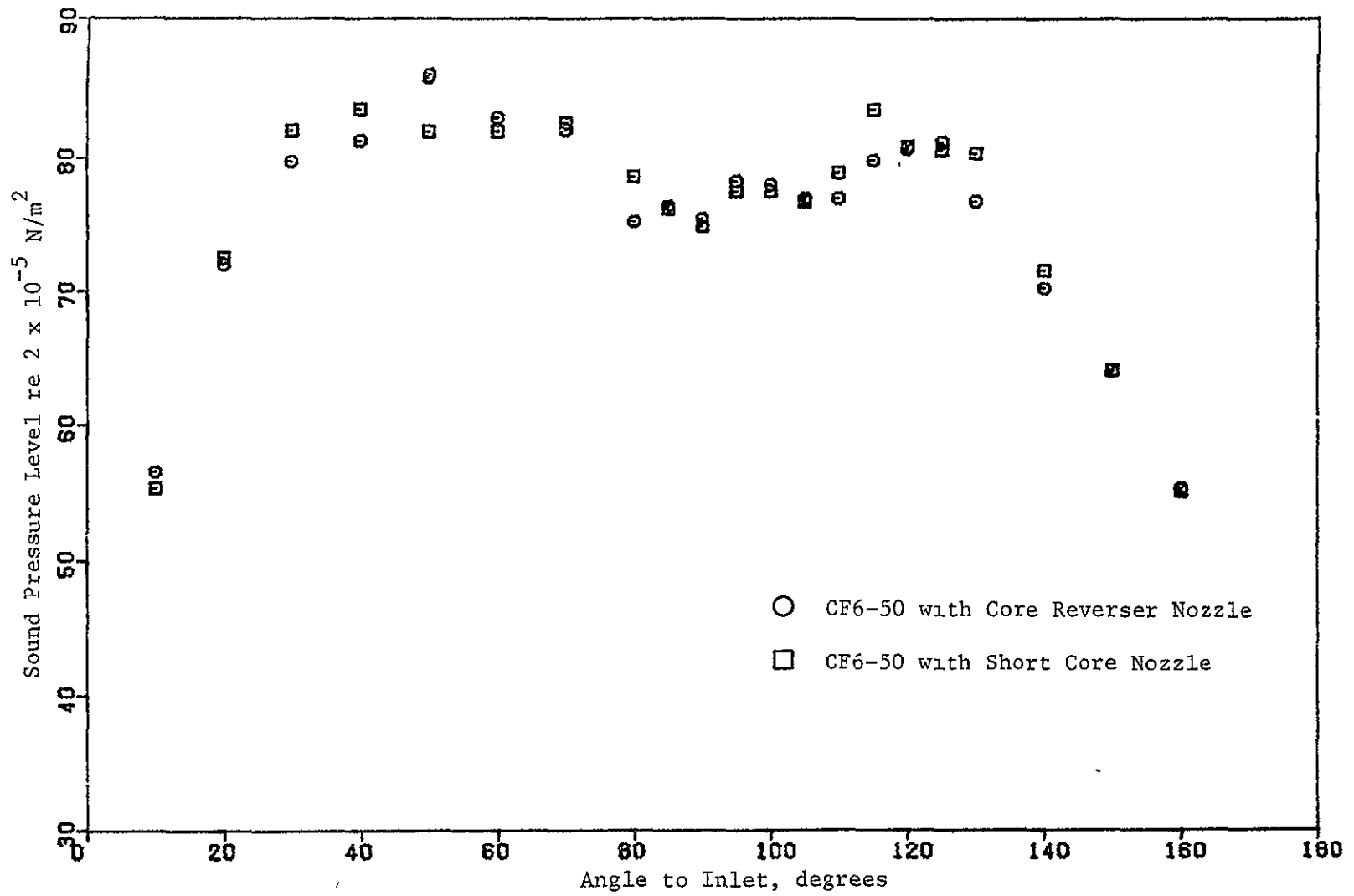


Figure 40. 4.0 kHz 1/3 Octave Band Directivity Comparison of Short Core Nozzle and Core Reverser Nozzle 122 m (400 ft) and 59 kN (13,300 lb) Corrected Thrust (Low Approach).

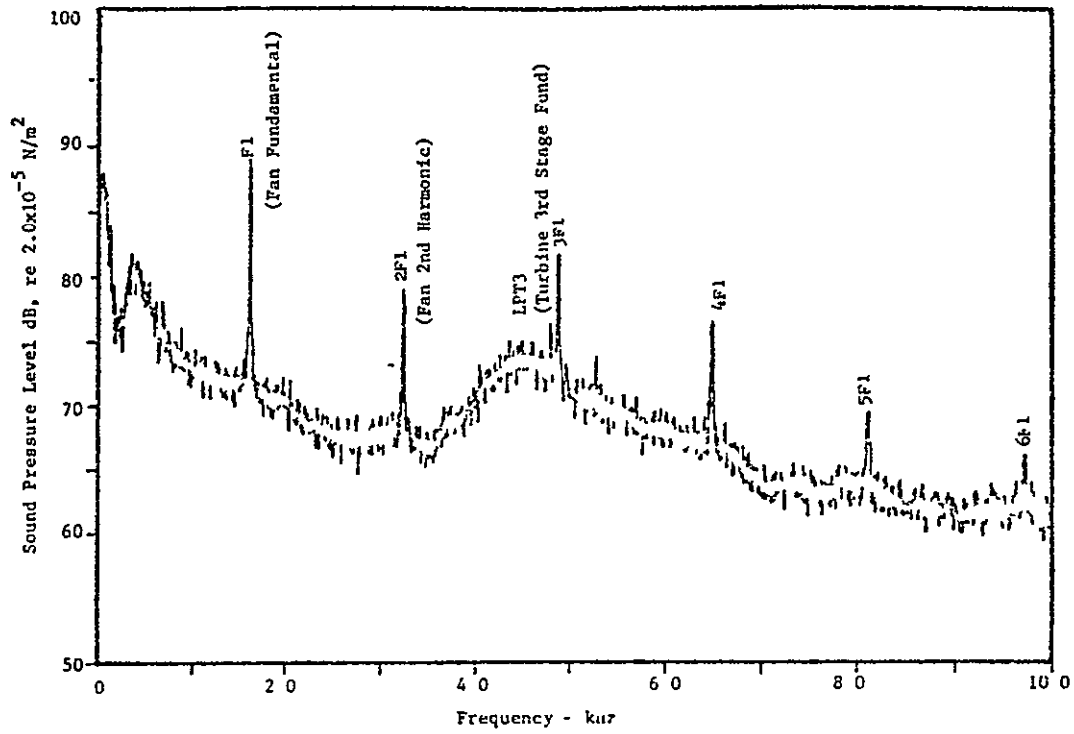


Figure 41. Short Core Nozzle Far Field Spectra at 100 Degrees, 45.7 m (150 ft) Arc 88 kN (19,800 lb) Corrected Thrust (High Approach).

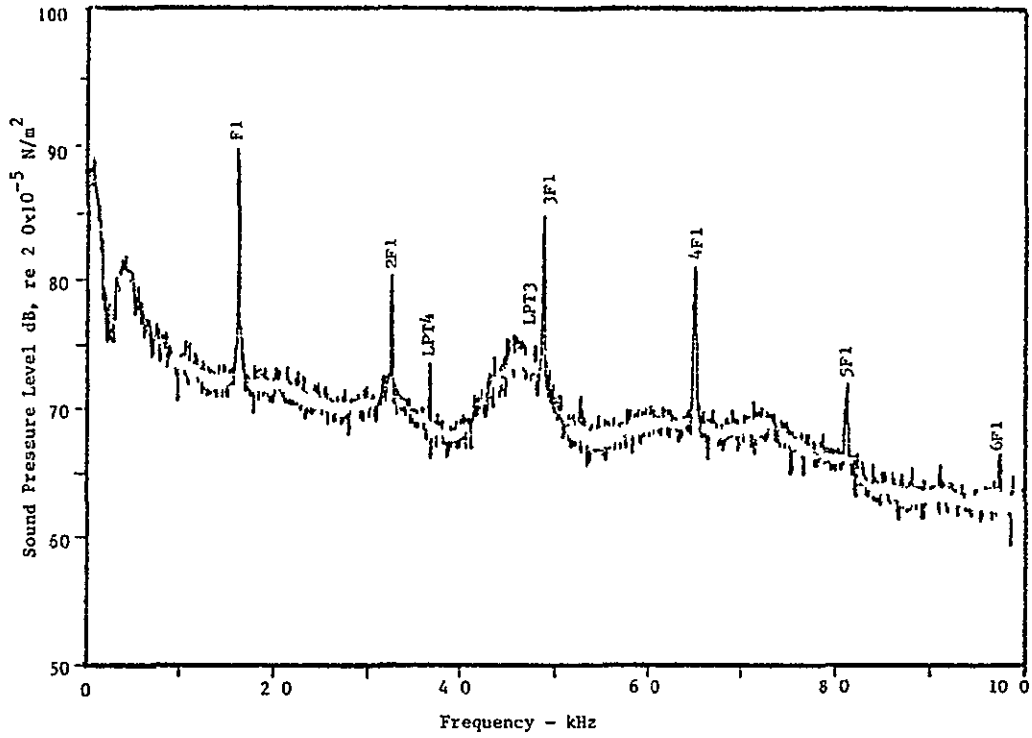


Figure 42. Short Core Nozzle Far Field Spectra at 105 Degrees, 45.7 m (150 ft) Arc 88 kN (19,800 lb) Corrected Thrust (High Approach).

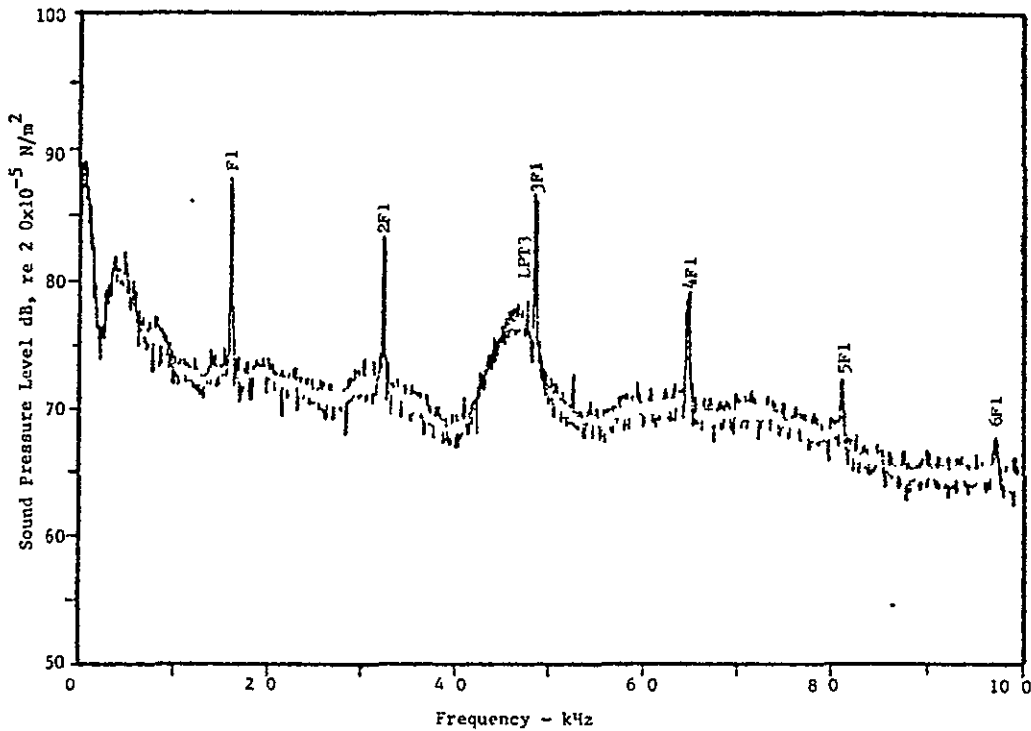


Figure 43. Short Core Nozzle Far Field Spectra at 110 Degrees, 45.7 m (150 ft) Arc 88 kN (19,800 lb) Corrected Thrust (High Approach).

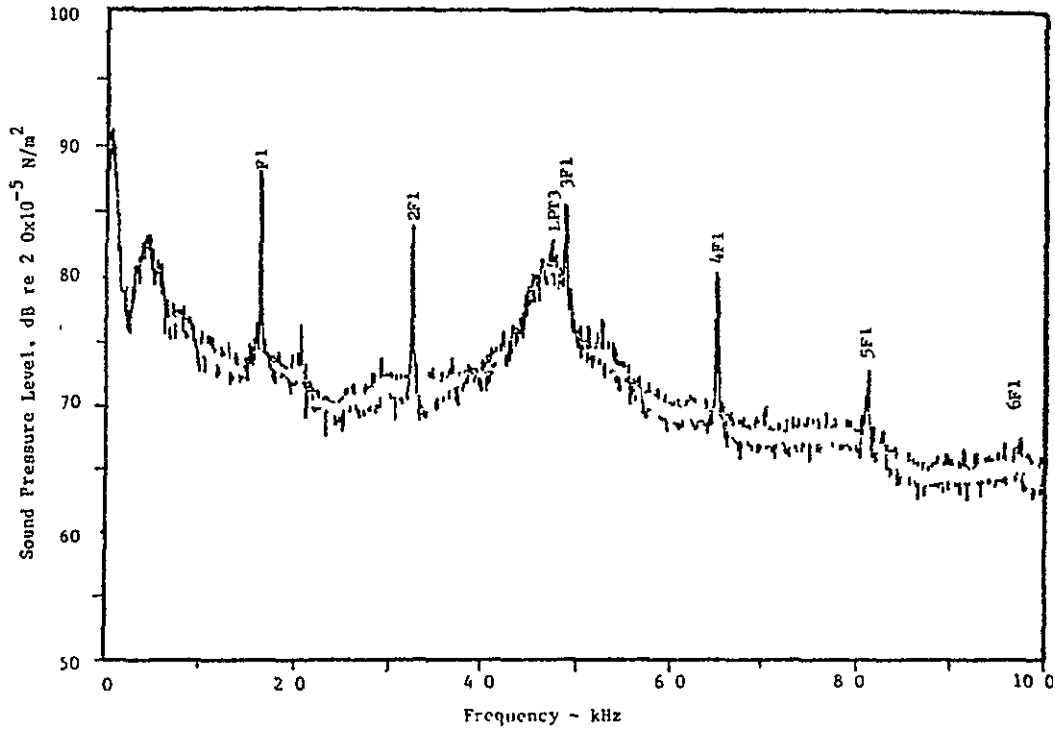


Figure 44. Short Core Nozzle Far Field Spectra at 115 Degrees, 45.7 m (150 ft) Arc 88 kN (19,800 lb) Corrected Thrust (High Approach).

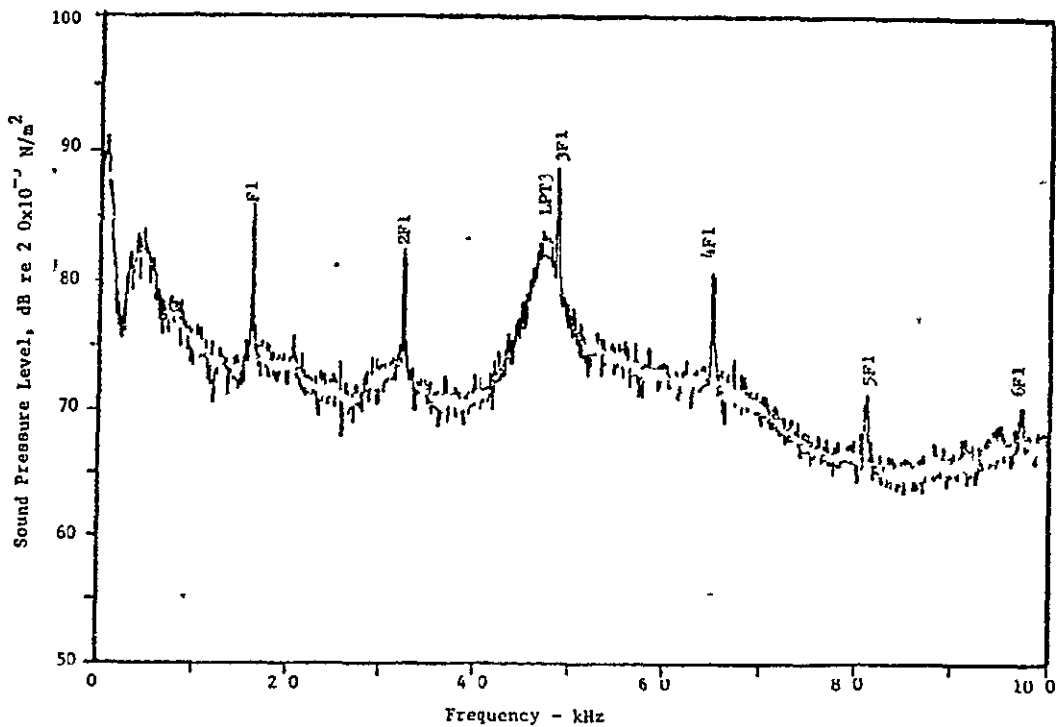


Figure 45. Short Core Nozzle Far Field Spectra at 120 Degrees, 45.7 m (150 ft) Arc 88 kN (19,800 lb) Corrected Thrust (High Approach).



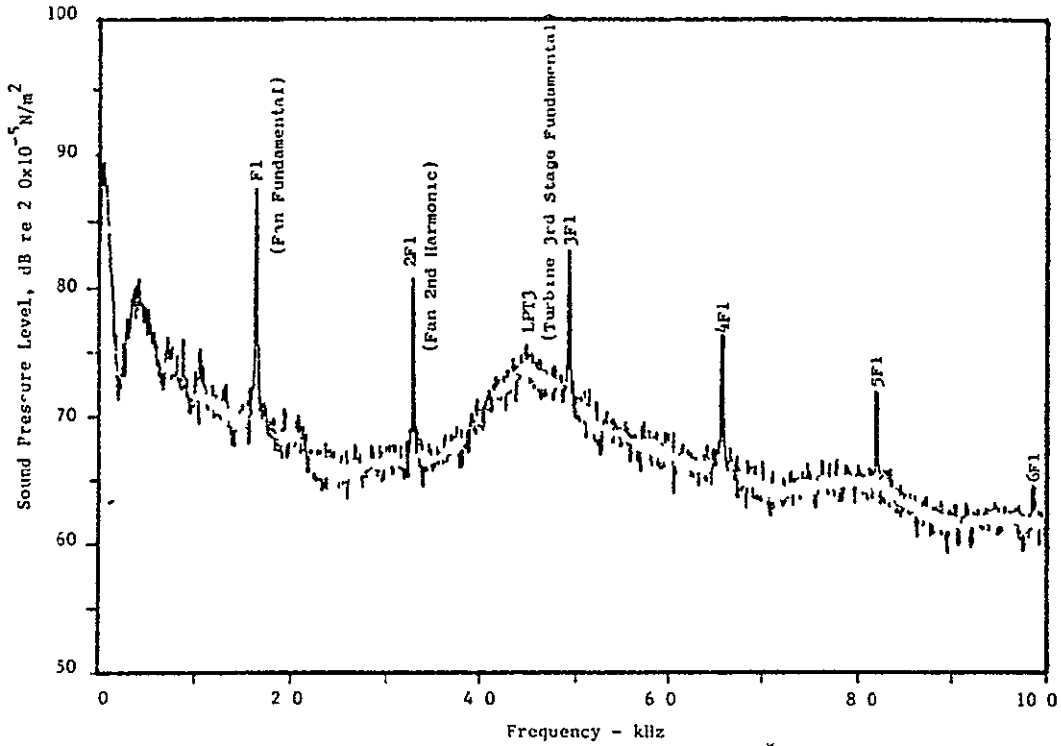


Figure 46. Core Reverser Nozzle Far Field Spectra at 100 Degrees, 45.7 m (150 ft) Arc 88 kN (19,800 lb) Corrected Thrust (High Approach).

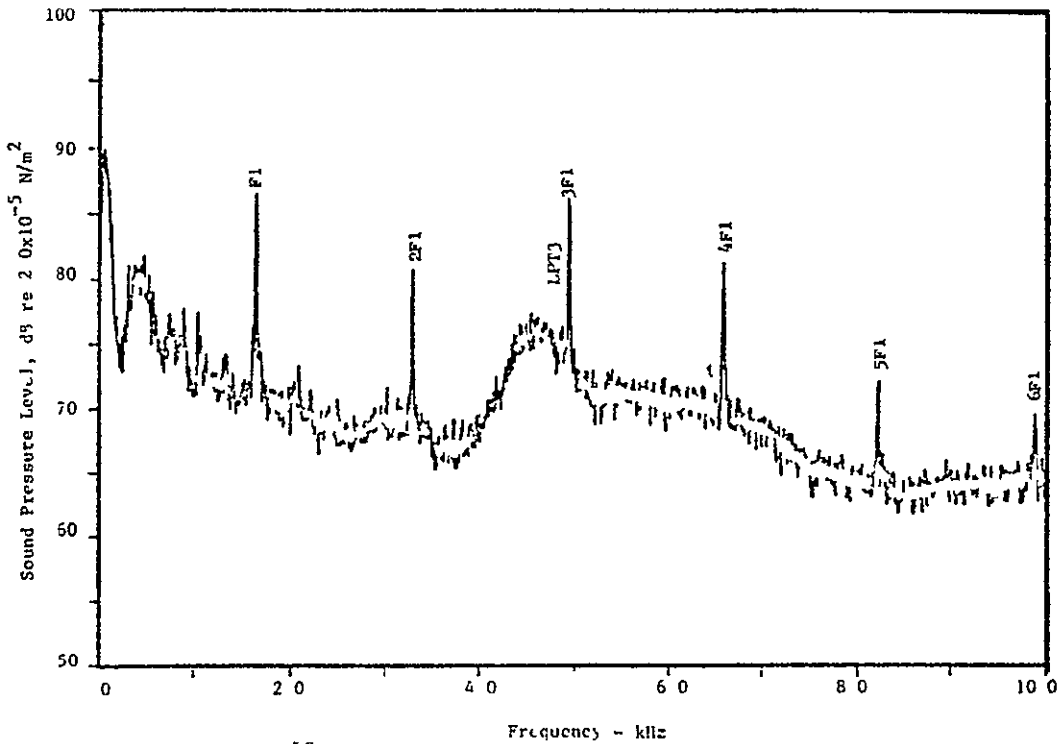


Figure 47. Core Reverser Nozzle Far Field Spectra at 105 Degrees, 45.7 m (150 ft) Arc 88 kN (19,800 lb) Corrected Thrust (High Approach).

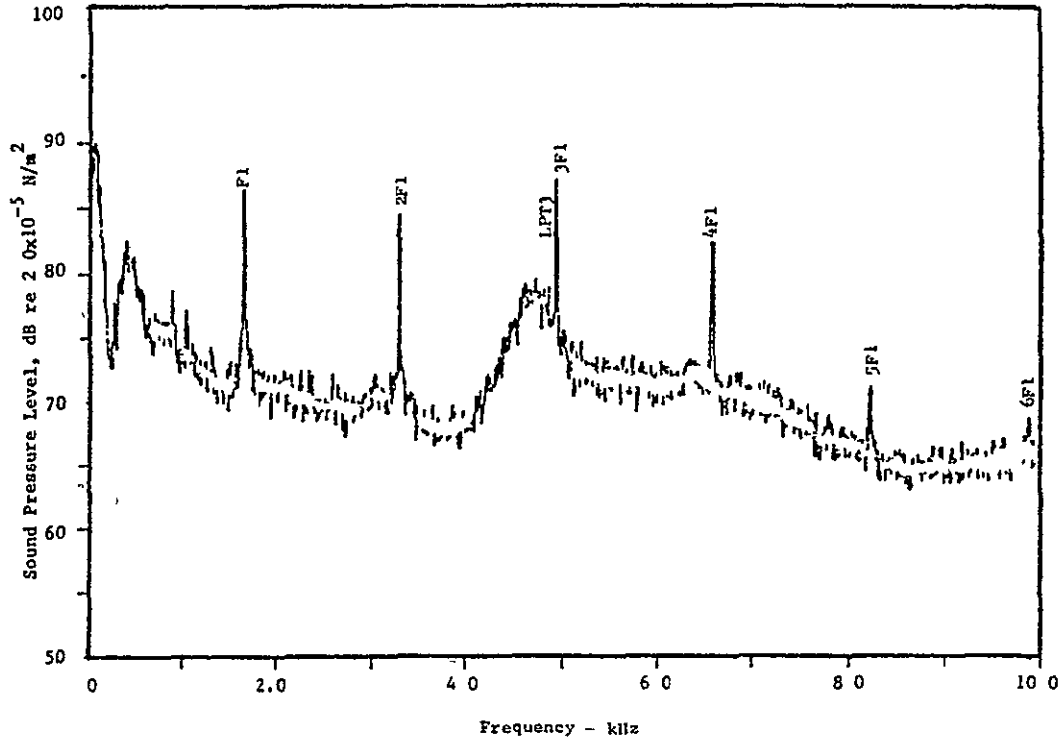


Figure 48. Core Reverser Nozzle Far Field Spectra at 110 Degrees, 45.7 m (150 ft) Arc 88 kN (19,800 lb) Corrected Thrust (High Approach).

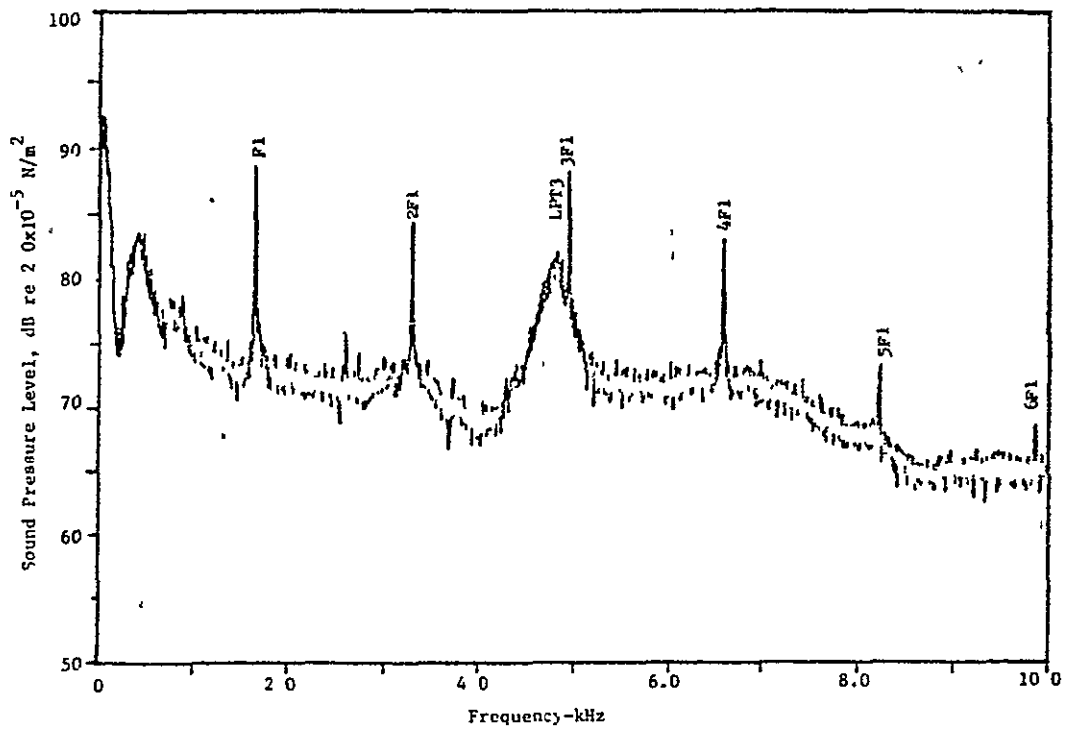


Figure 49. Core Reverser Nozzle Far Field Spectra at 115 Degrees, 45.7 m (150 ft) Arc 88 kN (19,800 lb) Corrected Thrust (High Approach).

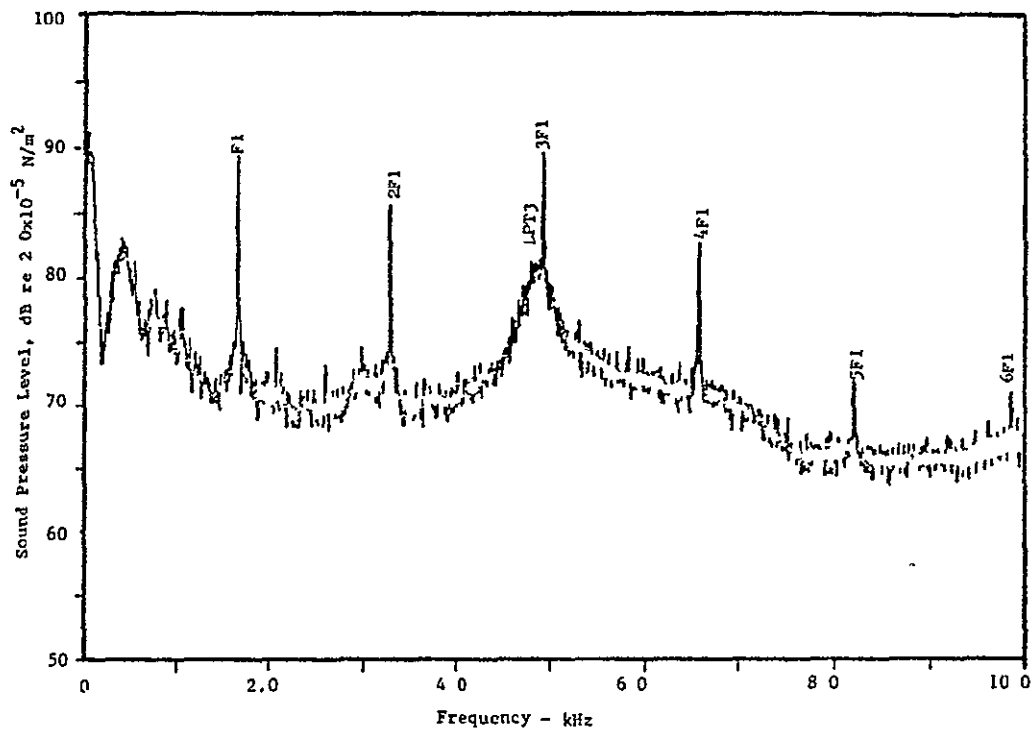


Figure 50. Core Reverser Nozzle Far Field Spectra at 120 Degrees, 45.7 m (150 ft) Arc 88 kN (19,800 lb) Corrected Thrust (High Approach).

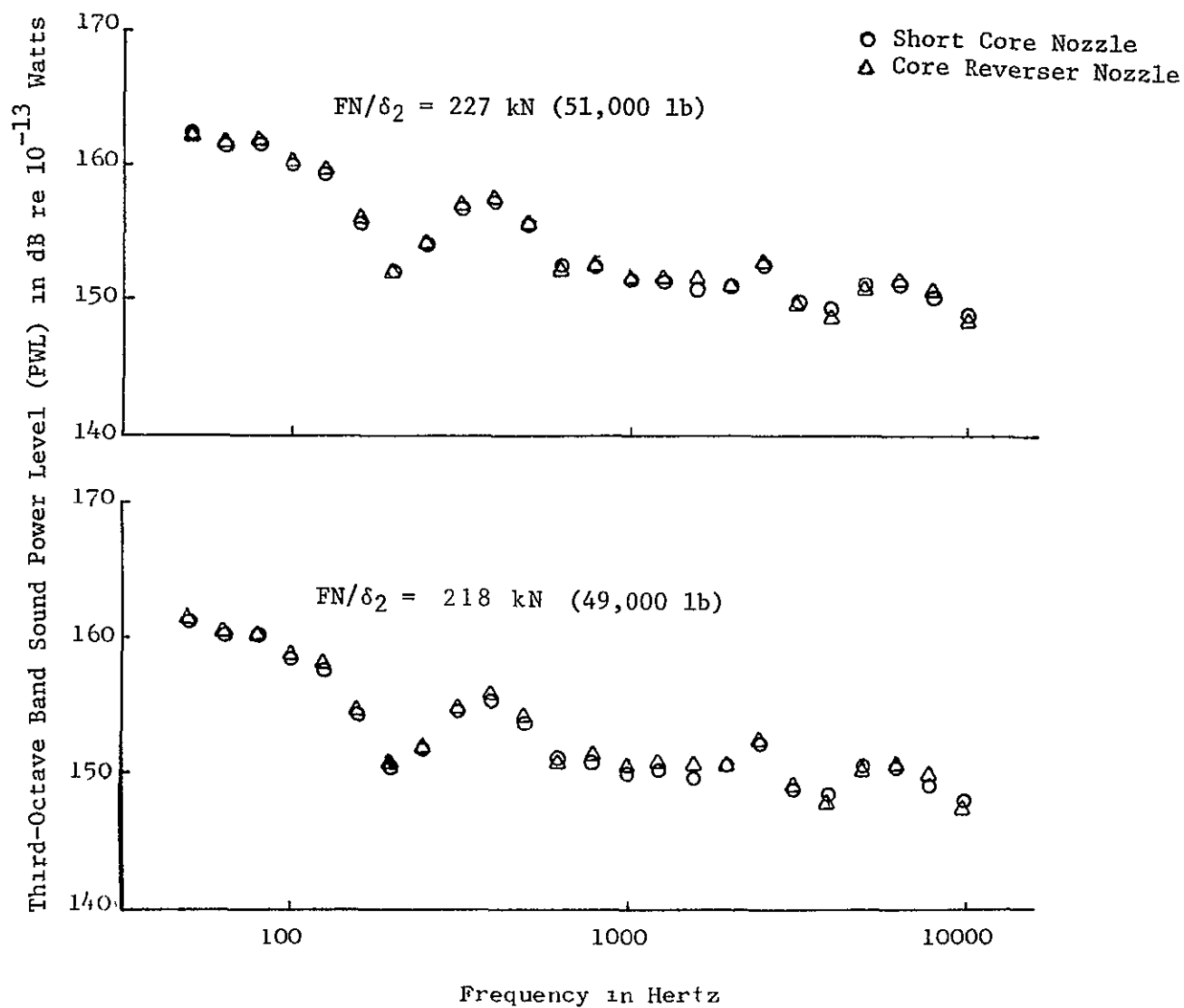


Figure 51. Power Level Comparison of Short Core Nozzle and Core Reverser Nozzle on CF6-50 Engine at Takeoff Power.

NO 31462 SOUND ANALYZER 1/3 OCTAVE BANDS  
 IN STOCK DIRECT FROM CODEX BOOK CO. NORWOOD, MASS 02062  
 PRINTED IN U.S.A.  
 Codex GRAPH PAPER

ADD 49 DB TO OBTAIN OCTAVE BAND LEVEL

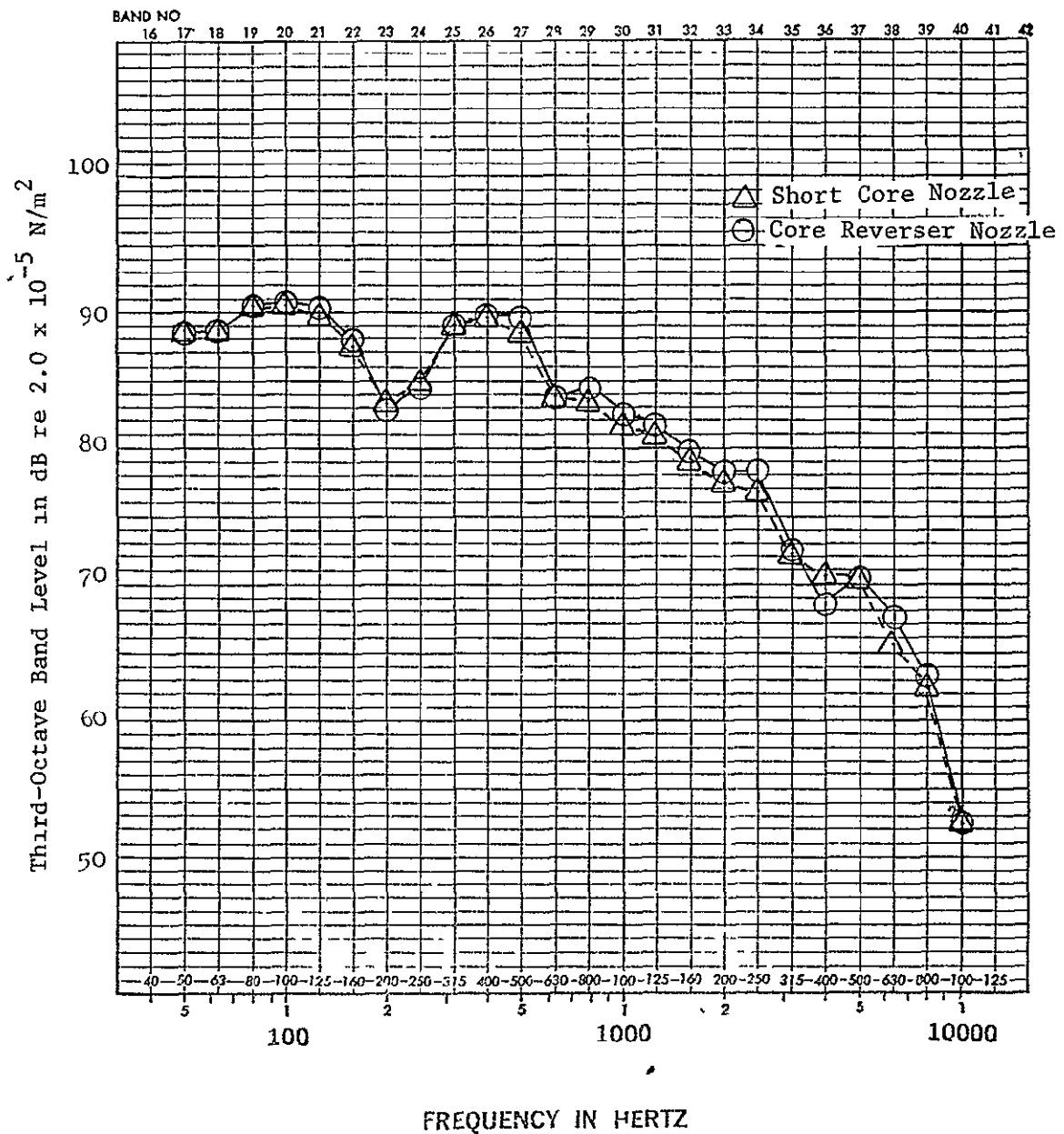


Figure 52. 1/3 Octave Spectrum Comparison of Short Core Nozzle and Core Reverser Nozzle at 130 Degrees 305 m (1,000 ft) Sideline and 217 kN (48,800 lb) Corrected Thrust (Takeoff).

ORIGINAL PAGE IS  
OF POOR QUALITY

ADD 4.9 DB TO OBTAIN OCTAVE BAND LEVEL

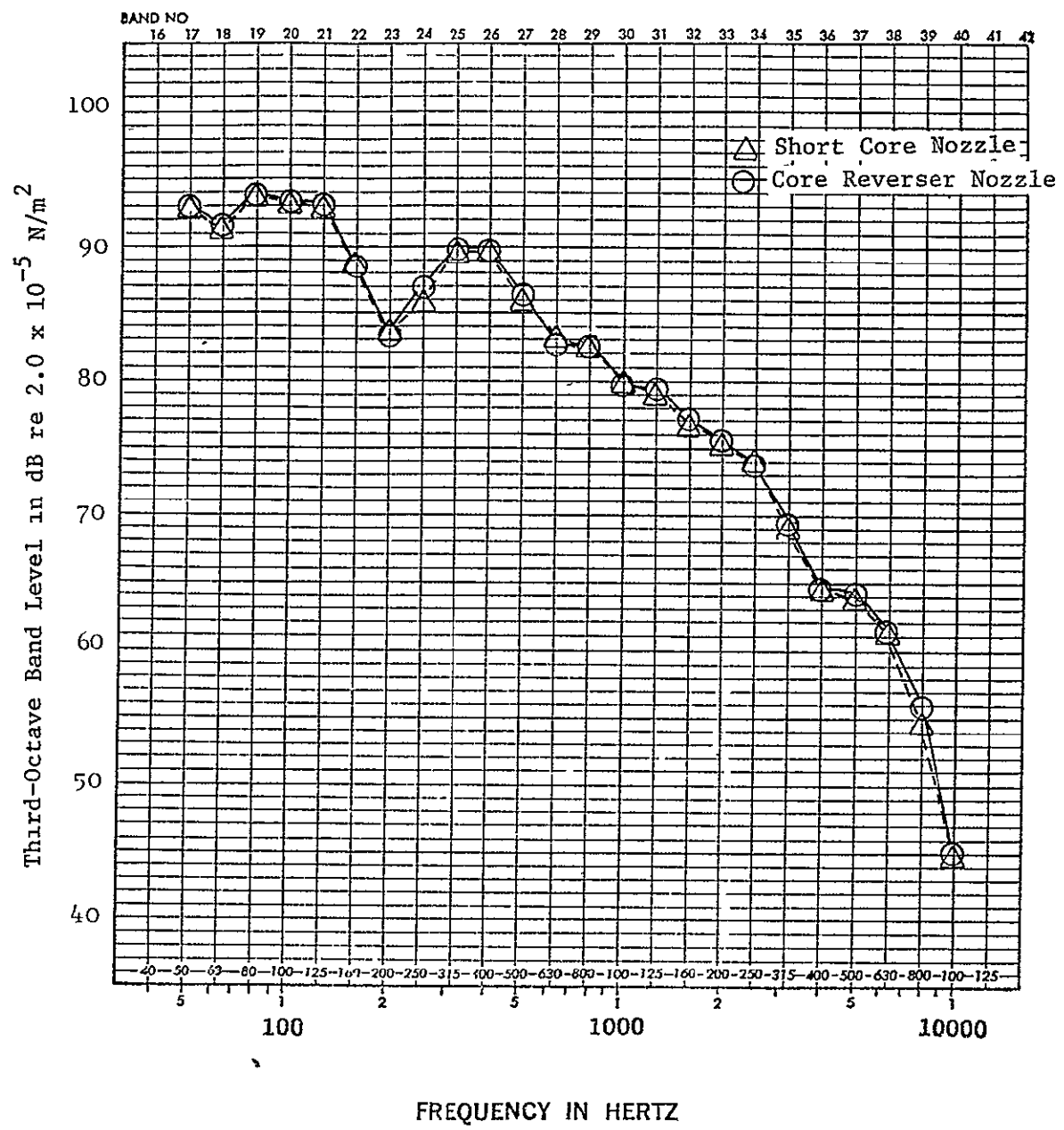


Figure 53. 1/3 Octave Spectrum Comparison of Short Core Nozzle and Core Reverser Nozzle at 140 Degrees 305 m (1,000 ft) Sideline and 217 kN (48,800 lb) Corrected Thrust (Takeoff).

ADD 49 DB TO OBTAIN OCTAVE BAND LEVEL.

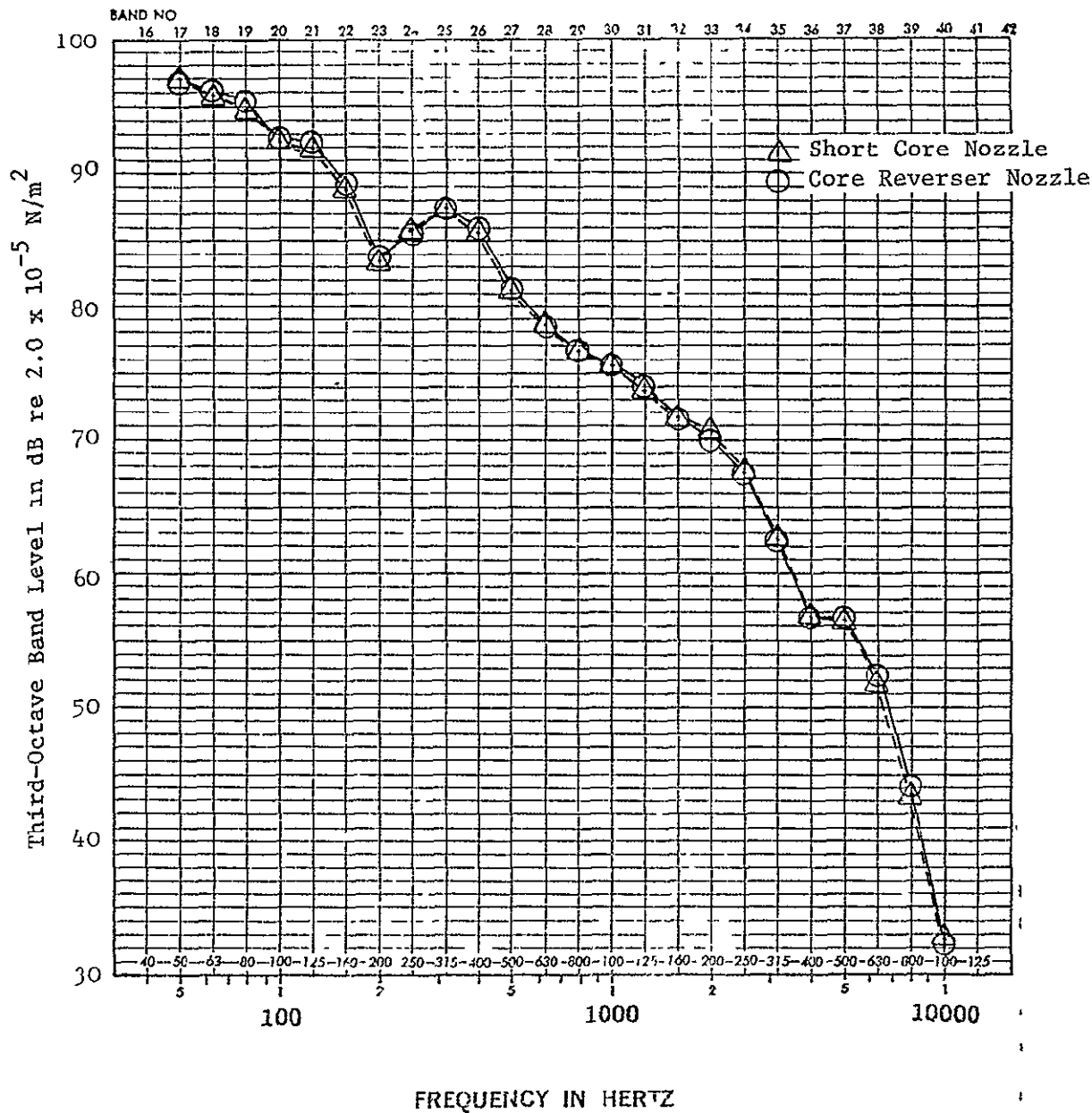


Figure 54. 1/3 Octave Spectrum Comparison of Short Core Nozzle and Core Reverser Nozzle at 150 Degrees 305 m (1,000 ft) Sideline and 217 kN (48,800 lb) Corrected Thrust (Takeoff).

ADD 49 DB TO OBTAIN OCTAVE BAND LEVEL

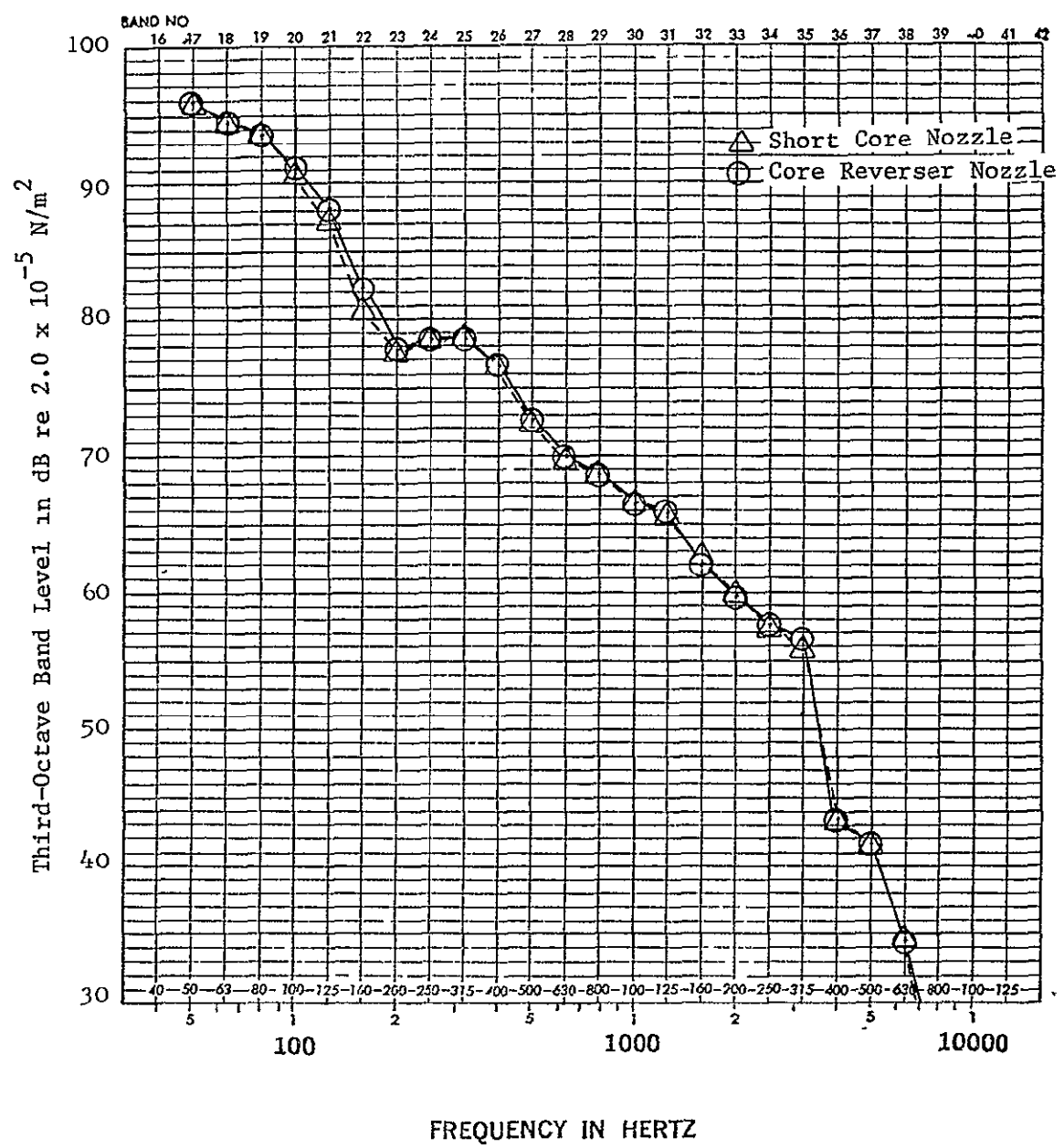


Figure 55. 1/3 Octave Spectrum Comparison of Short Core Nozzle and Core Reverser Nozzle at 160 Degrees 305 m (1,000 ft) Sideline and 217 kN (48,800 lb) Corrected Thrust (Takeoff).



ADD 49 DB TO OBTAIN OCTAVE BAND LEVEL

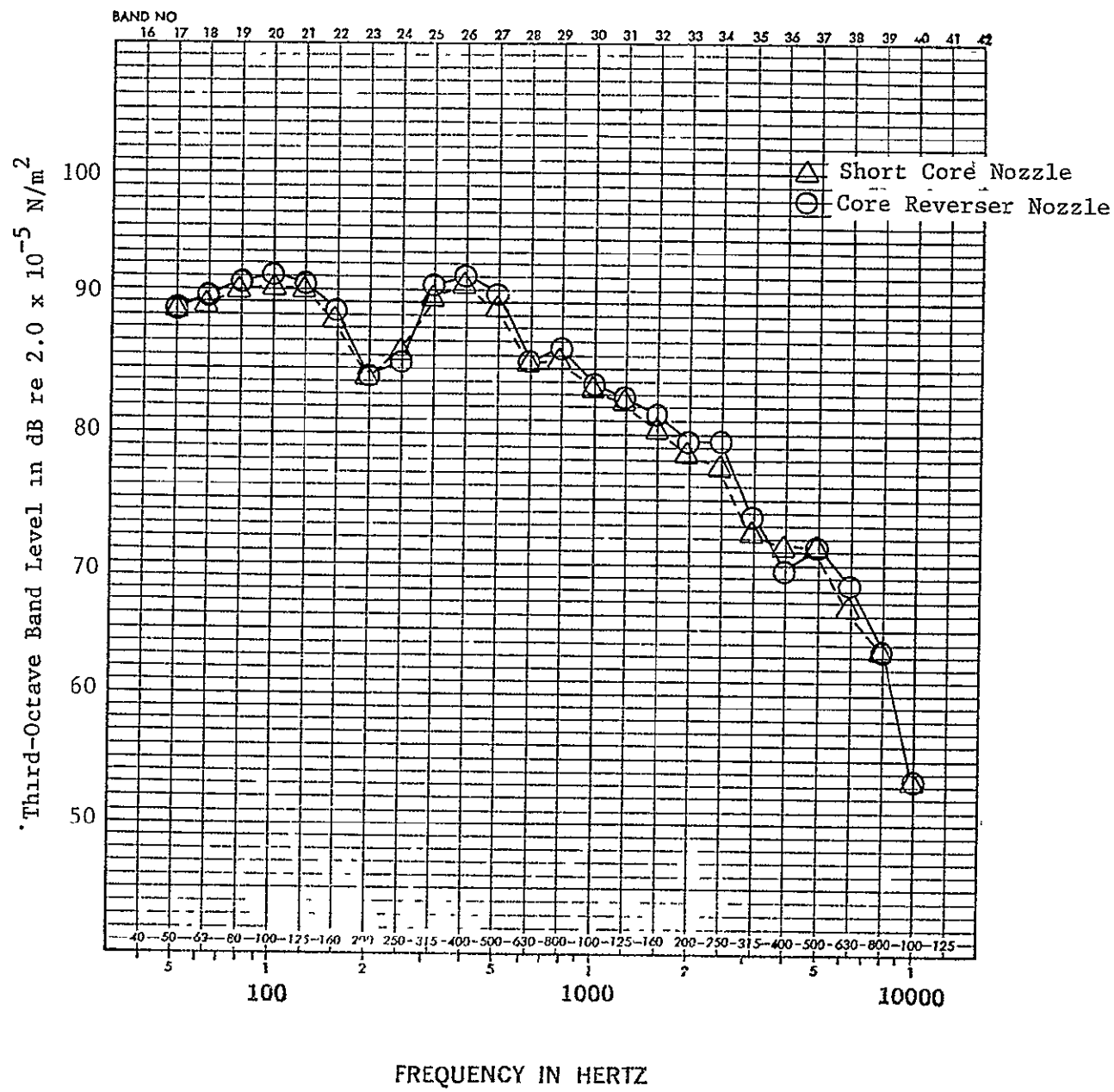


Figure 56. 1/3 Octave Spectrum Comparison of Short Core Nozzle and Core Reverser Nozzle at 130 Degrees 305 m (1,000 ft) Sideline and 228 kN (51,200 lb) Corrected Thrust (Takeoff).

PRINTED IN U.S.A.

GRAPH PAPER

ADD 4.9 DB TO OBTAIN OCTAVE BAND LEVEL

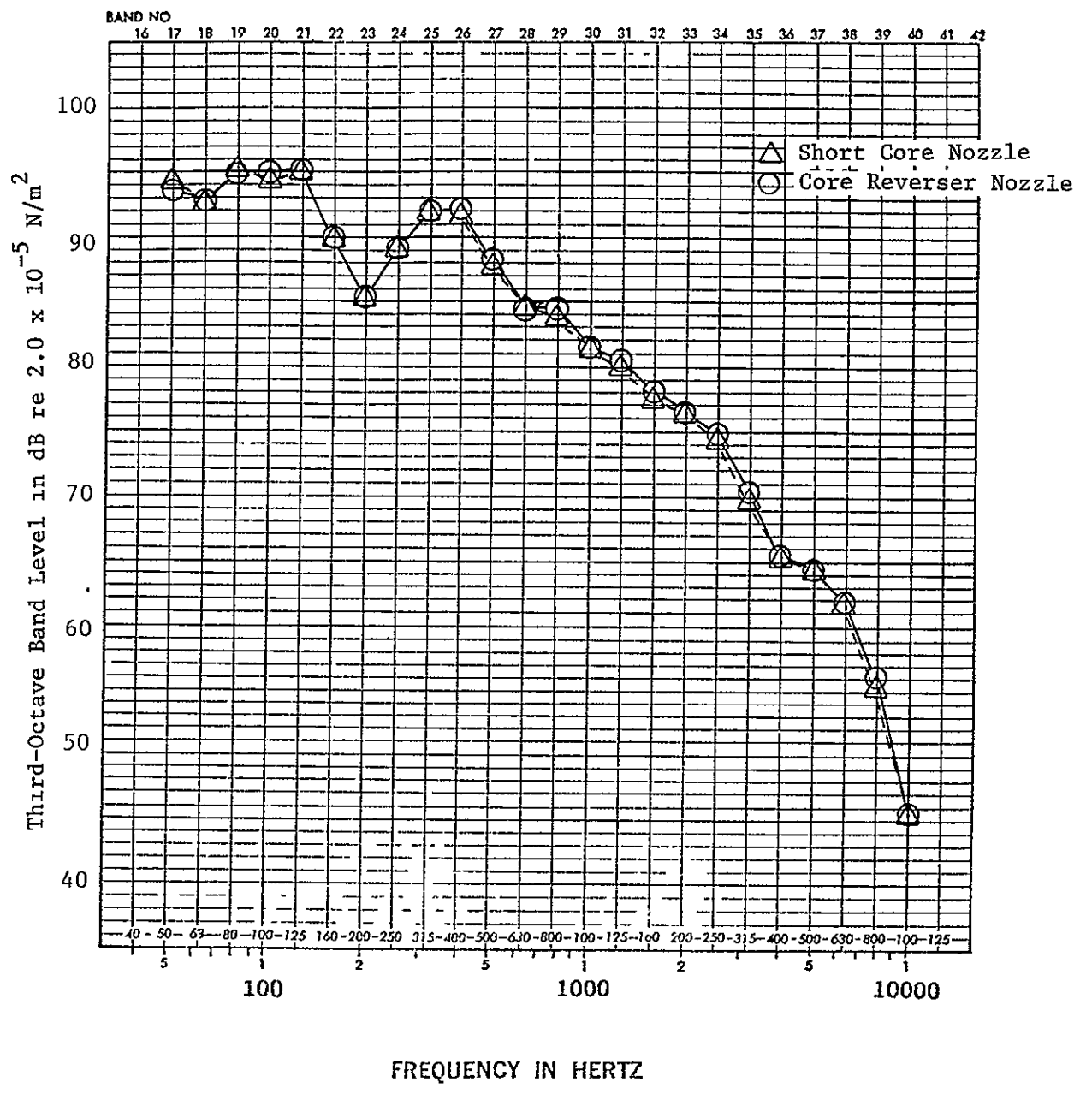


Figure 57. 1/3 Octave Spectrum Comparison of Short Core Nozzle and Core Reverser Nozzle at 140 Degrees 305 m (1,000 ft) Sideline and 228 kN (51,200 lb) Corrected Thrust (Takeoff).

ADD 49 DB TO OBTAIN OCTAVE BAND LEVEL

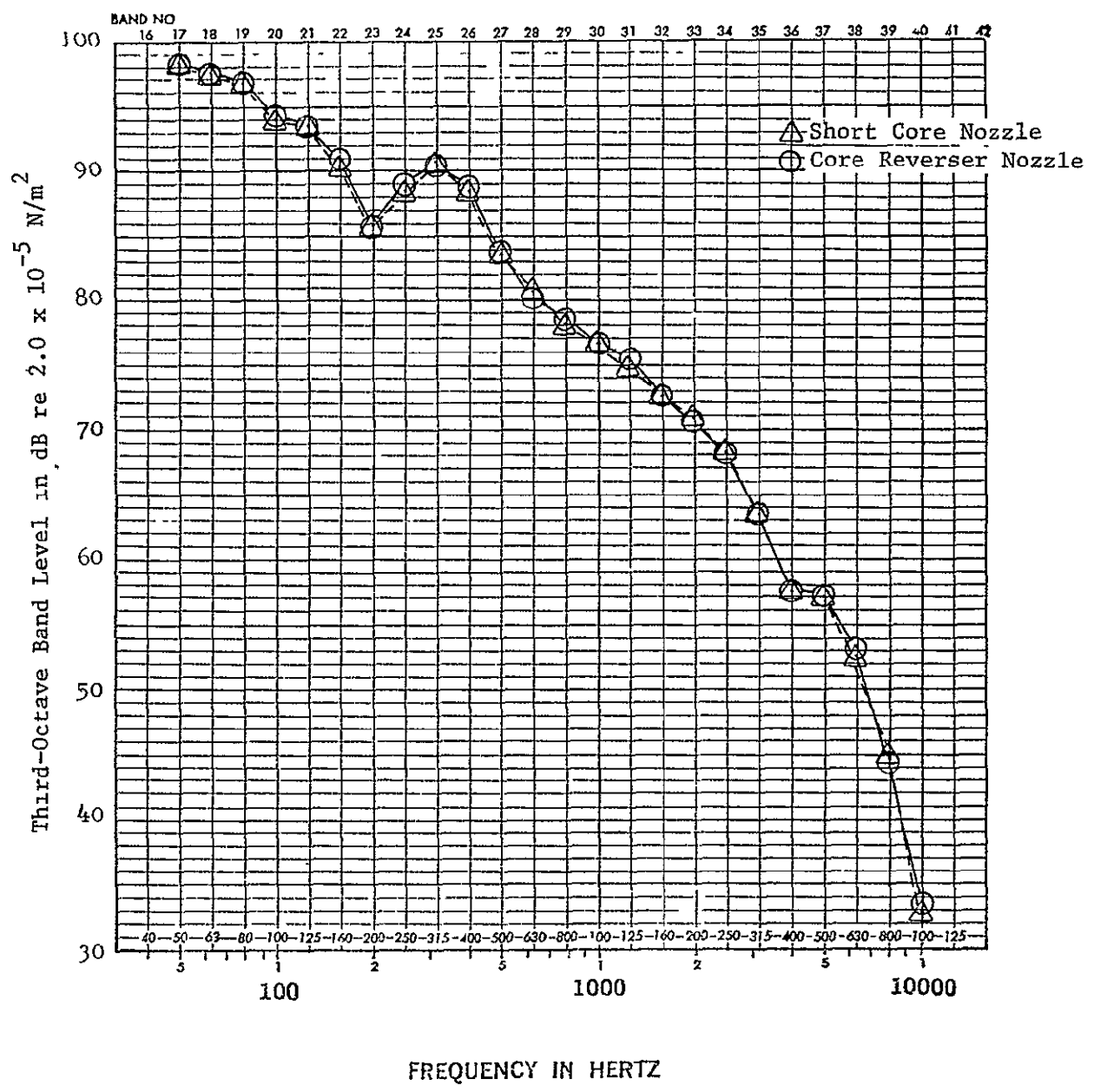


Figure 58. 1/3 Octave Spectrum Comparison of Short Core Nozzle and Core Reverser Nozzle at 150 Degrees 305 m (1,000 ft) Sideline and 228 kN (51,200 lb) Corrected Thrust (Takeoff).

ADD 4.9 DB TO OBTAIN OCTAVE BAND LEVEL

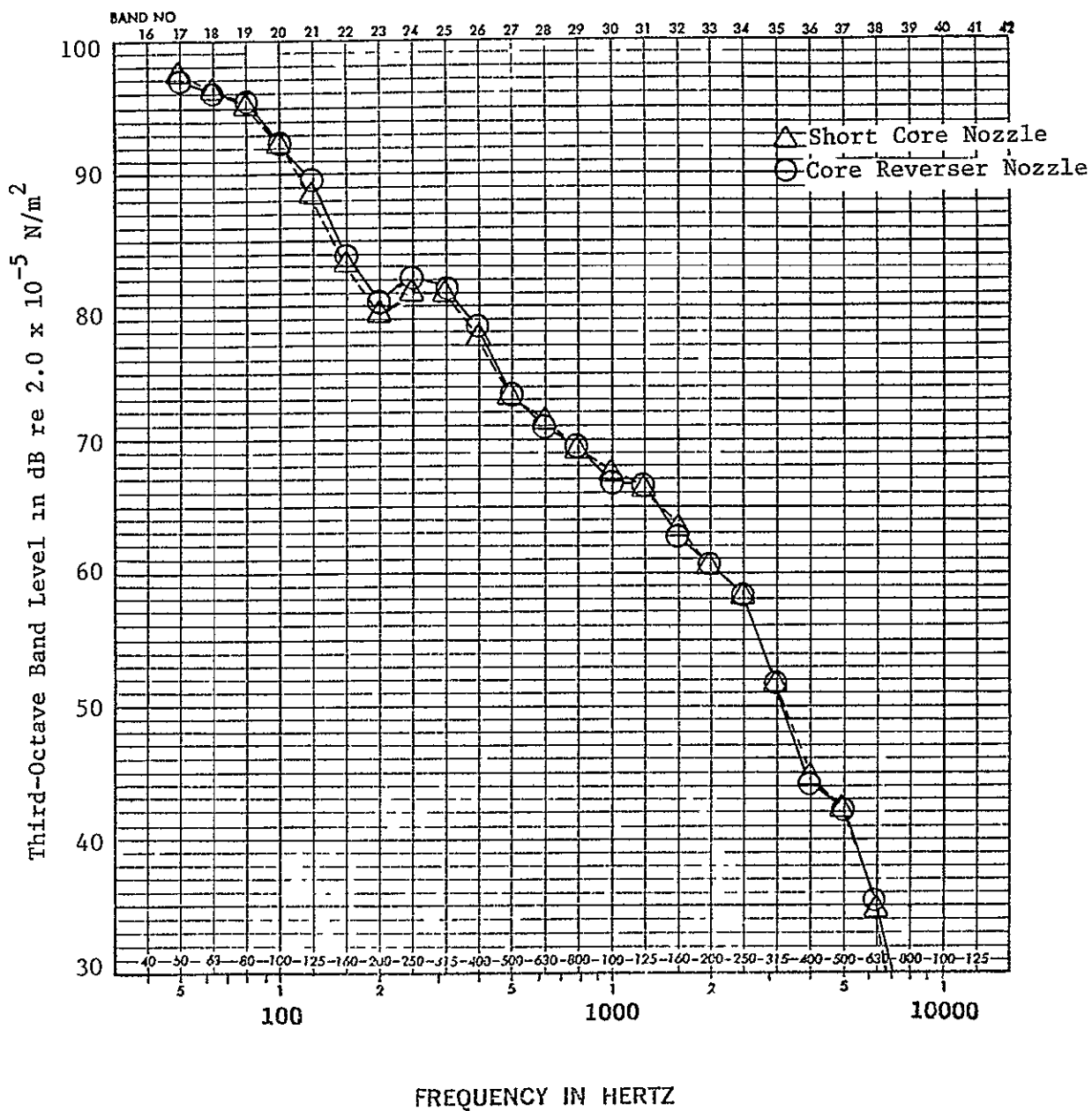


Figure 59. 1/3 Octave Spectrum Comparison of Short Core Nozzle and Core Reverser Nozzle at 160 Degrees 305 m (1,000 ft) Sideline and 228 kN (51,200 lb) Corrected Thrust (Takeoff).

## Low Pressure Turbine Noise

LPT noise suppression resulting from the acoustic treatment in the core nozzle was expected to be similar between the Short Core Nozzle and Core Reverser Nozzle configurations based on previous rectangular duct testing at temperatures and flow velocities which simulated the engine cycle. The rectangular duct testing, however, did not account for the complex shape of the real core duct. The design of the acoustic treatment proper was not changed between the core nozzles. Unfortunately, test scheduling difficulties, due to adverse weather conditions, did not permit comparative tests using the sound separation probe to evaluate treatment suppression performance between the nozzles.

Results from a 5 Hz band width spectrum analysis of the core nozzle data and from a narrow band analysis of the 45.7 m far field data at 100 through 120 degrees for a typical high approach power setting (88 kN) are shown in Figures 60 and 61. The Short Core Nozzle core probe data (immersion No. 1), as shown in Figure 60, clearly shows the fundamental BPF tones associated with each turbine stage, and the dominance of the third stage tone. By comparisons, the far field data show no discernible turbine tones.

The phenomenon of "haystacking" as observed in the far field narrow band spectra for the third stage tone has received considerable attention in the literature discussing turbine noise generation. Only the salient features of the mechanism will be discussed here. A detailed discussion of the phenomenon is given in Reference 3.

The transformation of the third stage turbine BPF tone into a "haystack" observed in the far field spectra is an apparent result of scattering of the acoustic wave by the core and fan jet turbulence. The observed spectral broadening and amplitude modulation is hypothesized to be primarily produced by propagation through the jet interface and shear layers. In addition to spectral broadening, the turbulence scattering centers act as the source of the scattered wave. The far field data will exhibit a Doppler shift dependent upon the relative velocity of the turbulent boundary layers at each far field microphone location. For conditions where the energy of the scattered wave is comparable to or less than that of the incident tone, the far field data will exhibit a haystack and an observable tone. The tone will not exhibit a frequency shift even though the peak frequency of the haystack exhibits a Doppler shift.

The far field properties of the third stage turbine BPF, as shown in Figures 41 to 50, are essentially as described above with both engine configurations exhibiting similar behavior. The fourth stage BPF fundamental tone is evident at 105 degrees for the Short Core Nozzle (Figure 42). Evidently, either there is an unknown mechanism that governs the far field propagation of this tone which differs from the scattering process described above, or the haystack amplitude is below the broad band noise in this frequency region.

A composite of pressure levels which represent the envelope of pressure amplitudes measured at the eight transducer positions (see Section 6.3) is

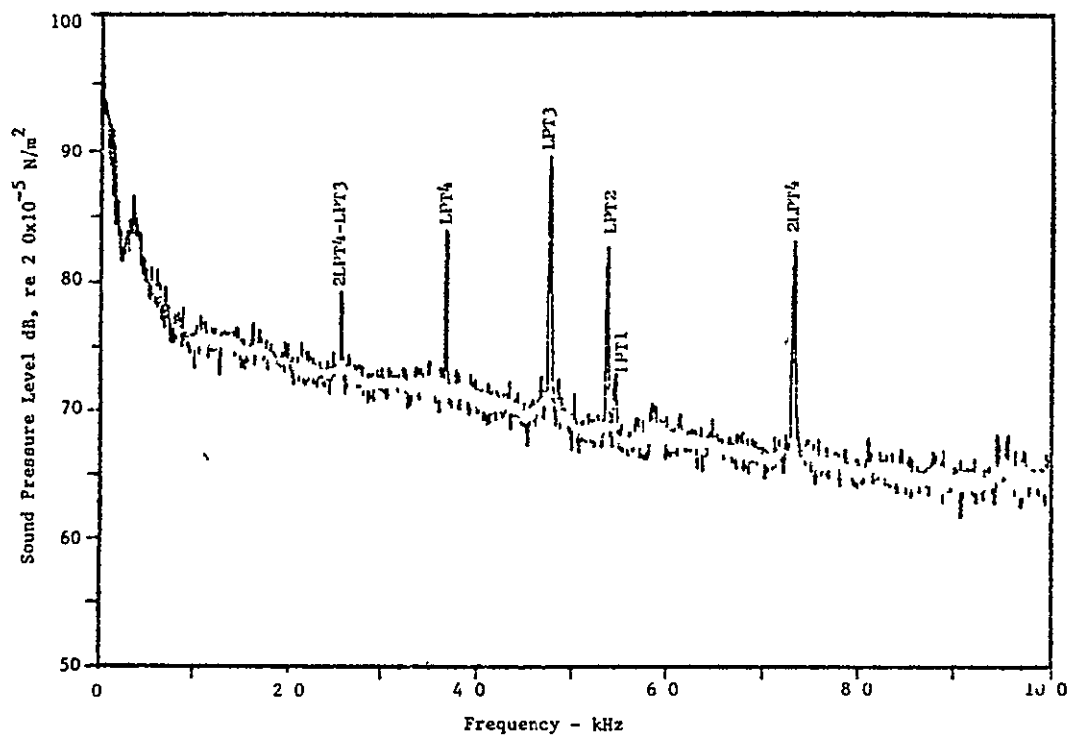


Figure 60. Short Core Nozzle Core Probe Spectrum at Immersion No. 1  
88 kN (19,800 lb) Corrected Thrust (High Approach).

Sound Pressure Level, dB re  $2.0 \times 10^{-5}$  N/m<sup>2</sup>

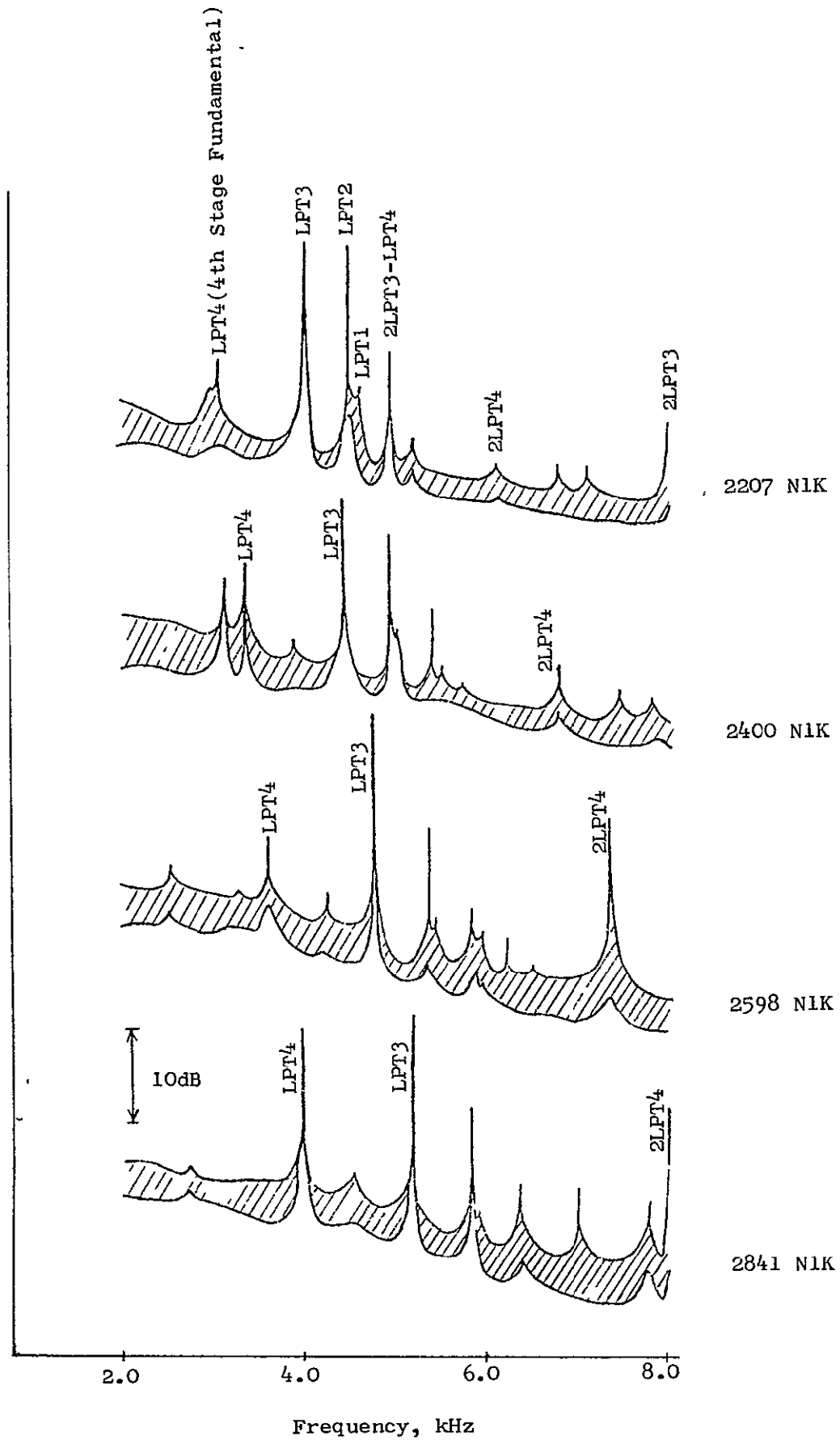


Figure 61. Short Core Nozzle Probe Measured Sound Pressure Level Envelope of Eight Spectra, 20 Hz Band Width.

shown in Figure 61 for four corrected fan speeds spanning the range of approach power settings. A 20 Hz band width tracking filter was used to reduce the data. The blade passing frequencies of the low pressure turbine (128, 126, 112 and 86 blades, respectively, for the first through fourth stages) are seen as distinct tones. The third stage fundamental is always a predominant feature of the core probe spectrum. Second harmonics of the tones as well as several sum and difference tones produced by tone modulation through blade rows are also observed. Broad band levels remained fairly uniform across the nozzle, but tone levels varied significantly, even between adjacent positions.

The power levels of the strongest tones were calculated from the logarithmic average of all the pressure measurements and are shown in Figure 62 for the four values of corrected fan speed. The duct cross section was assumed to be composed of eight equal area regions with uniform sound pressure level distributions over each area. The power level was calculated as shown below.

$$\overline{PWL} = \overline{SPL} + 10 \text{ Log } A + 20 \text{ Log } (1.0 + 0.707M) + 10 \text{ Log } (P_0/P_s \sqrt{T/T_0}) + 10 \text{ dB}$$

where.  $\overline{PWL}$  = space average PWL, dB re  $10^{-13}$  watts

$\overline{SPL}$  = space average SPL, dB re  $2.0 \times 10^{-5}$  N/m<sup>2</sup>

A = area of the nozzle (m<sup>2</sup>)

M = duct Mach number

$P_0/P_s$  = ratio of ambient to duct static pressure

$T/T_0$  = ratio of duct total temperature to ambient temperature

The spectral broadening of both the third stage low pressure turbine BFP fundamental and the fan BFP third harmonic tones in the far field results in an overlap of the broad band noise from each component. Correlation of the far field data with the source is inconclusive due to the nonlinear scattering process, preventing the determination of the spectral content due to each component in the frequency regions of interest. Hence, direct evaluation of treatment performance between the two configurations could not be performed. Any conclusions regarding treatment effectiveness drawn from comparing the small spectrum level differences in this frequency region should be regarded as questionable.

#### Community Noise Impact Assessment

Community annoyance as a result of noise produced from aircraft operation is inherently subjective. Annoyance produced by aircraft noise is dependent on sound level, spectrum content, tone content, time duration, and an individ-



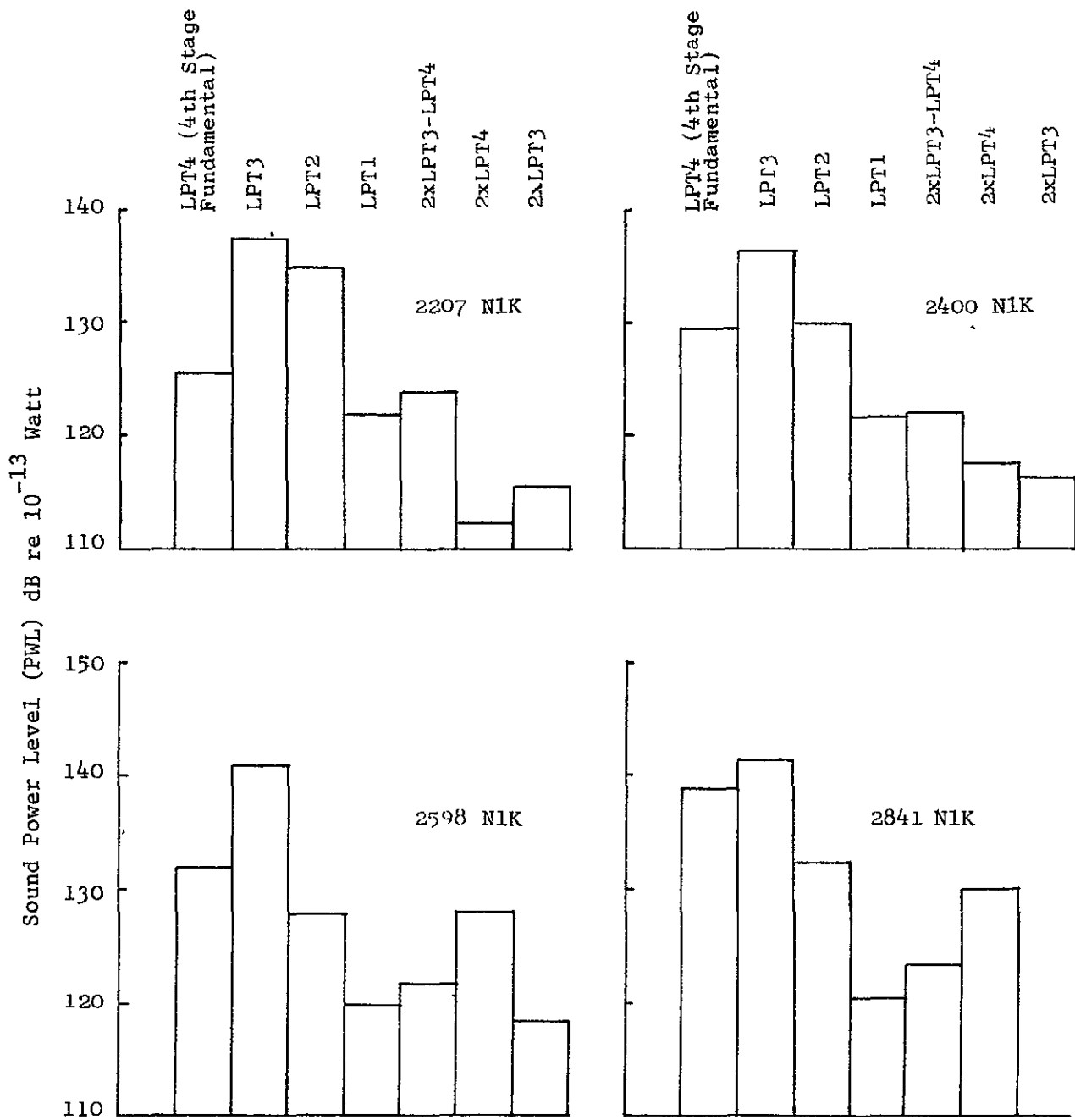


Figure 62. Duct Measured Power Level for the Short Core Nozzle.

ual's perception of the noise. In order to assess community noise annoyance as related to a statistical population sampling that accounts for all of the above variables, the effective perceived noise level (EPNL) was evolved. Current FAA regulations governing aircraft noise are based on EPNL. The regulations specify maximum EPNL as a function of gross takeoff weight for sideline, takeoff (flyover), and approach.

To evaluate the impact of the Short Core Nozzle on the CF6-50 engine community noise levels, simulated EPNL values were analytically obtained using the static noise data from this test. It was assumed that the static PNL data were measured flight levels recorded at typical aircraft velocities. No corrections were applied to estimate flight effects on engine noise. Simulated EPNL values were calculated at power settings typical of the DC-10-30, B-747, and A300B aircraft for approach and takeoff operating conditions. These power conditions and associated altitudes and velocities are presented in Table IV.

An analysis of the simulated EPNL values was performed to determine sample statistics for the population mean and variance for each engine configuration (CF6-50 with the Short Core Exhaust and the CF6-50 with the Core Reverser Nozzle). To assess the community noise impact of the Short Core Nozzle engine configuration, the differences between the average EPNL for each engine configuration at the same thrust were determined and the resulting delta evaluated against the hypothesis that the engine configurations are acoustically equivalent.

A least square fit of the EPNL data as a function of thrust was determined for each engine configuration using an orthogonal polynomial regression model. The EPNL data were then interpolated to the nominal power settings shown in Table V to remove data bias produced from thrust set-point scatter. Sample statistics for each power setting were calculated to obtain the sample mean, unbiased variance for the sample, and the pooled variance for the entire engine configuration data sample. The differences between the sample means (delta) were used to determine the change in community noise obtained with the Short Core Nozzle. The statistical parameters obtained from this analysis that were used to construct confidence bands for the deltas between sample means are summarized in Table VI.

The hypothesis that the engine configurations are acoustically equivalent was evaluated by comparing the magnitude of the deltas to the 90% confidence band for the difference between sample means obtained from the pooled variance, centered about zero. Results of this evaluation are shown in Figure 63. The Short Core Nozzle noise levels are "statistically equivalent" to those of the Core Reverser Nozzle if the delta value lies within the 90% confidence band, "statistically less than" if below the lower band limit, and "statistically greater than" if above the upper band limit.

As shown in Figure 63, the deltas between the subject engine configurations are always within or below the 90% band limits. Based on the above analysis, these results imply that community noise levels for the CF6-50 with the Short Core Nozzle are equivalent to or less than the CF6-50 with the Core Reverser Nozzle engine configuration.

Table IV Typical Flight Operating Conditions for CF6-50 Engine.

Condition	Thrust Range (Max/Min)		Altitude (Max/Min)		Flight Velocity (Max/Min)	
	kN	lbs	m	ft	m/sec	knots
Takeoff	230/200	52,000/46,000	610/305	2000/1000	103/93	200/180
Cutback	170/150	38,000/34,000	610/305	2000/1000	103/93	200/180
High Approach	100/65	23,000/15,000	122/113	400/370	85/77	165/150
Low Approach	70/50	16,000/12,000	122/113	400/370	85/77	165/150

Table V. Nominal Thrust Set Point For Data Groupings.

Thrust		Condition	Nominal Altitude		Nominal Flight Velocity	
N	lbs		m	ft	m/sec	knots
227,962	51,248	Takeoff	305	1000	103	200
216,810	48,741					
204,489	45,971					
168,921	37,975	Cutback	305	1000	103	200
158,477	35,627					
148,491	33,382					
101,686	22,860	High Approach	122	400	85	165
94,654	21,279					
88,079	19,801					
81,958	18,425					
76,291	17,151					
72,341	16,263	Low Approach	122	400	85	165
68,053	15,299					
59,094	13,285					
53,632	12,057					

Table VI. Statistical Parameters.

Condition	Engine Configuration	$\hat{\sigma}^2$	$\nu$	N	t( $\nu$ )	90% Confidence Band Limits on $\Delta EPNL$
Takeoff and Cutback	CF6-50 w/Short Core Nozzle	0.0280	19	3		
	CF6-50 w/Core Reverser Nozzle	0.0595	19	3		
	Pooled	0.0438	38		1.684	$\pm 0.29$
Approach	CF6-50 w/Short Core Nozzle	0.1473	25	3		
	CF6-50 w/Core Reverser Nozzle	0.1572	26	3		
	Pooled	0.1523	51		1.678	$\pm 0.54$
Notes:						
$\sigma^2$ = Pooled unbiased estimate of sample variance						
$\sigma_p^2$ = Pooled unbiased estimate of configuration sample variance						
$\nu$ = Degrees of freedom of sample						
N = Number of data samples comprising sample mean at each nominal thrust						
t( $\nu$ ) = "t" statistic for $\nu$ degrees of freedom, 95th percentile						
90% Confidence Band limits for $H_0: \Delta EPNL = 0$ , $\pm t(\nu) \sigma_p \sqrt{\frac{1}{N_1} + \frac{1}{N_2}}$						
$H_0$ = Statistical hypothesis						
$N_1$ = Number of data samples comprising sample mean of Core Reverser Nozzle at each nominal thrust						
$N_2$ = Number of data samples comprising sample mean of Short Core Nozzle at each nominal thrust						

$\Delta$ EPNL - dB re EPNL of the CF6-50 Engine with the Core Reverser Nozzle

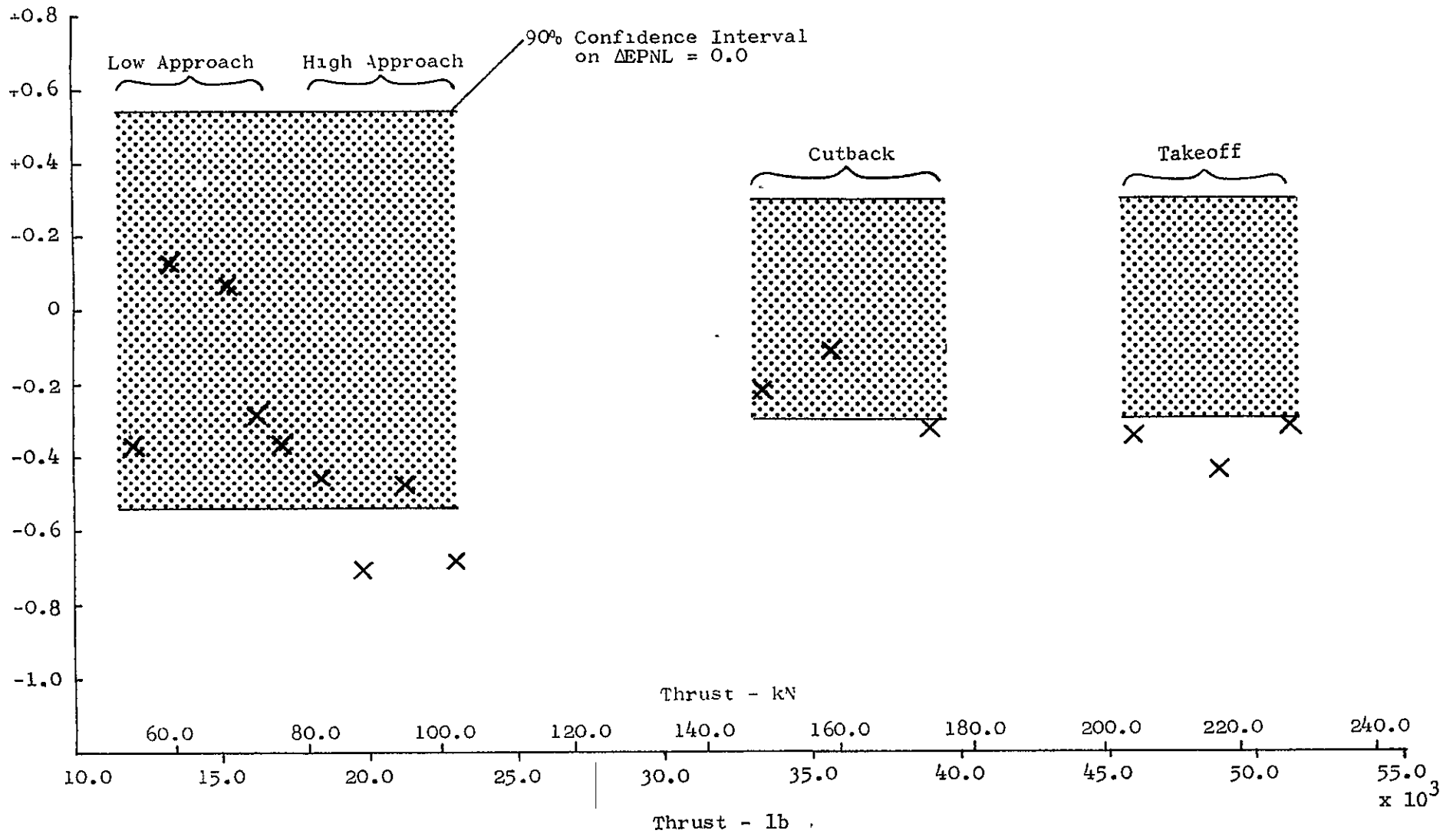


Figure 63. Change in Community Noise Obtained With the CF6-50 Engine With the Short Core Nozzle.

Based upon static back-to-back testing, the CF6-50 engine with a Short Core Nozzle produces almost identical community noise levels as the CF6-50 engine with a Core Reverser Nozzle when operated at identical corrected thrust and flight conditions. Results presented within this report document that the dominant noise components of the CF6-50 engine (fan, LPT, and core jet) were not significantly impacted by the Short Core Nozzle.

Small changes in the directivity pattern of the third stage LPT fundamental BPF tone were observed for the Short Core Nozzle when compared to the Core Reverser Nozzle. The acoustic treatment suppression performance of the Short Core Nozzle may have produced this change but no definitive conclusions could be drawn as a result of the LPT third stage tone modulation and scattering by engine exhaust turbulence. It is predicted that this result will not affect aircraft flyover noise characteristics with the possible exception of aircraft operating at very low power approach flight conditions. Even at this condition, however, the overall system EPNL should not increase.

## 7.0 ENDURANCE TEST

### 7.1 TEST CONFIGURATION

Endurance testing of the Short Core Nozzle was conducted on a CF6-50C configuration engine. Standard flight-type fan reverser doors and prototype core cowling were installed on the engine. The Short Core Nozzle outer cowl and centerbody shown in Figures 64 through 66 were installed.

### 7.2 TEST FACILITY

In endurance testing of engine cowling, it has proven more representative to perform these tests in an outdoor test site rather than an enclosed test cell to avoid pressure/noise perturbations from the cell walls. For reasons of site availability, it was decided to utilize the Edwards Flight Test Center outdoor test facility for endurance testing. The test site used was General Electric's Test Site MB4 which is shown in Figure 67.

### 7.3 TEST PROCEDURE

Following the mechanical checkout, break-in run, and a short engine performance analysis test, the engine was placed on "C" cycle endurance. A "C" cycle is a 15 minute cycle that simulates the transient movements made during a typical airline flight. Figure 68 gives a graphical presentation of the cycle. The mission mix of exhaust gas temperatures was selected to simulate the distribution of takeoff temperatures seen in airline service. If the required exhaust gas temperature could not be reached without exceeding fan speed limits, the engine was shut down and bleed pipes were installed. The mixture of cycle was.

<u>Takeoff EGT, ° C (° F)</u>	<u>Number of Cycles</u>
Below 878 (1613)	150
879 (1614) - 914 (1678)	350
915 (1679) - 942 (1728)	300
943 (1729) - 950 (1742)	100
951 (1743) - 960 (1760)	<u>100</u>
Total	1000

### 7.4 TEST RESULTS

A detailed visual inspection upon completion of endurance testing of the Short Core Nozzle indicated that there was no sign of distress after the completion of the 1000 endurance cycles. A formal dye-penetrant inspection corroborated these findings.



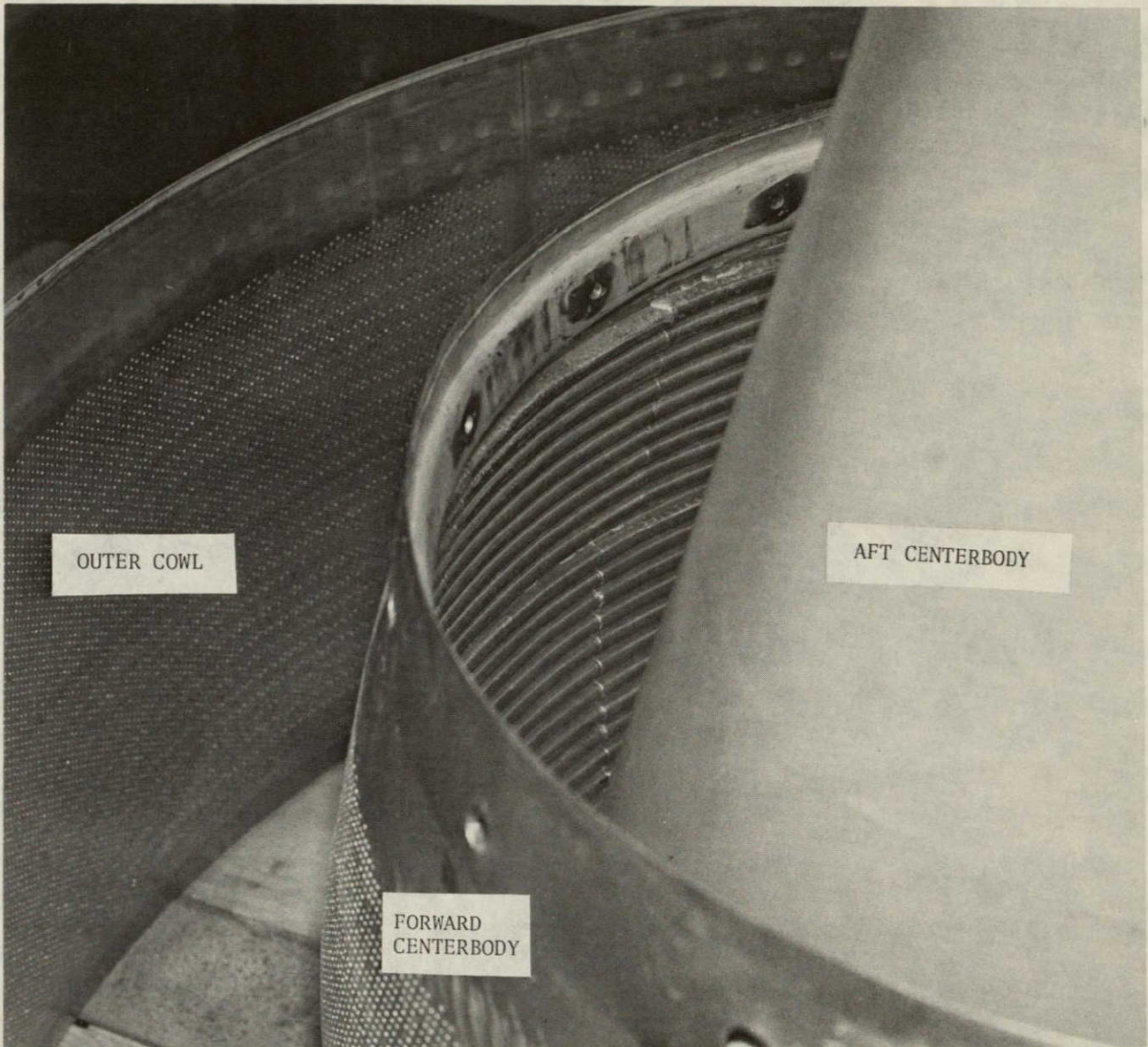


Figure 64. Disassembled Short Core Nozzle - View A.

ORIGINAL PAGE IS  
OF POOR QUALITY



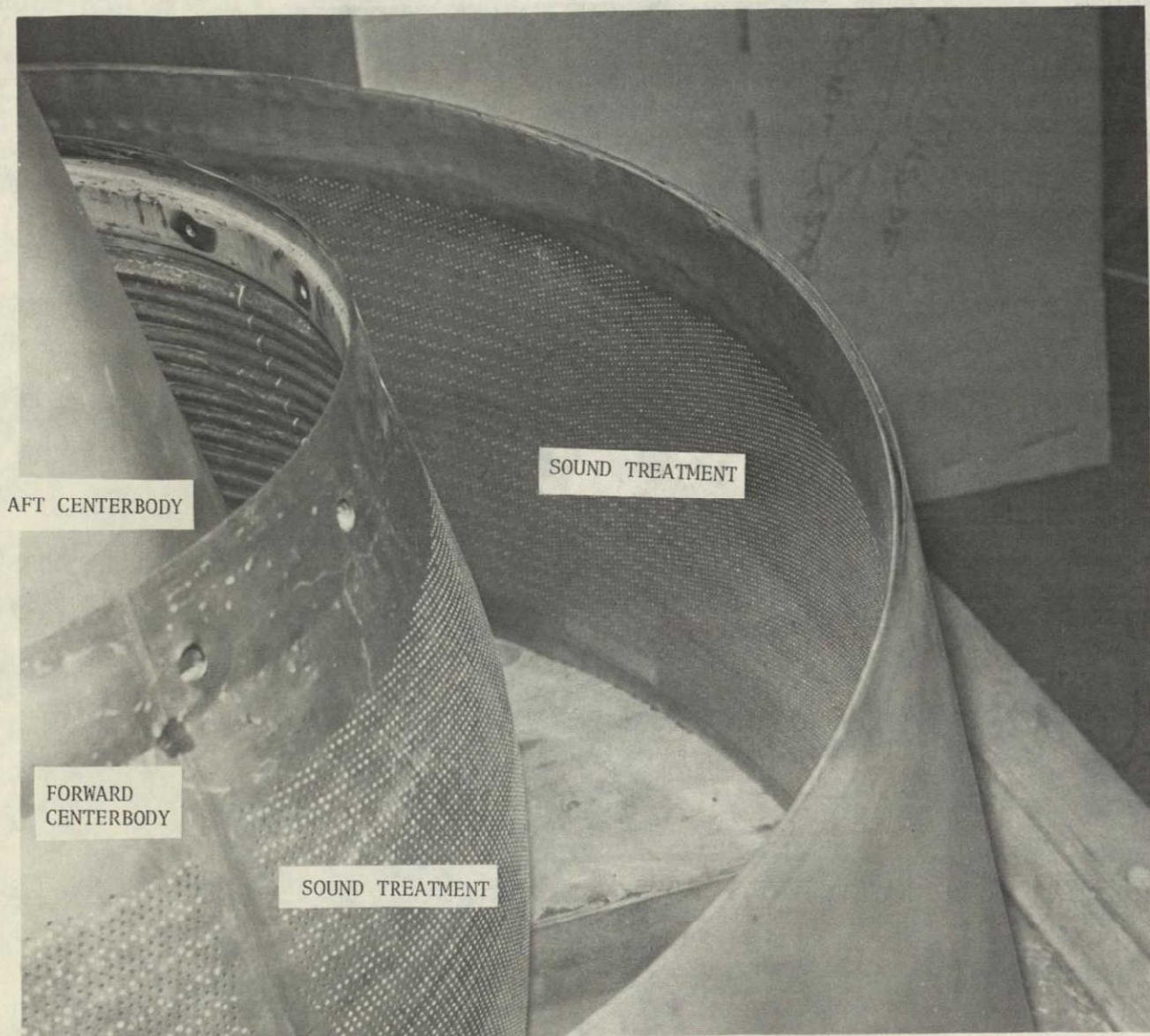


Figure 65. Disassembled Short Core Nozzle - View B.

21 3049  
PAGE 12  
FOUR QUALITY

ORIGINAL PAGE IS  
OF POOR QUALITY

c-2



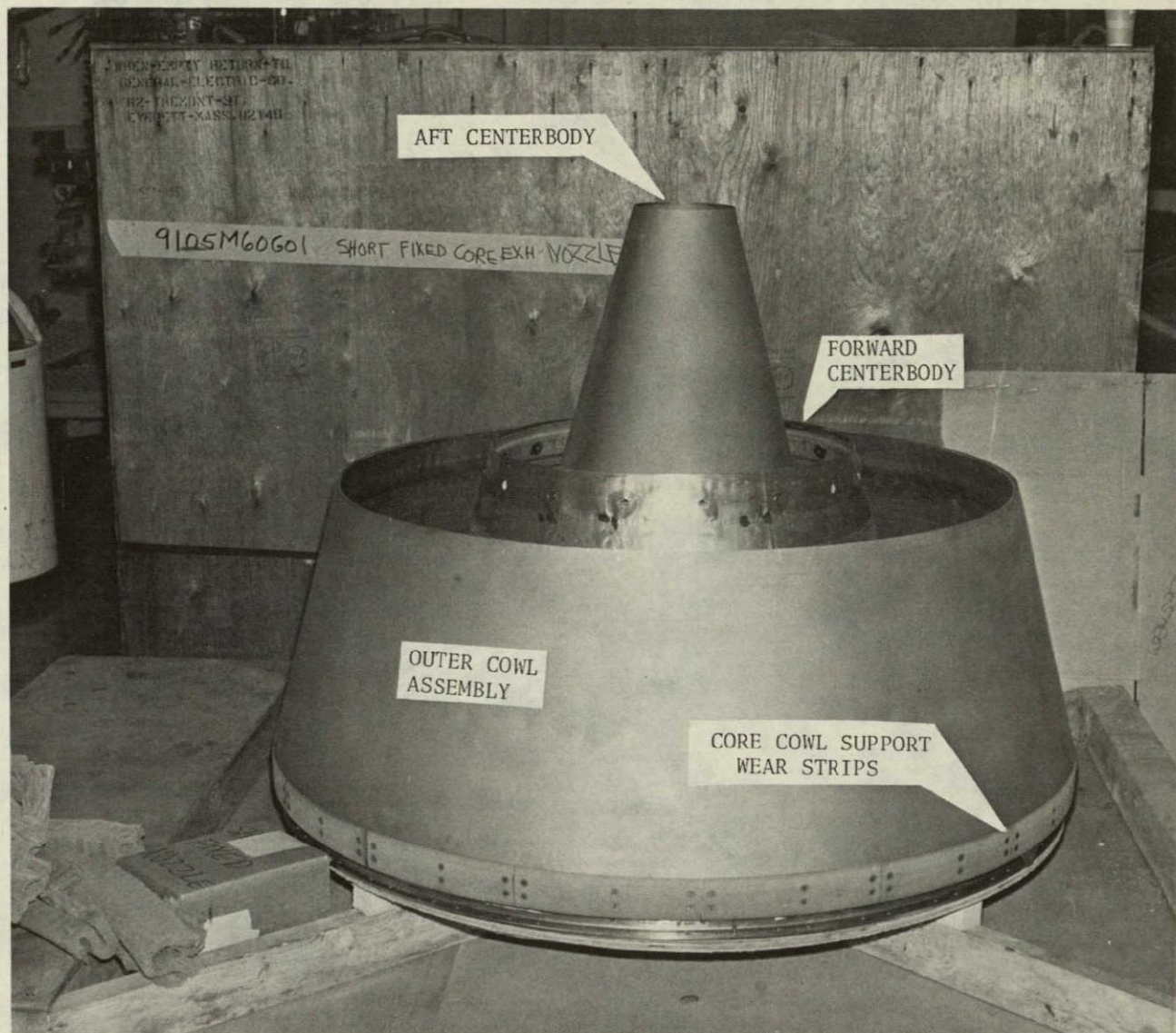
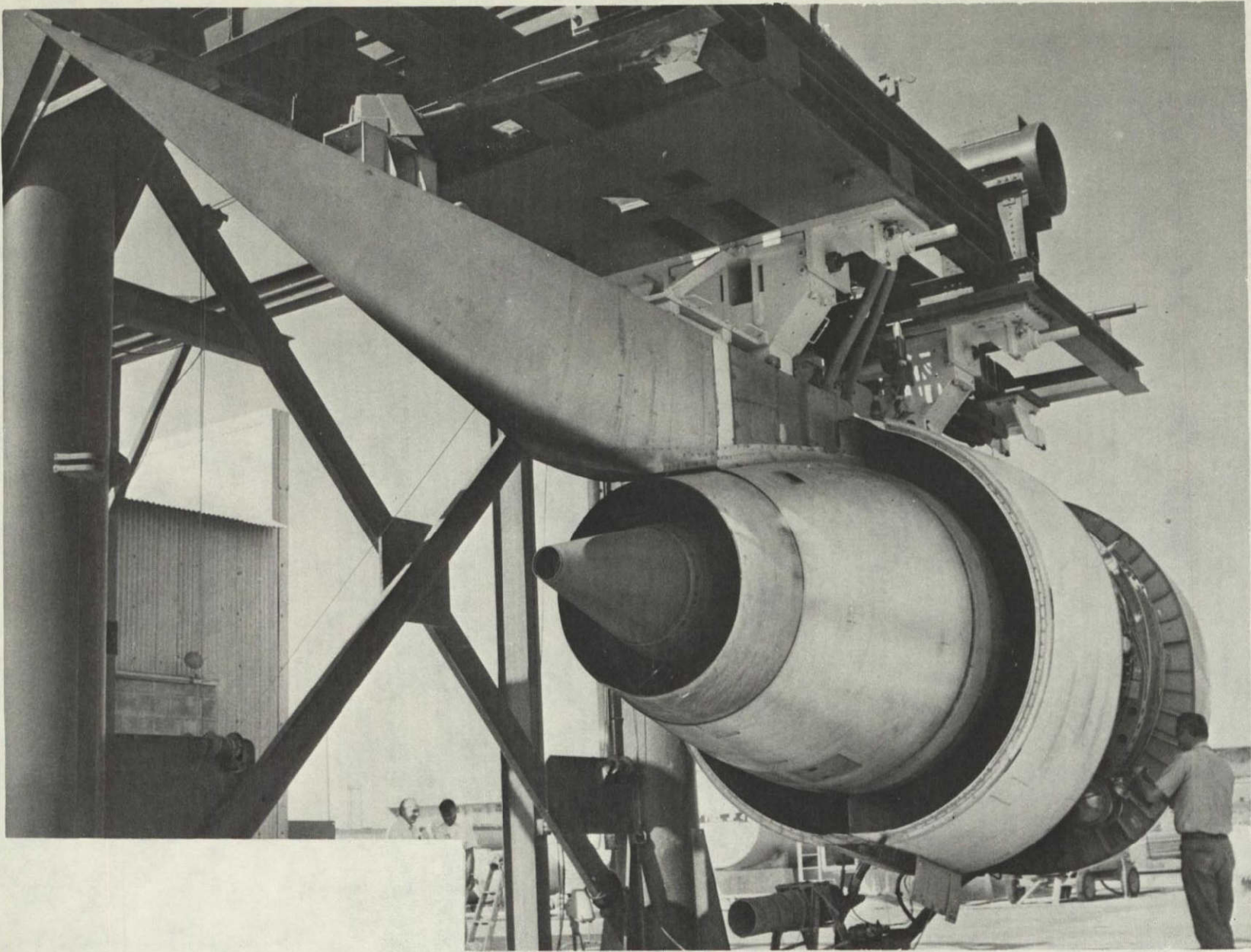


Figure 66. Disassembled Short Core Nozzle - View C.





ORIGINAL PAGE IS  
OF POOR QUALITY

Figure 67. CF6-50 Engine at General Electric Test Site MB4, Edwards AFB.

The visual inspection was made with suspect areas being examined at 10X with the following results

- Aft Centerbody - No dents or visual damage. Two nutplates "frozen" and not free to slide in their holders
- Forward Centerbody - No distress evident including weld line of skin to forward flange. The radial access holes had not been properly positioned at three locations and had to be elongated for wrench clearance at the factory. Up to 30% hole elongation was required.
- Exhaust Nozzle - No distress evident including the circumferential weld of the liner skin to the forward flange. Evidence of rewelded areas in this joint with minor undercutting and overlapping due to initial fitup
- Outer Cowl - An indentation approximately 25 mm (1 in.) in diameter and 5 mm (3/16 in) deep is visible at the 9 o'clock location, aft looking forward, approximately 200 mm (8 in.) aft of the front flange which appears to be handling damage. An indication of cowl door wear on outer cowl wear pads is evident. Leading edge of wear pad at 6:30 position, aft looking forward is well polished locally and worn halfway into the forward retaining countersunk rivet diameter. Wear coating material (tungsten carbide) is in place but locally worn. No other distress was discernible
- Channel - Particular attention was paid to the "U" channel corner radii (see Figure 6). No evidence of cracking or other distress.

The unit was then inspected to the requirements of the quality control instructions which had been previously prepared for the inspection of the Short Core Nozzle prior to shipment to Airbus Industrie for flight test and after completion of a short instrumented endurance test at Peebles. The results of the zygo inspection on the endurance test nozzle revealed no zygo discrepancies.

## 8.0 ECONOMIC ASSESSMENT

The Short Core Nozzle concept was evaluated by Boeing and Douglas under Task 1 of this program (Reference 1). Boeing studied the concept for the 747-200 aircraft for 1% cruise sfc improvement and Douglas evaluated the concept for 2% sfc improvement, 1% for internal performance improvement and 1% for reduced interference drag.

The engine ground test demonstrated a gross thrust coefficient improvement of approximately 0.3% which is equivalent to a cruise sfc improvement of 0.9%. Preliminary assessments of flight testing conducted by Airbus Industrie on the A300B airplane and by Douglas on the DC-10-30 aircraft outside this program support the sfc improvement.

The 0.9% reduction in cruise sfc due to the internal thrust coefficient improvement results in the block fuel savings shown in Table VII for the minimum fuel consumption mission. This is based on the data presented in Reference 1.

Table VII. Short Core Nozzle Block Fuel Savings for Internal Thrust Coefficient Improvement.

(Minimum Fuel Analysis)

Aircraft	Range	$\Delta^1$ Fuel	
	km	kg	%
DC-10-30	805	-58	-0.5
	2735	-211	-0.8
	6275	-599	-1.0
B-747-200	770	-37	-0.4
	3460	-49	-0.1
	6195	-98	-0.1

For the Boeing 747-200 aircraft, a block fuel savings of 0.4% was projected for the 770 km flight and 0.1% for the longer flights. The benefit in reduced nacelle weight and improved internal performance is accounted for along with the increased external nacelle drag on block fuel savings. The effect of the increased external nacelle drag has a greater impact on the long-range flights than on the short-range flights. Thus, a smaller savings is shown for the longer flights.

The estimated annual fuel savings per aircraft for the above block fuel savings are shown in Table VIII.

Table VIII Estimated Annual Fuel Savings Per Aircraft for Internal Thrust Coefficient Improvement

(Minimum Fuel Analysis)

Aircraft	Range km	Fuel l/AC/Year
DC-10-30	805	145,900
	2735	258,500
	6275	526,900
B-747-200	770	109,900
	3460	42,400
	6195	49,900

The economic assessment for the medium fuel price of 14 5¢/l (55¢/gal) for the DC-10-30 and 11 89¢/l (45¢/gal) for the B-747-200 is summarized in Table IX for a 0.9% sfc reduction

Table IX. Economic Assessment of Short Core Exhaust Concept for 0.9% SFC Reduction Due to Internal Thrust Coefficient Improvement

(Medium Range, Medium Fuel Price, Minimum Fuel Analysis)

<u>Aircraft</u>	<u>Payback (Years)</u>	<u>ROI (%)</u>
DC-10-30	0.02	4106
B-747-200	13.1	2

## 9 0 SUMMARY OF RESULTS

The Short Core Nozzle has been evaluated in three full scale engine ground tests. The main results of these tests are summarized below

### Performance Test

The CF6-50 engine back-to-back static performance test verified within data accuracy the scale model test results and indicated a thrust coefficient improvement of approximately 0.3%. This improvement results in a cruise sfc reduction of 0.9% at M 0.85, 10,668 m (35,000 ft) altitude for a thrust level of 37,800 N (8,500 lb).

At equal effective exhaust nozzle area, the Short Core Nozzle showed improvements in gross thrust at engine pressure ratio and fan speed over the Long Fixed Core Nozzle. Therefore, the Short Core Nozzle does not require a power management change to meet minimum thrust at fan speed

### Acoustic Test

The CF6-50 engine back-to-back static acoustic test demonstrated that the Short Core Nozzle produces almost identical community noise levels as the Core Reverser Nozzle at identical thrust levels. Dominant noise components of the CF6-50 engine, such as fan, low pressure turbine, and core jet were not significantly impacted by the Short Core Nozzle.

### Endurance Test

The CF6-50 engine static endurance test demonstrated the life capability of the Short Core Nozzle hardware in 1000 flight cycles without any indication of distress.

Flight tests conducted outside the program indicate that a cruise sfc reduction of at least 0.9% is attainable on the Airbus Industrie A300B and the DC-10-30 aircraft with the installation of the Short Core Nozzle. The estimated annual fuel savings per aircraft for the DC-10-30, assuming only a 0.9% improvement, amounts to 146,000 to 527,000 liters, depending on range.



## APPENDIX A

### QUALITY ASSURANCE

#### INTRODUCTION

The quality program applied to this contract is a documented system throughout the design, manufacture, repair, overhaul, and modification cycle for gas turbine aircraft engines. The quality system has been constructed to comply with military specifications MIL-Q-9858A, MIL-I-45208, and MIL-C-45662 and Federal Aviation Regulations FAR-145 and applicable portions of FAR-21.

The quality system and its implementation are defined by a complete set of procedures which has been coordinated with the DOD and FAA and which has their concurrence. In addition, the quality system as described in the quality program for this contract is consistent with the requirements established by NASA-Lewis Research Center. The following is a brief synopsis of the requirements established by this system.

#### QUALITY SYSTEMS

The quality system is documented by operating procedures which coordinate the quality-related activities in the functional areas of Engineering, Manufacturing, Materials, Purchasing, and Engine Programs. The quality system is a single-standard system wherein all product lines are controlled by the common quality system. The actions and activities associated with determination of quality are recorded, and documentation is available for review.

Inherent in the system is the assurance of conformance to the quality requirements. This includes material verification and the performance of required inspections and tests. In addition, the system provides change control requirements which assure that design changes are incorporated into manufacturing, procurement and quality documentation, and into the products.

Measuring devices used for product acceptance and instrumentation used to control, record, monitor, or indicate results of readings during inspection and test are initially inspected and calibrated and periodically are reverified or recalibrated at a prescribed frequency. Such calibration is performed by technicians against standards which are traceable to the National Bureau of Standards. The gages are identified by a control number and are on a recall schedule for reverification and calibration. The calibration function maintains a record of the location of each gage and the date it requires recalibration. Instructions implement the provisions of MIL-C-45662 and the appropriate FAR requirements.

Work sent to outside vendors is subject to quality plans which provide for control and appraisal to assure conformance to the technical requirements. Purchase orders issued to vendors contain a technical description of the work to be performed and instructions relative to quality requirements

Engine parts are inspected to documented quality plans which define the characteristics to be inspected, the gages and tools to be used, the conditions under which the inspection is to be performed, the sampling plan, laboratory and special process testing, and the identification and record requirements

Work instructions are issued for compliance by operators, inspectors, testers, and mechanics. Component part manufacture provides for laboratory overview of all special and critical processes, including qualification and certification of personnel, equipment and processes.

When work is performed in accordance with work instructions, the operator/inspector records that the work has been performed. This is accomplished by the operator/inspector stamping or signing the operation sequence sheet to signify that the operation has been performed.

Various designs of stamps are used to indicate the inspection status of work in-process and finished items. Performance or acceptance of special processes is indicated by distinctive stamps assigned specifically to personnel performing the process or inspection. Administration of the stamp system and the issuance of stamps are functions of the Quality Operation. The stamps are applied to the paperwork identifying or denoting the items requiring control. When stamping of hardware occurs, only laboratory approved ink is used to assure against damage.

The type and location of other part marking are specified by the design engineer on the drawing to assure effects do not compromise design requirements and part quality.

Control of part handling, storage, and delivery is maintained through the entire cycle. Engines and assemblies are stored in special dollies and transportation carts. Finished assembled parts are stored so as to preclude damage and contamination, openings are covered, lines capped and protective covers applied as required.

Nonconforming hardware is controlled by a system of material review at the component source. Both a Quality representative and an Engineering representative provide the accept (use-as-is or repair) decisions. Nonconformances are documented, including the disposition and corrective action if applicable to prevent recurrence.

The system provides for storage, retention for specified periods, and retrieval of nonconformance documentation. Documentation for components is filed in the area where the component is manufactured/inspected.

A buildup record and test log are maintained for the assembly, inspection and test of each major component or engine. Component and engine testing is performed according to documented test instructions, test plans and instrumentation plans. Test and instrumentation plans are submitted to NASA for approval to the testing.

Records essential to the economical and effective operation of the quality program are maintained, reviewed, and used as a basis for action. These records include inspection and test results, nonconforming material findings, laboratory analysis, and receiving inspection.

Maintainability, reliability, and safety are items considered in the basic design concept and are covered in Section 4.0.

APPENDIX B

LIST OF SYMBOLS

BPF	Blade Passing Frequency, kHz
$C_F$	Flow Coefficient
$C_{F15}$	Fan Nozzle Flow Coefficient
$C_T$	Gross Thrust Coefficient
DMS	Data Management System
EGT	Exhaust Gas Temperature, ° C (° F)
EPNL	Effective Perceived Noise Level, EPNdB
FGM	Measured Gross Thrust, N (lb)
$F_{iCore}$	Ideal Thrust of Core Nozzle, N (lb)
$F_{iFan}$	Ideal Thrust of Fan Nozzle, N (lb)
$F_n, FN$	Net Thrust, N (lb)
Hum	Humidity, Grains
LPT	Low Pressure Turbine
M	Mach Number
N	Number of Samples in Data Grouping
$N_1$	Fan Speed (rpm)
$N_{1K}$	Corrected Fan Speed (rpm)
$N_2$	Core Speed (rpm)
$P_{Bar}$	Barometric Pressure, N/cm <sup>2</sup> (lb/in <sup>2</sup> )
PEDS	Portable Environmental Data Station
PNL	Perceived Noise Level, PNdB

PNLT	Tone Corrected Perceived Noise Level, PNdB
$P_o$	Ambient Pressure, N/cm <sup>2</sup> (lb/in <sup>2</sup> )
$P_s$	Static Pressure, N/cm <sup>2</sup> (lb/in <sup>2</sup> )
$P_{T \text{ Fan}}$	Fan Nozzle Total Pressure, N/cm <sup>2</sup> (lb/in <sup>2</sup> )
PWL	Sound Power Level dB re 10 <sup>-13</sup> Watts
RMS	Root Mean Square
sfc	Specific Fuel Consumption, kg/hr N (lbm/hr lbf)
SPL	Sound Pressure Level dB re 20 x 10 <sup>-5</sup> N/m <sup>2</sup>
T	Total Temperature, ° C, (° F)
$T_o$	Ambient Temperature ° C (°F)
t(v)	"t" Statistic for (v) Degrees of Freedom, 95th Percentile
V	Velocity, m/sec (ft/sec)
$\theta$	Polar Angle Referenced to Engine Centerline, Clockwise from Inlet
$\sigma$	Unbiased Estimate of Sample Standard Deviation
$\sigma^2$	Unbiased Estimate of Sample Variance
$\delta_2$	Standard Pressure Correction, $P_{T2}/10133$ ( $P_{T2}/14696$ )
v	Degrees of Freedom of Sample

## REFERENCES

1. Fasching, W.A., "CF6 Jet Engine Performance Improvement Program, Task 1 - Feasibility Analysis", NASA Report CR-159450.
2. "Aerospace Recommended Practice ARP866A", Society of Automotive Engineering Revised March 15, 1979
3. Kazin, S.B and Matta, R K., "Turbine Noise Generation, Reduction and Prediction", AIAA Paper No. 75-449, March 1975.

COMPANY/PERSONNEL

Nielsen Engineering & Research  
510 Clyde Avenue  
Mountain View, CA 94043  
Dr. William Roberts

TRW Equipment, TRW Inc.  
23555 Euclid Avenue  
Cleveland, OH 44117  
C. S. Kortovich

Richard A. Whitaker

Electronic Supply Division  
ESB/OCNG MS 34  
Hanscom AFB, MA 01731  
Major Robert P. Couch

Computer Avionics Corporation  
120 Charcot Avenue  
San Jose, CA 95131  
Milton E. Gregory

General Electric Company  
AFPRO (Det. 28)  
Cincinnati, OH 45215  
R. Glindmeyer/Mail Drop N-1  
Chief, Plans Requirements & Eval. Branch

NASA/LeRC Approved Distribution List

<u>COMPANY/PERSONNEL</u>	<u>COMPANY/PERSONNEL</u>
National Aeronautics & Space Administration Washington, DC 20546 Dr James J. Kramer/R	Robert E. Jones/60-6
Dr. Raymond S. Colladay/RJP-2 (3_copies)	Lawrence P. Ludwig/23-2
George C. Deutsch/RT-6	Harold E. Rohlik/77-2
William S. Aiken/RD-5	Tito T. Serafini/49-1
Harry W. Johnson/RJG-4	Kenneth E. Skeels/500-305
C. Robert Nysmith/RP-4	Lewis Library/60-3 (2_copies)
Richard A. Rudey/RTP-6	Report Control/5-5
Stafford W. Wilbur/RJP-4	NASA Langley Research Center Hampton, VA 23665 Robert W. Leonard, Dr./158
Roger L. Winblade/RHG-5	Ray V. Hood/158
NASA Lewis Research Center 21000 Brookpark Road Cleveland, Ohio 44135 Dr. John M. Klineberg/3-3	NASA Ames Research Center Moffett Field, CA 94035 Louis J. Williams/237-9
Warner L. Stewart/3-5	NASA Dryden Flight Research PO Box 273 Edwards, CA 93523 James A. Albers, Dr./2089
Donald L. Nored/301-2	William L. Ko/34820
Joseph A. Ziemianski/301-4 (3_copies)	Frank V. Olinger/2093
John E. McAulay/301-4 (20_copies)	NASA Scientific and Technical Information Facility PO Box 8757 Balt/Wash Intl Airport, MD 21240 Accessioning Department (30_copies)
Edward M. Szanca/301-4 (20_copies)	Federal Aviation Administration DOT/FAA/NAFEC ANA-410, Bldg. 211 Atlantic City, NJ 08405 Gary Frings
Milton A. Beheim/86-1	Department of Transportation 21000 Second St., SW Washington, DC 20591 Harold True/ARD 550
Robert W. Hall/49-1	William T. Westfield/ARD 500
Melvin J. Hartmann/5-3	Robert S. Zuckerman/ARD 550
Richard A. Rudey/60-4	
Robert W. Schroeder/500-207	
William J. Anderson/23-2	
Salvatore J. Grisaffe/49-3	
Marvin H. Hirschberg/49-1	



COMPANY/PERSONNEL

Civil Aeronautics Board  
Washington, DC 20428  
J. E. Constantz/B-68

Wright-Patterson Air Force Base  
Dayton, OH 45433  
Everett, E. Bailey/AFAPL/TBD

R. C. Cochran/ASD/SDUB

R. M. Cox/AFFDL/DA

Lt. Col. D. S. Dickson/ASD/YZI

Lt. John Edens/ASD/ENFPA

Lt. Col. Reynald E. Fitzsimmons/AFAPL/TBD

Keith R. Hamilton/AFAPL/TBC

C. M. High/ASD/YZE

Capt. Charles M. Hutcheson/ASD/YZET

Maj. C. L. Klinger/ASD/YZET

Lt. Col. James L. Pettigrew/ASD/YZEA

Perry Shellaberger/ASD/ENFPA

E. C. Simpson/AFAPL/TB

Lt. E. Whonic/ASD/YZN

Offutt Air Force Base  
Headquarters  
Omaha, NE 68113  
Col. J. Streett/SAC/LGME

Oklahoma City Air Logistics Center  
Tinker AFB, OK 73145  
Capt. P. Davis/OC-ALC/MM

Capt. Steven Erickson/OC-ALC/MA USAF

E. Reynolds, Engine Test Branch (MAET)

COMPANY/PERSONNEL

Naval Air Propulsion Center  
1440 Parkway Avenue  
Trenton, NJ 08628  
Walter L. Pasela (PE 63)

Naval Weapons Center  
Code 3271  
China Lake, CA 93555  
J. A. O'Malley

Arnold Engineering and Development  
Center  
Arnold AFS, TX 39389  
Dr. James G. Mitchell/AEDC/XRFX

R. Roepke/AEDC/XRFX

Air Transport Association  
1709 New York Avenue, NW  
Washington, DC 20056  
E. L. Thomas

General Electric Company  
One Neumann Way  
Evendale, OH 45215  
Al Schexnayder/H4 (10\_copies)

Ray Wulf/F117

General Electric Company  
5300 Riverside Drive  
Cleveland, OH 44135  
Meade Rudasill

United Technologies Corp.  
Pratt & Whitney Aircraft  
400 Main Street  
East Hartford, CT 05108  
William O. Gaffin (10\_copies)

G. Phillip Sallee

United Technologies Corp.  
Pratt & Whitney Aircraft  
20800 Center Ridge Road, Rm. 105  
Rocky River, OH 44116  
George C. Falkenstein

COMPANY/PERSONNEL

United Technologies Corp.  
Hamilton Standard Division  
Bradley Field  
Windsor Locks, CN 06096  
K. Liebing

Louis Urban/MS3-2-36

The Boeing Company  
PO Box 3707  
Seattle, WA 98124  
Don Nordstrom

William B. Anderson

Kenneth H. Dickenson 3N-33

Paul G. Kafka

Richard L. Martin MS 73-07 2 copies

John L. White

McDonnell Douglas  
3855 Lakewood Blvd.  
Long Beach, CA 90846  
Ronald Kawai MC 36-41

F. L. Junkermann 36-41

Max Klotsche 35-31

Technical Library 36-84

Lockheed-California Co.  
PO Box 551  
Burbank, CA 91520  
John L. Benson

Tom Laughlin, Jr.

Allegheny Airlines, Inc.  
Greater Pittsburgh Int'l Airport  
Pittsburgh, PA 15231  
William G. Pepler

American Airlines, Inc.  
N. Mingo Road  
Tulsa, OK 74151  
Keith Grayson

Bob B. Cooper

Ray G. Fenner

COMPANY/PERSONNEL

Braniff International  
Braniff Tower  
PO Box 35001  
Dallas, TX 75235  
Hank Nelson

Continental Air Lines, Inc.  
Los Angeles Inter. Airport  
Los Angeles, CA 90009  
Frank Forster

Delta Air Lines, Inc.  
Hartsfield-Atlanta Int'l Airport  
Atlanta, GA 30320  
James Goodrum

Eastern Air Lines, Inc.  
Miami International Airport  
Miami, FL 33148  
M. Dow, Bldg. 21

Arthur Fishbein, Bldg. 21

P. M. Johnstone

The Flying Tiger Line, Inc.  
7401 World Way West  
Los Angeles Inter. Airport  
Los Angeles, CA 90009  
James M. Dimin

Bruno Lewandowski

J. R. Thurman

National Airlines, Inc.  
PO Box 592055  
Airport Mail Facility  
Miami, FL 33159  
R. A. Starner

Northwest Airlines, Inc.  
Minn.-St. Paul Int'l Airport  
St. Paul, MN 55111  
Al Radosta

Pan American World Airways  
JFK International Airport  
Jamaica, NY 10430  
John G. Borger

Lewis H. Allen

Niels B. Andersen

Robert E. Clinton, Jr.

Anqus MacLarty

COMPANY/PERSONNEL

Piedmont Airlines  
Smith Reynolds Airport  
Winston-Salem, NC 27102  
H. M. Cartwright

Paul M. Rehder

Seaboard World Airlines, Inc.  
Seaboard World Bldg.  
John F. Kennedy Int'l Airport  
Jamaica, NY 11430  
Ralph J. Barba

Jere T. Farrah

Trans World Airlines  
Kansas City Inter. Airport  
PO Box 20126  
Kansas City, MO 64195  
Ken Izumikawa 2-280 MCI

D. L. Kruse 2-280 MCI

Walter D. Sherwood

United Airlines, Inc.  
San Francisco Inter. Airport  
San Francisco, CA 94128  
John Curry

P. Hardy

James Uhl

Western Air Lines, Inc.  
6060 Avion Dr. Box 92,005  
World Way Postal Center  
Los Angeles, CA 90009  
Walter Holtz

Cooper Airmotive, Inc.  
4312 Putman Street  
Dallas, TX 75235  
B. Carter

Terry Harrison

Pacific Airmotive Corporation  
2940 N. Hollywood Way  
Burbank, CA 91503  
Oddvar O. Bendikson

Joseph R. Gast

COMPANY/PERSONNEL

Aerojet Manufacturing Company  
Vice President - Engineering  
601 S. Placentia  
Fullerton, CA 92634  
John Kortenhoeven

Air Research Manufacturing Company  
402 South 36th Street.  
PO Box 5217  
Phoenix, AZ 85010  
Karl R. Fledderjohn  
Dept. 93-200/503-3S

Dr. M. Steele  
Dept. 93-010/503-4B

F. Weber  
Dept. 93-200/503-3S

AVCO Lycoming Division  
550 South Main Street  
Stratford, CN 06497  
A. Bright

W. L. Christensen

General Motors Corporation  
Detroit Diesel Allison Division  
PO Box 894  
Indianapolis, IN 46206  
R. A. Sulkoske MS V19

G. A. Williams MS T8

The Aerospace Corporation  
PO Box 92957  
Los Angeles, CA 90009  
Ronald R. Covey

The Aerospace Corporation  
2350 East El Segundo Blvd.  
El Segundo, CA 90245  
W. Roessler

Advanced Technology, Inc.  
7923 Jones Branch Drive  
McLean, VA 22101  
Bernard C. Doyle, Jr.

Delco Electronics  
Avionics Sales Office  
7929 S. Howell Avenue  
Milwaukee, WI 53207  
J. Sheldrick